AN ABSTRACT OF THE THESIS OF

Jeffry Liem for the degree of Master of Science in Forest Products presented on February 29, 2000. Title: Carbon Fiber as a Resistive Heat Generator to Accelerate Adhesive Cure in Reinforced Wood Laminates.

Signature redacted for privacy.

Abstract approved: _____

Philip E. Humphrey / Robert J. Leichti

As a result of its atomic structure, carbon fiber produced from mesophase pitch has a high electrical conductivity and high tensile strength. Others have used carbon fiber as a resistive heating unit to accelerate matrix solidification in carbon fiber-polymer matrix composites.

In this study, a unidirectional carbon fiber reinforced polymer (CFRP) strip, which is usually used as a reinforcement material, was used to generate heat by the application of direct current (DC) power. A CFRP strip measuring 955 × 50 × 1 mm was successfully used to form a reinforced wood laminate using the CFRP resistive heating method. The CFRP strip was a pitch-based unidirectional composite of carbon fibers (9-μm diameter) in a 60 percent carbon fiber volume fraction. The polymer matrix was an epoxy. Due to the carbon fiber alignment and its molecular structure, the thermal-electrical properties of the CFRP strips were orthotropic.

To connect the electrical circuit to the CFRP strip, the ends of strip were first electroplated with copper. It was found that a tapered end-geometry and low plating power density combined with a long period for electroplating resulted in an

advantageously porous copper deposit. The CFRP strip was subsequently connected to the electrical circuit with solder. It was found that the circuit could produce approximately 34 percent energy conversion efficiency. Measurements showed that the CFRP strip heated quite uniformly over its length.

The bonding compatibility of CFRP to wood was explored with phenol resorcinol formaldehyde (PRF) and phenol formaldehyde (PF) adhesives. For this purpose, the effects of temperature on isothermal strength development rates were explored using an Automated Bonding Evaluation System (ABES). These studies were conducted to anticipate the strength development with time of resistively heated bonds. The responsiveness of adhesive-adherend combinations in relation to temperature has been tested under a range of time and temperature conditions in miniature adhesive test bonds.

The bonding strength of CFRP-to-wood after three minutes pressing at 100 ^{0}C using PRF adhesive were around 3 MPa. At this bonding strength, some of the carbon fiber was pulled out from the CFRP strip. Additional bond strength up to 150 percent (up to 4.5 MPa.) was gained when the glueline has cooled to room temperature. However, PF adhesive had weaker bonding strength and very little strength development at the same temperature. PF adhesive was therefore considered not to be viable at this stage.

A numerical prediction technique has been established that could give information on how much energy and pressing time are needed to reach optimum bond strength to make a reinforced glulam using resistive heating. The CFRP is concluded to have potential for wood laminate products, since it can be used to accelerate the adhesive cure and act as a reinforcement.

Carbon Fiber as a Resistive Heat Generator to Accelerate Adhesive Cure in Reinforced Wood Laminates

by

Jeffry Liem

A THESIS

Submitted to

Oregon State University

In partial fulfillment of
the requirements for the
degree of

Master of Science

Presented February 29, 2000
Commencement June 2000

Master of Science thesis of Jeffry Liem presented on February 29, 2000.

APPROVED:

Signature redacted for privacy.

Co-Major Professor, Representing Forest Products

Signature redacted for privacy.

Co-Major Professor, Representing Forest Products

Signature redacted for privacy.

Head of Department of Forest Products

Signature redacted for privacy.

Dean of Graduate School

I understand that my thesis will become part of the permanent collection of Oregon State University libraries. My signature below authorizes release of my thesis to any reader upon request.

Signature redacted for privacy.

Jeffry Liem, Author

ACKNOWLEDGMENT

I would like to thank many people who contributed to this project. My father for supporting me to go abroad and encourage me in any circumstance. His encouragement and love are the source of strength to finish this degree. Dr. Humphrey as my major advisor and Dr. Leichti as my co-major advisor for their guidance and support in these studies. Especially Dr. Humphrey, he is always very instructive and patience whenever I had problems during my study here. Dr. McLain for supporting me financially while my country was hit by economy crisis. Dr. Holbo for his ideas that helps me to overcome the CFRP connection problem. Mr. Clauson for his help to setup the instruments. It was very helpful having them around and as technical consultants for my experiments. Also people in Dr. Humphrey's lab: Jahangir, Jaewoo, Heiko, Clovis and also from other labs Andrew, Mark, Rachel, Jim, Wenlong, Jiqing. Their friendship made my life in lab much more interesting. My friends: Phil, Hendrik, Ridwan, Johnwan, Meifei, Sam and family, Herawan and family and the ICF members from the Baptist church.

CONTRIBUTION OF AUTHORS

Dr. Humphrey was involved in the experimental design, technique, analysis of all experiments, especially the bonding kinetics essay in chapter 4 and in preparation of manuscripts. Dr. Leichti was involved in preparation of manuscripts.

TABLE OF CONTENTS

TABLE OF CONTENTS (Continued)

Page

LIST OF FIGURES

LIST OF FIGURES (Continued)

Figure: Page

LIST OF FIGURES (Continued)

Figure: Page

LIST OF TABLES

CARBON FIBER AS A RESISTIVE HEAT GENERATOR TO ACCELERATE ADHESIVE CURE IN REINFORCED WOOD LAMINATES

CHAPTER 1

INTRODUCTION

One of the recently developed composite materials in the wood products industry is the reinforced glulam beam. A glulam beam is a laminate of several structural lumbers which are glued together to form a useful load-bearing member. Reinforced glulam beams are beams with additional high strength synthetic fiber reinforcing layers that are applied at the highest stress-concentration zones. These zones usually lie at the lower and upper extremes of the beam cross-section when the beam is loaded in bending mode. With such reinforcement, the strength of the wood beam may be greatly improved compared to ordinary glulam beams (Tingly 1996). Reinforced glulam beams allows the use of lower lumber grades, smaller size of lumber, and they may be made in unlimited sizes as long as appropriate pressing equipment is available. Because of the advantages mentioned above, reinforced glulam beams have great potential as a future structural building component.

The types of reinforcement materials that have been explored to date include glass fiber, aramid fiber and some carbon fiber. The fibers have most often been in the form of pre-impregnated sheet with a resin matrix. The fibers have usually had a unidirectional orientation in order to maximize the reinforcement strength in the longitudinal axis of beams. At the present time, the use of carbon fiber as a reinforcement material in wood

composites is limited. The relatively high price of carbon and non-standardized performance of reinforced products have, to date, largely prevented its commercial utilization in the forest products industry. However, in the near future, when the supply of large wood members becomes less available and the demand for wood products increases, reinforced wood may provide a viable solution.

The present manufacturing methods for these reinforced glulam beams involves cold pressing with phenol resorcinol formaldehyde (PRF) adhesive: a strong thermosetting glue that can cross-link at room temperature. The PRF glue is commonly used in glulam and in the manufacture of many other structural wood products. In the manufacture of experimental beams, the fibers are usually incorporated within an ordinary glulam beam, glued to wood in the desired position, then pressed for at least 8 hours to let the glue solidify. With the current slow manufacturing process, there are niches to improve the manufacturing method. Improvements in manufacturing speed together with the incorporation of reinforcement could greatly improve economic viability.

A study of reinforcement in glulam products has led to a potential method to directly heat the interfacial glueline. Carbon fiber, when embedded within a polymerized epoxy matrix (CFRP), can be used as a heat generator by application of a controlled voltage (Humphrey and Leichti 1998), while also acting as the reinforcement in the finished beam. By generating heat at the interface layer, the processing time of reinforced glulam beams may become shorter. This potential will be studied in this thesis.

This research will introduce the alternative method that can significantly increase the production of the reinforced beams. By accelerating the thermoset adhesive curing time, the production time to manufacture reinforce glulam beams may be greatly reduced.

An Automated Bonding Evaluating system (ABES) will be used to study the kinetics of bonding development between wood and carbon fiber reinforcement materials. A repetitive test with progressively increased pressing time at several fixed temperatures can be used to study the bonding kinetics. The results of this study can be used to determine optimal conditions under which to apply the resistive heating for beam formation.

It is estimated that the production of glulam beam material will increase significantly from 232 million board feet (0.54 million m^3) in 1995 to 326 million board feet (0.77 million m^3) by the year 2003 (APA 1998). With processing improvements, productivity can be increased, the quality can be improved, and reinforced glulam can fill the increasing demand.

CHAPTER 2

LITERATURE REVIEW

HISTORY OF FIBER REINFORCED POLYMER (FRP) COMPOSITES

The use of FRP began in the early 1940's, when the military and aerospace programs needed lightweight materials of high strength. These materials also needed to have resistance to chemicals, have non-magnetic properties and good fatigue resistance. They were used in rockets and satellites, wing skins for aircraft, and helicopter's rotor blades (Ballinger 1994). This progress led to the development of many types of fiber-resin systems and manufacturing methods that are now used for civilian applications. A range of basic composite manufacturing methods is reviewed below.

Composite Manufacturing Methods

Lay-up methods. - Civilian development started in the 1950's, when 'lay-up' manufacturing processes were used to build heavy-duty fiberglass-boats. These structures had to resist salt water and impact loading and resist winter freezing cycles. Lay up was by hand or machine to build sheets of fabric or fiber that were bound together with a resin so that the thickness of the composite could be customized (Ballinger 1994).

Pultrusion methods. - The 'Pultrusion' manufacturing method was developed in 1956 to make components for structural purposes such as I-beams, channels, and tubes. Some Japanese and European companies produce pre-tensioned and post-tensioned concrete using this manufacturing method. The pultrusion process is a continues process

of pulling fibers through a resin bath and pushing assemblages of such coated fibers through a heated die to produce desired cross-sectional shapes (tube, I-shape, box, etc.) (Ballinger 1994).

Filament-winding methods. - The 'filament-winding' manufacturing process was developed in 1955 to produce filament wound fiberglass pipe for above and below ground applications that can withstand severe chemical environments. Filament winding is an automated process of winding resin-wetted fibers around a mandrel to produce circular shapes (Ballinger 1994).

Wrapping methods. - Recently FRP has been used for strengthening structures by wrapping or adhesively bonding glass or carbon materials around them. This wrapping process was developed in Japan for strengthening structures to avoid earthquake damage. This process was commercialized in Switzerland to strengthen existing timber and concrete structures by adhesively bonding carbon fiber laminates (prepreg) (Ballinger 1994).

Induction heating methods. - Carbon fiber reinforced polymer (CFRP) materials were formed into Cross-Ply Composites using a 'Magnetic induction' heating method (Fink *et al.* 1992). In this process, the thermosetting resin was cured between plies using a non-contact and localized electromagnetic field (EMF) with a frequency 50 – 200 kHz and typical power of 15 kW. Such an alternating field led to the generation of the 'Eddy-current' effect (Halliday 1998 and Dorf 1993). The eddy-current loop generated heat in a conductive thin layer of cross-carbon-fiber that was placed between two laminae. Fink's study was devoted to finding ways of patching or covering holes in aerospace applications.

Advantages and Disadvantages of Using FRP

The development of FRP has been rapid but has not been commercialized widely. Obstacles to wide acceptance seem to have been a lack of precise stress analysis and structural design. Those are caused by wide range of fibers and matrixes properties that makes the FRP composite products become not uniform and difficult to apply for general purpose products. This non-uniformity is causing difficulty to standardize and manufacturers are reluctant to use any standards that are developed.

With regard to economic benefits, FRP can reduce shipping, installation and costs, and may have longer life cycle than competitive materials. Although the prices of the constituents is high, potential reduction in labor costs and necessary equipment needed can make composite components may offset the high cost.

HISTORY OF REINFORCEMENT OF LAMINATED WOOD STRUCTURES

Reinforced glulam beams

Metal reinforcement. - Mark (1961, 1963) and Sliker (1962) used *aluminum plates* for the reinforcement of laminated wood beams in order to enhance stiffness and strength. Mark (1961) positioned continuous aluminum plates in the compressive and tensile zones of beam vertical cross-sections, where longitudinal stress are high when beams are loaded in bending. Sliker (1962) used 1/16-inch aluminum plates to reinforce glue-laminated beams on the outer faces. Again, Mark (1963) used a trapezoidal aluminum casing to reinforce trapezoidal wood sections.

Bohannon (1962) *prestressed the wood* in the outer tension lamination of glu-laminated beams by placing 3/8-in steel diameter rods to hold the glulam in tension between steel blocks at the ends of the beam. When a force was applied to the beam, the beam's tensile zone will suffer less tensile stress due to the prestressed bars placed in it. This prestressing method had been used in prestressed concrete since 1800.

Subsequently, Lantos (1970) used phenol-resorcinol formaldehyde (PRF) adhesive to bond *steel rods* within beams along their length in the high stress zones.

Coleman (1974) used *steel plates and U-shaped* sections surrounding the compressive and tensile zones to reinforce laminates of wood. The steel plates were inserted between wood laminations, and increases in stiffness and strength were observed. Krueger and Sandberg (1974) used a woven steel wire and epoxy glue to reinforce the tensile zone of glulam.

In addition Bulleit (1989)] used steel bars that are used in concrete to reinforced glulam. Gardner (1991) has successfully patented a reinforcing system using high strength deformed steel bar for concrete reinforcement using epoxy glue. The reinforcement bars were applied at the outer glueline of the tensile and compressive zones.

Synthetic fiber reinforcement. - The concept of bonding synthetic fibers to wood was first reported in the 1960's when Wangaard (1964) and Biblis (1965) used glass-fiber reinforced plastic strips to reinforce the compression and tensile zones of solid wood samples loaded in bending mode. Spaun (1981) used E-Glass to reinforce finger jointed wood in the high stress region of beams. Rowland (1986) subsequently used unidirectional and cross-woven carbon and Kevlar ® fibers and various adhesive types

(epoxy, resorcinol formaldehyde, phenol resorcinol formaldehyde, and phenol formaldehyde) in studies of reinforcement.

After thirty years of reinforcement studies to enhance the strength and stiffness of laminated wood composite systems, none of them went into mass production. The viability was not realized until Moulin (1990) and Tingley (1990) used high strength fiber reinforced polymer (FRP) as a partial length reinforcement that was then approved by the International Conference of Building Material (ICBO 1995).

The study of reinforcing wood has progressed over the last decades toward the use of high strength synthetic fibers. Those who have reported research studies on these types of reinforcement include Tingley and Leichti 1994, Triantifillou and Deskovic 1992, Davalos *et al.* 1994, Barbero *et al.* 1993, Moulin *et al.* 1990, and Kirlin 1996. The present discussion will be largely limited to the use of carbon fiber since this combines high stiffness and strength with the ability to conduct electricity: a pre-requisite of the resistive heating method.

Reinforced panel board. - In enhancing and reducing waste in wood products, reinforced particleboard (1,200 × 90 × 38 to 88 mm) made from solid wood residue (particle-wood), has been reinforced with high tensile fibers and pressed in a continuous-belt press (Saucier and Holamn 1975). Incorporated with the wood-particles, which are weak in flexural bending strength, the prestressed strands (fiberglass, aluminum wire, etc.) can improve the flexural strength of the composites. Three adhesive types (urea, phenolics, and resorcinol) were investigated although only the resorcinol had a positive result.

Reinforcement using fiberglass and phenol formaldehyde resins with petroaltum additives (30 percent of fiber weight) has been conducted to improve dry-process hardboard products (Smulski and Ifju 1986). Sandwich lay-up with fiberglass at the top and bottom parts (yarn and laminate forms) was used to reinforce the hardboard. The result was an increase of flexural stiffness and strength of the hardboard reinforced with continuous fiberglass. By increasing fiber volume fraction (0.7 to 2.6 percent), the composite's mechanical properties (MOE and MOR) were increased by up to 10 percent. All the composites failed in the tensile fracture mode because the strain at maximum stress of the hardboard is much less than that of the fiberglass (0.3 mm/mm and 1.0 mm/mm or 0.012 in/in and 0.041 in/in). The result of this study may assist the future design of reinforced fiberboard.

Manufacturing Reinforced Glulam Products

Hand lay-up. - The most common process to make reinforced structural members is 'hand-lay-up' using carbon-fabric or Kevlar ® fabric. This may be done by applying a base coat resin on the surface, placing fabric on the wetted surface, closing the laminate and clamping under a pressure of around 0.34 MPa (50-psi) for 24 hours to ensure complete cure of room temperature cure adhesive.

FRP can be laid up at the same time as glue spreading or as a separate process after the glulam has cured. The inert surface and lack of porosity of FRP apparently requires longer times to be cured using typical wood bonding. Some have reported that it generally takes up to seven days before the reinforced product can be used (Tingley and Leichti 1994a, and Dailey *et. al.* 1995). This delay may, in part, be due to the need for

internal stresses to relax after the glue has cured. Such stress may be the result of moisture migration in the vicinity of the glue line (Humphrey 1999).

A significant increase in stiffness and strength of glulam reinforced FRP can reduce the depth of glulam beams which also reduces their weight and need for bracing to prevent lateral buckling (Davalos *et al.* 1994). In spite of some promising results, Triantafillou and Deskovic (1992) mentioned that 'no practical and economical processes have yet been developed for the commercial production of wood beams reinforced with FRP'.

Oven cure. - 'Oven-cure' manufacturing methods have been explored. In this method, unidirectional Kevlar ® prepreg is heated to make the resin matrix flow. Following this, the hot-prepreg is applied to the wood beam which is then clamped at around 75 psi (0.5 MPa), and placed into an oven at around 121 ^{0}C (250 ^{0}F) for one hour to cure the adhesive (Abdel-Magid 1994). Without additional adhesive applied at the interface area, a wood-FRP delamination problem did occur that indicates a weak bond between adherends. The attempt in this approach was to use the thermoplastic nature of the matrix as an adhesive to bond it to the wood. Clearly there were problems of wetting and bond formation with the wood.

Pultrusion. - Attempts to use 'Pultrusion' methods have been made to manufacture FRP-wood composite beams (Mufti *et al.* 1992). Spruce wood with cross-section area 5 × 24 mm was fed manually into the 'inlet-die' with continuous fiber feeding (with V_f = 20 percent of E-glass, S-glass, Kevlar, or carbon). Pressurized-injection-melted-resin (55 to 45 percent total weights) was pumped into the middle part of the die with pressure and temperature controls ranging from 0.27 to 0.41 MPa (40- to

60-psi) and 180 to 190 ^{0}C respectively. At the 'outlet-die' a pultruded specimen was produced at a speed of 150 mm per minute. Material produced at 0.41 MPa (60-psi) pressure and 190 ^{0}C temperature in the resin injection had the highest shear and flexural strength. At the interface area, the wood absorbs a lot of resin and leaves the fibers drier than usual; this is likely due to the penetration of matrix micro-cavities. The cured wood-matrix-fiber composites with 41 percent wood volume fraction had 4 times greater stiffness than the wood itself and had 115 times greater load capacity than pure woods in a four-point bending test.

A pultruded vinylester FRP for wood reinforcement that bonds with RF glue are suggested and can reduce the product cost (Gardner *et al.* 1994). The test of sapwood and heartwood with or without FRP bond strength were tested using a shear-block test (ASTM D 905). The glues were Resorcinol-formaldehyde (RF), epoxy, and emulsified polymer isocyanate (EPI) with a specimen size of 63.5 × 50 × 9.5 mm. In the wet test (ASTM D 1101), RF shows better bond strength than epoxy and EPI, but in the dry test, epoxy is superior. Because of the poor performance of epoxy, further tests will focus on using RF glue. The result of shear-block test shows wood-FRP values lying between 7.5 to 8.5 MPa (dry) and 5 to 6.5 MPa (wet). For use in timber construction, shear strength values of 7.38 MPa are required. These results therefore suggest that pultruded wood-FRP is reliable for interior purposes.

Bending Strength of Wood Composite Beams

One of the benefits of using reinforcement is to increase composite strength. Full scale reinforced and unreinforced glulam beams (16.15 × 1 × 0.2 m) were tested by

Tingley and his co-workers according to ASTM D198 (Tingley and Leichti 1994). The aramid-reinforced plastic (ARP) material used in the study had a tensile strength of 1,380 MPa and a modulus of elasticity (MOE) of 127,650 MPa. The ultimate shear strength of unidirectional ARP, 60 percent fiber volume fraction (V_f) with epoxy matrix, is 82.8 MPa. This compared to Douglas-fir *sp.* tensile property, at 12 percent moisture content (MC) of 103.5 MPa and the MOE is 12,420 MPa. The beams were produced using conventional PRF glue with 80-minutes open time, 8-hour close time, and a standard pressure of 0.862 to 0.897 MPa. With 1.5 percent concentration of Aramid-FRP in the cross section of the above beams, the bending strength of reinforced and unreinforced beams can be compared as shown below in Table 2.1.

Table 2. 1. Mechanical properties improvement using AFRP at the top and bottom of the glulam beam (Tingley and Leichti 1994).

MOE bending	Reinforced	13,455 MPa	30%
	Unreinforced	11,247 MPa	increase
MOR bending	Reinforced	46,368 MPa	88%
	Unreinforced	24,626 MPa	increase
Ultimate shear strength	Reinforced	1.876 MPa*	40%
	Unreinforced	1.345 MPa**	increase

Notes: (*) NFPA-NDS 1991 approved value
(**) American Plywood Association (APA) approved value test of Douglas-fir *sp.*

SHEAR TESTING OF ADHESIVE TO WOOD BONDS

In the present work, the strength development of wood-to-C-FRP bonds will be studied as they cure. This is with a view to designing and optimizing the resistive heating approach. For this reason, the use of lap-shear testing methods for bond assessment are briefly reviewed here.

A large number of analyses of stresses in single-lap joints have been conducted over the past 60 years or so. Volkerson (1938) published the first known analysis of stresses arising from differential shearing. The analysis was then extended to calculate stresses due to both bending and shearing. Eventually, Goland and Reissner (1944) described the shear and transverse tensile stresses in the adhesive.

Further improvements in stress analysis were made by using finite element methods (FEM). An investigation using the then quite new method was conducted by Cooper and Sawyer (1979). These workers compared solutions, including non-linear behavior, with the results of Goland and Reissner who developed closed-form solutions. At the same time, the influence of thickness on stresses in the adhesive layer was explored by Ojalvo and Eidinoff (1978), who produced a more complete shear-strain equation.

Many researchers have investigated stress distributions in other test joint configurations. The intention of these investigations was often to determine the effect on bond strength of altering joint geometry and also to develop test methods which provided results which were independent of sample size. Improvement of test sample geometry by tapering edges and stepping joints was, for example, analyzed by Erdogan and Ratwani (1971).

Bond Delamination in Lap Shear Test

Using the automated bonding evaluation system (ABES), the bonding reactivity of thermosetting adhesives can be evaluated in a small lap-shear testing method developed by Humphrey (1999). This instrument affects a hot-pressing action on a miniature scale by the use of small test bonds and controlled pressure and temperature blocks. The testing method enables bond strength development kinetics and the effect of modification of specific bond conditions to be investigated. Groups of small lap-shear tests are pressed at a range of target temperatures, and tensile load is applied after certain designated time periods. Adherends are made thin or heat diffusive so that block temperature is reached at the glueline quickly; near isothermal conditions therefore prevail for most of each pressing period. Derived bond test data can be used to construct plots of isothermal shear strength development with time. Providing that such isothermal strength development plots display linearity in their early stages, then a value of bond formation speed can be derived by regressing bond strength against time. The effect of temperature on bonding rate may then be explored by collecting data for a range of pressing temperatures and then plotting the regressed isothermal bonding rates against temperature.

Several factors effect the results of ABES testing for a given adhesive; these include (but are not limited to) adherend properties, adhesive distribution over the glueline, and overlap area. When using ABES, adherend thickness must be sufficient to enable the maximum shear load to be transferred to the bond area without tensile failure in the wood away from the bond. The thickness must also be sufficient to prevent adhesive penetration right through the wood sample during the bond pressing; this would

interfere with bond formation. On the other hand, if near-isothermal conditions are to be reached quickly at the bond line (necessary for the above mentioned kinetics analysis), the adherend material must not be too thick. The adherend's thermal conductivity (or diffusivity) should therefore also be considered before selecting adherend sample thickness.

The overlap area used in ABES testing must be selected so that the loading capacity of the instrument is not exceeded when bonds are allowed to reach high levels of cure. When strong adhesive or well cured bonds are to be tested, a small overlap area is therefore preferred. In single lap joint tests, the effect of adherend geometry on the shear stress as considered by Goland and Reissner (1944), may expressed in the following way:

$$S_s = \sqrt{2\frac{G \cdot c^2}{E \cdot n \cdot t}} \qquad (1)$$

$$S_n = \sqrt[4]{\frac{3E_c \cdot c^4}{8 \cdot E \cdot n \cdot t^3}} \qquad (2)$$

Where:

S_s = shear stress concentration (Pa)

S_n = normal stress concentration (Pa)

G = adhesive shear modulus (Pa)

E = adherend tensile elastic modulus (Pa)

E_c = adhesive tensile elastic modulus (Pa)

c = overlap length (mm)

n = adhesive layer thickness (mm)

t = adherend thickness (mm)

The predicted variation of shear stress along the interface layer in the axial direction is parabolic (Figure 2.1). This is caused by material interactions imposed by the tensile load. Furthermore, a bending effect occurs within the joint due to its transverse asymmetry. The interaction of such forces can promote propagation of fracture from the ends of the overlap towards its center and thus cause premature catastrophic failure. These effects can mask the measurement of true shear strength values. All of the above factors were considered in the design of the test method used in the present study.

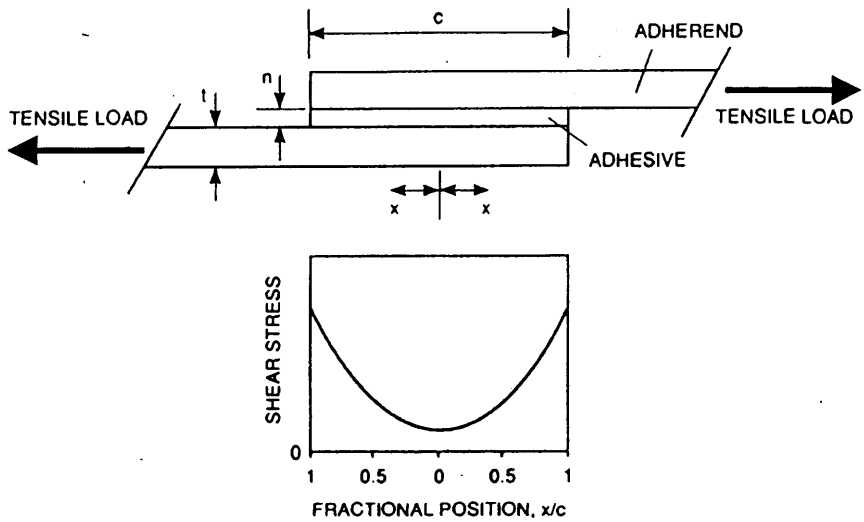

Figure 2. 1. Variation of lap shear stress at the interface area (Humphrey 1989).

Delamination Mode

The delamination because of fracture initiation and propagation modes may possibly be explained with Frank's seismic fault model. "The physics of propagation of shear cracks in the resin-rich material between plies in a laminate is not unlike that for the

propagation of shear cracks (earthquakes) in the crust and upper mantle of the earth" (Ashbee 1993). The concentric stress around the edges (both ends at the overlap area) at the interface zone must be large, and when the stress from both ends approach and meet each other and a larger stress concentration is formed. Those stress concentrations reinforced each other and a rapid release of elastically stored energy will cause fractures and it can undergo a catastrophic rapid growth delamination.

The effect of concentrated stress at the edges is detailed that 'the maximum shear and peel stresses are found at or near the boundary of the joints'. Since the composite material is made of adherends and adhesive, ' the maximum shear bond are higher in joints with non-identical material' and 'stiffer material carries greater portion of the loads' (Leichti *et al.* 1991).

These considerations are beyond the scope of the present work, however. Indeed, the main use of the ABES system is to explore the strength development of glue bonds. Most tests are therefore on bonds which are only partially cured. Under these conditions, the wood is likely to be significantly stiffer than the adhesive and stress uniformity will therefore be greater. Finite-element analysis is presently being applied to the test bond configuration. This is with a view to considering fracture mechanisms more fully. Still, all such analysis depends upon known adhesive layer thickness and elastic (or viscoelastic) properties. The glueline in wood joints are not, however, well understood. It is likely that it is of variable thickness (microscopically) and the adhesive penetrates the porous wood to create gradients in material properties through the bond. These gradient in properties almost certainly change as the adhesive penetrates and polymerizes during cure (Humphrey 1999).

In spite of the above complexity, the ABES testing method has been found to be a highly effective way of exploring adhesive bonding reactivity.

ELECTRO HEATING PROCESSES

Electrothermal technology separates the electrical heating process into two major categories (Orfeuil 1987) which may be termed 'indirect heating' and 'direct heating' methods. Each will be considered in turn.

Indirect Heating Methods

Indirect heating suggests a transfer of energy from a heat source to the heated object using a medium, such as water or oil. A common application using this method is the central heating in buildings where heated water is transported in a closed loop as an energy-transporting agent.

Resistance heating. - Indirect resistance heating is heating through a refractory wall as the medium and as the heat conductor. The energy source is electrical resistors that generate heat when currents flow through them. This method is used in resistance furnaces that can generate 600 to 700 ^{0}C.

Infrared radiation heating. - Infrared heating depends on energy transmission of electromagnetic radiation that is generated electrically from a radiation emitting source with wavelengths between 0.76- and 1000-μm. Infrared heating can perform localized heating with high accuracy and very high power density. This method is mostly used in the drying, heating, polymerizing and sterilization industries.

Plasma heating. - A plasma consists of matter (molecules or atoms) obtained by an ionizing gas; it consists of positively charged ions and negatively charged free electrons, which remains electrically neutral. Ionization is an electron separation process using very strong electric fields to break the valence bond. The ionized plasma is a good conductor. With a current flow in the gas stream, magnetic forces are generated and these contact the gas stream, and result in high increase of energy. Plasma heating is only used in very high thermal applications since it ranges from 2,000 to 50,000 ^{0}K for partially ionized plasmas. Plasmas with a high degree of ionization (thermonuclear fusion) can generate several million degrees Kelvin.

Direct Heating Methods

Direct heating is relatively common in electronic applications. In this process, heat is generated when the current flows through the object and releases energy. Many home appliances use this method.

Resistance heating. - The direct resistive method is similar with to indirect one, the only different is that there is no medium to transfer the heat. This direct resistance heating will be discussed in detail since it is used in the present work.

Induction heating. - In these methods, heating is obtained by placing a conductor in a variable magnetic field and is usually called electromagnetic induction (EMI) heating. Applying an alternating potential difference of frequency '*f*' in the coils generates a variable magnetic field inside and around the coils. When a conductor is inserted into the coil, a variation of magnetic fields creates magnetic flux passing the body and induces eddy currents (Dorf 1993, and Halliday 1974). The eddy current is then

converted into heat due to the Joule effect in a heating body. This system is usually run in 50-Hz to 10-MHz and often requires a huge power supply.

Dielectric heating (microwave and radiowave). - Dielectric heating is a successive distortion or polarization of a non-conductive material that is placed within alternating electric fields. The molecular distortion causes heating and it is also known as the dielectric hysteresis heating effect. This system runs in the 10- to 300-MHz radiowave band and 300- to 30,000-MHz microwave band, and requires a huge power supply.

Electron beam heating. - In the 1900's von Pirani discovered the electron-beam heating method where the kinetic energy of an electron beam is converted to heat when it strikes the targeted heated body. The mechanism of heating depends upon extracting the electrons from a surface (a cathode) in a vacuum chamber and providing them with kinetic energy by accelerating them in an electric field and then focusing them on the target. The speed of the electrons is in the order of 85,000 km/sec when an accelerating voltage of 20 kV is used. This method is mostly used in welding or melting special alloys and surface deposit coating.

Laser heating. - Laser heating (invented in the 1960's) uses a continuously releasing photon energy pulse with 0.6443-μm wavelength acting on a very small area. Using a bank of capacitors, the population of energy pulses can be increased and pumped into a large energy. The pulse is then concentrated in a crystal (often ruby and then called an optical solid state laser) or a semi-conductor material (and then called semiconductor solid-state laser). The focused and dense energy pulse comes out from the reflector tube through a narrow hole of a semi-transparent mirror and generates a laser beam. The light

emission energy (emission of photons) is created because of the change in the path of the electrons, which jump from their normal orbital position to a higher one (thermal for incandescent source) and attain an unstable equilibrium state. Upon their return to their original orbit, they release energy. This laser heating is used for high precision cutting, micro-machining, and special welding operations. Efficiency of around 10 percent is typical and a large power supply is therefore needed for most applications.

Electric arc heating. - Electric arc heating, found by Davy in 1880, is a heating method that uses current flow between two electrodes in an ionized gas environment. An incandescent cathode emits electrons, which move toward the anode due to the electric field existing between the electrodes. The electron flow through and encountered gas molecules ignite ionization due to the shock within the gas. This heating is used for example, in furnaces to produce steels. In such electric-arc-furnace, an electrode is submerged into the furnace chamber containing molten iron. Ions are accelerated by an applied electric potential and strike the cathode to generate heat in the vault. The heating can generate 3000 ^{0}C and requires a huge power supply when used in a furnace. It has, however, proven useful in a wide range of smaller applications, including arc welding.

Resistive Heating Methods

The electro-thermally-heated furnaces have been used since 1920. The principle of resistive heating depends upon *Joule's law* which states that *"any electrically conductive substance through which an electric current flows gives off heat"* (Orfeuil, 1987). From the *Ohm's law*, the relation between voltage (V), current (I), and resistance (R) in a closed circuit can be described as:

$$V = IR \qquad (1)$$

The power derived from the electric flow will follow equation:

$$P = VI = RI^2 = \frac{V^2}{R} \qquad (2)$$

Where:

P = power (W)

V = potential (V)

I = Current (A)

R = resistance (Ω)

Resistance is effectively a constant of proportionality between current and voltage and is a body or material property. Figure 2.2 illustrades the realizationship between the parameters of equation (2).

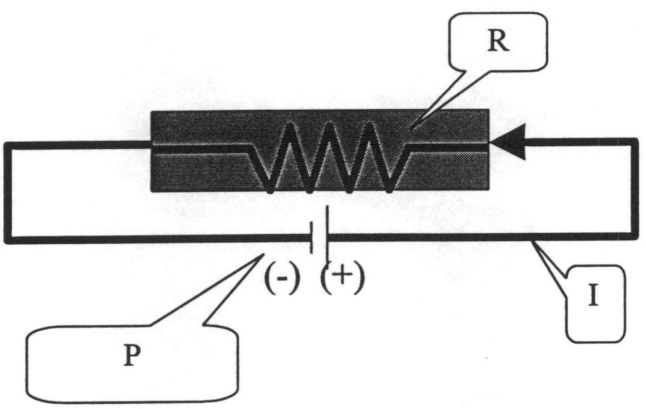

Figure 2. 2. Resistance heating principle.

When the electric power is applied for a certain period of time, the electrical energy converted into heat can be described as:

$$Q = Pt = RI^2t \qquad (3)$$

Where:

Q = heat flux (J)

t = time (sec)

To measure the energy emitted with an alternating voltage heating:

$$Q = \int_0^t VI \cdot dt \qquad (4)$$

This thesis only involves the use of direct current power supply, but if an alternating current power supply is used of phase angle φ with respect to the voltage, the active power P is equal to:

$$P = VI\cos\varphi \qquad (5)$$

Once the heating concept is proven in the present work with direct current, the use of alternating current will be explored. Conduction heating can use metallic or non-metallic materials, but it has to be a conductor of electricity. A conductive material is placed between two connections, where the potential is applied and the heat develops within the body. The heat generation is uniform if the resistivity and the cross-section are uniform and isotropic. In some cases, heat due to irregularity of material density and texture may cause temperature heterogeneity. This is the case in the present application where the CFRP is orthotropic and contact resistance may be high compared to the resistivity of the CFRP.

Uneven heating problems commonly occur in the contact area of the material junction between two different materials. Improper connection design can cause excessive local heating effects in the body.

Generally a conduction heating system requires the following:

- Electrical power supply
- Electrical control and regulation system
- Current input (contact) to heating material
- Appropriate resistive heating load

The advantages of conduction heating are as follow:

- High energy conversion with efficiencies often between 70 to 90 percent
- Very short heating times, with a high power density
- Flexible placement
- Inexpensive process.

The limitations of this method are:

- Allowable current at the contacts with the heating material is limited
- Uneven heating effect may occur when the material is anisotropic
- Frequency interference when operated at 50-Hz.

Most resistive heating studies have involved analysis of heat production, heat transfer, and heat utilization (absorption and efficiency). In this thesis, the characteristics of carbon fiber as a heat generator are studied.

Electrical Heating Method in Wood Products

In the 1960's a laminating process called 'Silverlam-process' was reported by Kootenay Forest Products Ltd. BC, Canada (Kootenay Ltd. 1964). This process involves the use of thin aluminum foil as a resistive heating element which is sandwiched between wood laminates (Western Hemlock, Douglas Fir, and Western Larch) at the glueline. The purpose of this method is to cure glue at the interface layers, by electrically heating the aluminum foil, in minutes to form a glulam product.

This Silverlam process offered an increase of productivity with rapid curing and a moderate endurance to the wet environment because of the thermoset resin. There is no record of any increase in composite strength using this method but the record states that the products pass the CSA 0122-1959 shear block test and CSA 0122-1959 delamination test. Beams up to 6.5-m (20-ft) were produced by this method. Indeed the tensile properties of aluminum foil are very low and more likely to represent a plane of weakness. There have also been concerns that the aluminum-to-wood bond is not as strong as that between wood and wood. Due to these concerns and the conservatism of the wood industry, this technology has not been adopted. This innovation in the present work does, however, offer greater promise since it combines resistive heating and reinforcement in the same component (the CFRP).

CARBON FIBER

Carbon Structure

Carbon fibers are made of carbon atoms, which are arranged in polynuclear aromatic hexagonal ring arrays that is shown in Figure 2.3. Hexagonal arrays are oriented

parallel to the "a" crystallographic axes. Illustration in Figure 2.4 shows that these arrays form sheets in the 'X-Y plane' direction and are called graphene layers, a honeycomb like structure. All the graphene layers are stacked in the 'C' crystallographic axis (Chung 1994).

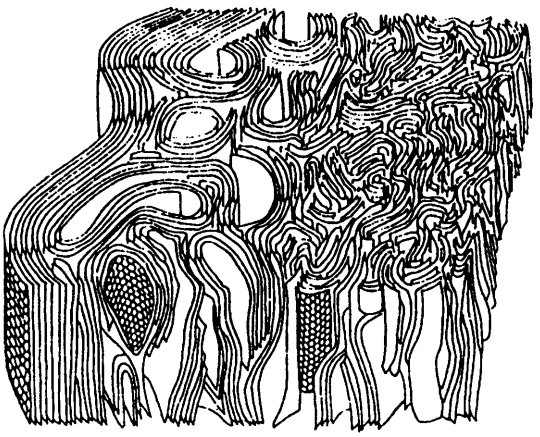

Figure 2. 3. Texture model of Carbon fiber showing skin-core heterogeneity (from Chung 1994).

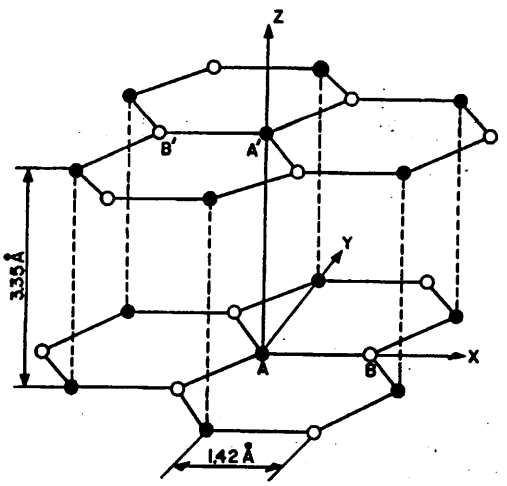

Figure 2. 4. The crystal structure of graphite or Graphene layers (from Chung 1994).

Illustration in Figure 2.5 shows that the C atoms in the graphite structure are in a sp^2 hybridized (planar-triangular of four C atoms formation that shows the central atoms is surrounded by three others with 120 ^{0} bond angle.

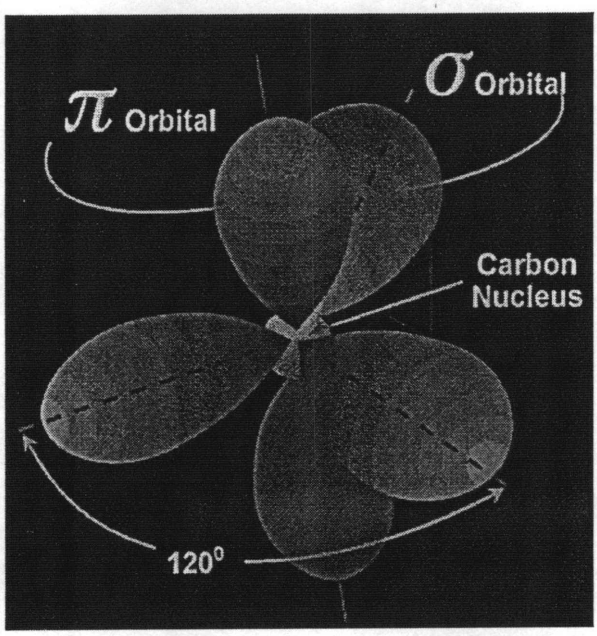

Figure 2. 5. Schematic version of sp^2 hybridized Carbon (Ashbury Carbon Ltd. 1996).

The C-atom within a layer ('X-Y'-plane) are bonded by (1) covalent bond, provided by the overlap of the sp^2 hybridized orbital and (2) metallic bonds provided by delocalization of the p^z orbital. This delocalization of the p^z orbital makes the graphite become a good thermal-electrical conductor. In the perpendicular direction, electrical field-type bond or Van Der Walls bonding is represented by 'Pi' (π) that has a 360^0 field of influence around its own carbon atom bond and provides the bond between the graphene layers. These 'Pi' bonds are weaker than the 'sigma' bonds. Two-dimensional

graphene layers of aromatic rings are stacked one to another parallel to the 'C' crystallographic axes. Each carbon in each benzene ring joints to three other carbon atoms through 'strong-covalent-bond', except the 'C' atom at the edge, illustrated in Figure 2.6.

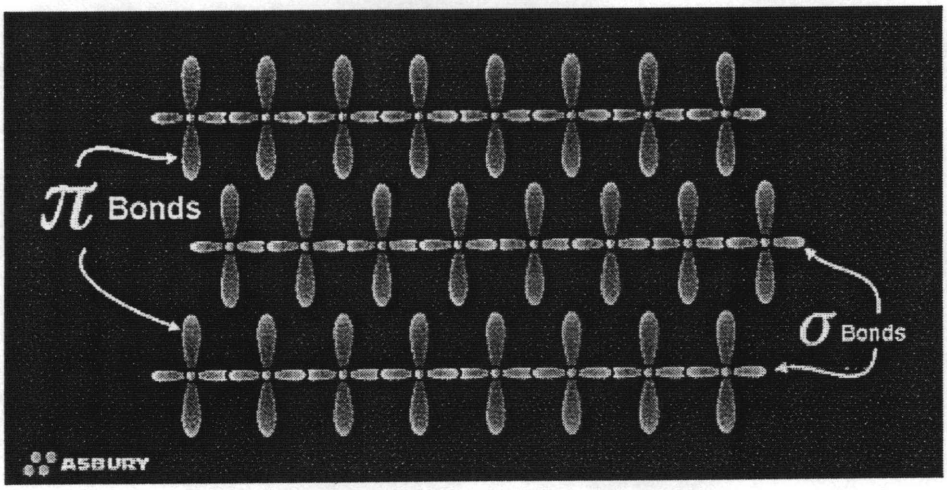

Figure 2. 6. Schematic representation of Pi bonding parallel to the 'a' plane of graphene (Ashbury Carbon Ltd. 1996).

Each graphene layer is held in a stacked arrangement by weak Van-Der Walls bonds, resulting from overlapping 'Pi' bond of the sp^2 carbon network, illustrated in Figure 2.7. The results of these two types of bonding can cause a high degree of anisotropy in different crystallographic directions.

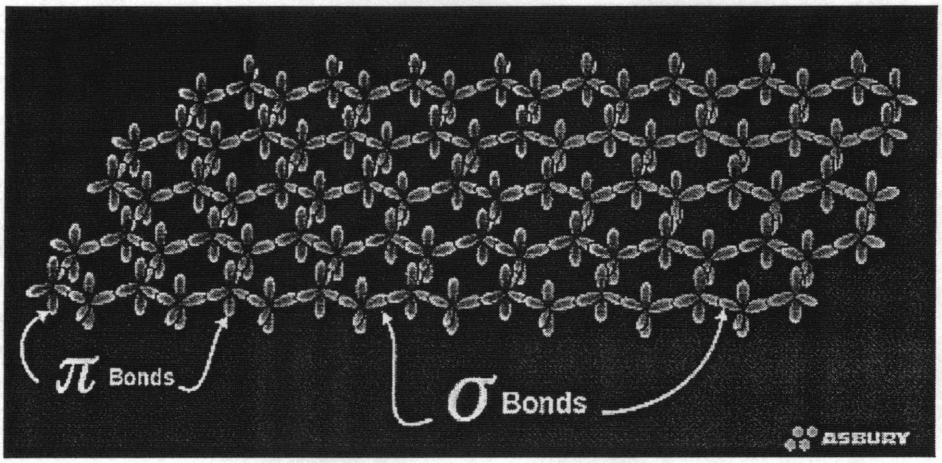

Figure 2. 7. Schematic representation of Pi bonding parallel to the 'a' plane of graphene in three dimension illustration (Ashbury Carbon Ltd. 1996).

Conductivity of Carbon Fiber

The electrical and thermal conductivity of carbon fiber have not been explored and published as extensively as the mechanical material properties. The resistivity of carbon fibers along the axis can be as low 15×10^{-8} Ωm at room temperature; this is almost as low as metallic materials such as pure silver or copper that have values in the order of 1.6×10^{-8} Ωm (Halliday 1988). However, when carbon fibers are embedded in a polymer matrix with 60 percent fiber volume fraction, the resistivity can significantly increase and reach value of 1×10^{-2} Ωm (Ashby 1994).

The thermal conductivity of carbon fiber is orthotropic. In the longitudinal direction the thermal conductivity is 650 to 1,100 W/mK and in the transverse direction it is 15 to 50 W/mK. The orthotropic behavior suggests that carbon fiber can function like a thermal pipe (Spicer *et al.* 1999).

The crystalline molecular form of carbon-graphite, with carbon attached in the x-y plane by covalent and metallic bonding, gives carbon fiber its good electrical and thermal

conductivity properties. In the direction perpendicular to the layers, Van Der Waals bonding provides the bonding between layers and gives thermal and electrical insulating properties to the material (Chung 1994). This makes carbon fiber a good electrical and thermal conductor along the fiber axis, and a good thermal insulator across the fiber axis.

Blaszkiewicz *et al.* (1992) studied the resistivity of carbon fiber embedded in a polymer matrix. Using general effective media computer modeling, they tried to simulate the resistivity and thermal conductivity of the carbon-polymer composite, based on the media theories (Lounder 1987). The carbon-polymer composite resistivity was found to depend on the volume fraction of the carbon fiber. As one would expect, the resistivity values of graphite-epoxy and carbon-epoxy composites are highly dependent on the fiber volume fraction and temperature applied.

At elevated temperatures, the resistivity of carbon-polymer composite increases, and a low filler volume fraction also will increase the resistivity. A low value of fiber volume fraction in the composite leads to a segregation of the fiber network inside the composite body. A high value of the fiber volume fraction can result in a random array of graphite flakes with many inter-fiber contacts. Studies near the critical fiber volume fraction suggest a reasonable linear relationship and correlation between resistivity and temperature.

Researchers tried to make a conductive polymer by mixing the carbon fiber into polyethersulfone with extrusion and injection molding at high temperature (Guoquan and Ping 1997). They found that a network of discontinuous carbon fiber (length = 2.00-mm) with a high fiber aspect ratio (length/diameter = 285) made an excellent conductive composite.

ELECTROPLATING

A major challenge in the present project concerned establishing an electrical connection with the CFRP. After careful consideration, electroplating was identified as a possible means of establishing such contact. Therefore, electroplating processes related to synthetic fiber were reviewed.

Many studies relating CFRP coating processes have been conducted since 1992. The purpose of these studies was to affect heating, enable current conduction, or to improve specific mechanical properties of the composites. Kim and Mai (1991) tried to coat aramid (Kevlar®) fiber and carbon fiber with polyvinyl-alcohol (PVA) to increase the transverse fracture toughness of the fibers by promoting interface bond between fiber to matrix. They found that coating the aramid and carbon fibers with PVA lead to enhanced fiber toughness that the brittleness was also increased. Embrittlement can lead to catastrophic failure when objects are subjected to impact loading.

Abraham and Satyanarayana (1992) tried to coat carbon fiber with copper and nickel by an electroless coating and cementation surface deposition technique. They used the electroless coating technique to deposit a copper layer onto the carbon fibers with a copper thickness up to 0.2-μm. This was done so that the copper would act as a coupling agent for the carbon fiber when it was embedded in an aluminum matrix. The copper and nickel layers on the carbon fiber enhanced the wettability of carbon fiber with molten aluminum. A metal layer on the fiber surface also prevented surface deposits of refractory materials on the carbon fiber and reduced the chemical reaction of the carbon fiber surface during wetting with molten aluminum. This research demonstrated that the use of an electroless-coating technique is feasible and that the coating does not reduce the

ultimate tensile strength of the fiber. However, cementation coating resulted in lower ultimate tensile strength values of the product. It was thought that surface discontinuities in the coating lead to stress concentrations and consequent fracture initiation.

Lin and Warrier (1993) studied the electroless silver coating of carbon fiber using a silver-nitrate solution when working on a project for the aerospace and electrical industries. They found that the rate of coating deposition and the coating thickness depended on the carbon fiber degree of graphitization. They found that the rate of the coating and the coating thickness depends on the carbon fiber degree of graphitization in Table 2.2. Their findings suggested that the PAN-based carbon fiber could not be electroplated.

Table 2. 2. Degree of graphitization (Lin and Warrier 1993).

Type of Material	Degree-Graphitization (%)
Pure Graphite	99.5
CVD fiber	95.9
Pitch	65.8
PAN	0

Specifications:

CVD fiber : Chemical Vapor Deposition (CVD), a carbon filament that is grown catalytically when a carbonaceous gas is in contact with small metal particles at elevated temperatures (from Chung 1994).

Pitch : A precursor of carbon fiber that is originally from coal or petroleum pitch obtained from the distillation of crude oil in a reduced pressure or by pyrolysis of naphtha, a by product of tar (from Chung 1994).

PAN : polyacrylonitrile (PAN) polymer is a precursor of Carbon fiber in the form of a textile fiber that is made by a pyrolysis in an inert atmosphere (from Chung 1994).

This Silver coating on carbon fiber protected the fiber when in high temperature environments and prevents the carbon from reacting with molten aluminum. Coating of carbon fiber also improves fiber surface wettability, and reduces of the viscosity of the molten aluminum matrix. The method can promote matrix infiltration in a pressureless process. A slight increase was gained in the UTS of coated carbon fiber when compared to the non-coated ones. This is likely due to the fact that the coating reduces the number and severity of surface defects.

CONCLUSION

Pitch-based CFRP with a high degree of carbon fiber graphitization is to be utilized to generate heat that also can cure the adhesive in a wood lamina with a resistive heating method. This material is a good reinforcement material in a composite, electroconductive, and available in a strip of cured unidirectional carbon fiber orientation. The conductivity of carbon fiber itself in longitudinal direction is better than in transverse direction.

When a CFRP plate will be used as a heating plate, a continuous direct contact of current from a power supply to individual unidirection carbon fiber is necessary. An electroplating method that can provide a contact surface for the wires to be soldered at both ends of CFRP strip can be used to connect the ends of carbon fiber in CFRP plate to contact the power supply.

Connecting the CFRP strip to a power supply and applying potential into the strip may cause heat generation because of the strip resistance itself.

REFERENCES

Abel-Majid, B., H. J. Dagher, and T. Kimball. 1994. The effect of composite reinforcement on structural wood. Infrastructure: New materials and methods of repair. American Society of Civil Engineers, p.: 417-424.

Abraham, S., B.C. Pai, and K.G. Satyanarayana. 1992. Copper coating on Carbon fiber and their composites with aluminum matrix. Journal of the Material Science (27): 3479 – 3486.

Ashby, M. 1994. Cambridge material selector 2.0 (CMS). Granta Design Ltd., Trumpington, Cambridge CB2 2LS, UK.

Asbury Carbons, Inc. 1966. P O. Box 144. Asbury, NY, 08802.

Ashkinazi, L.A. 1993. New opportunities for applicartion of carbon as a material for heaters, Pribory I Tekhnika Eksperimenta, n 3, May-Jun 1993, p 224-227

Ballinger, C. A. 1994. Specification needs for FRP composite products. Infrastructure: New material and methods of repair. Proceeding of the Third Material Engineers Conference in San Diego, CA, Nov 13-16, 1994, Published by American Society of Civil Engineers, (ASCE) 1852 p.: 56-63.

Barbero, E.J., J.F. Davalos, and U. Munipalle. 1993. Bond strength of FRP-wood interface. Journal of Reinforced Plastics and Composites, 13(9): 835-854.

Biblis, E. J. 1965. Analysis of wood fiberglass composite beams: Within and beyond the elastic region. Forest Products Journal 25(24): 81-88.

Blaszkiewicz, M., D. Mclachan, and R.Newnham. 1992. The volume fraction and temperature dependence of the resistivity in carbon black and graphite polymer composites: An effective media-percolation approach. Polymer Engineering and Science 32(6): 421-425.

Bohannan, B. 1962. Prestressing wood members. Forest Products Journal 12(12): 596-602.

Bulleit, M. W., B. L. Sandberg, and G. J. Woods. 1989. Steel reinforced glued laminated timber. Journal of Structural Engineering 115(2): 433-444.

Chung, D. D. L. 1994. Carbon fiber composites. Butterworth-Heinemann, Newton, MA.

Coleman, G. E. and H. T. Hurst. 1974. Timber structures reinforced with light gage steel. Forest Products Journal 24(7): 45-53.

Cooper P.A., and J.W. Sawyer. 1979. A critical examination of stresses in an elastic single lap joint. NASA, Langley Res Cent, Hampton, Va, Source: NASA Technical Paper n 1507. p:58.

Davalos, J. F. and E. J. Barbero. 1991. Modelling of glass-fiber reinforced glulam beams. International Timber Engineering Conference London, UK, p.:3.234-3.241.

Davalos, J.F.; H. V. S. Ganga Rao S. S. Sonti, R. C. Moody, and R. Hernandez. 1994. Bulb-T and glulam-FRP beams for timber bridges. Proceedings of the Structures Congrees '94, Apr 24-28 1994. Sponsored by: ASME, Published by ASCE. p: 1316-1321.

Dailey, T. H. Jr. 1995. Hybrid composites: Efficiency utilization of resources by enhancement of traditional engineered composites with pultruded sheets. In proceeding of the Composites Institute's 50th Annual Conference and EXPO'95, Cincinnati, OH.

Dorf, R. C. 1993. The electrical engineering handbook. CRC Press, Inc. Boca Raton, Florida, FL, 33431.

Guoquan, W. and Z. Peng. 1997. Electrical conductivity of poly (vinyl chloride) plastisol-short carbon fiber composite. Polymer Engineering and Science 37(1): 96-100.

Erdogan, F., and M. Ratwani. 1971. Stress Distribution in Bonded joints. Journal of Composite Materials, 1971(5): 378-393.

Fink, B. K., R. L. Mccullough, and J. W. Gillespie Jr. 1992. Local theory of Heating in Cross-Ply Carbon Fiber thermoplastic Composites by Magnetic Induction", University of Delaware, Newark, Delaware. Polymer Engineering and Science 32(5): 357 – 369.

Galligan, P.E. 1999. Personal references. 5223 Verda Line NE., Salem, Oregon, 97303.

Gardner, G. P. 1991. A reinforced glued laminated timber system. International Timber engineering Conference London p.: 3.295-3.300.

Gardner, D. J., J. F. Davalos, and U. M. Munipalle. 1994. Adhesive bonding of pultruded fiber-reinforced plastic to wood. Forest Product Journal 44(5): 62-66.

Goland, M. and E. Reissner. 1994. The stresses in cemented joints. Journal of Applied Mechanic, 1994 (1): A17-127.

Halliday, D. and R. Resnick. 1988. Fundamentals of Physics. Third Edition. John Willey & Sons, Inc. NY

Humphrey, P. E. and S. Ren. 1989. Bonding kinetics of thermosetting adhesive system used in wood-based composites: the combined effect of temperature and moisture content. Journal Adhesion Science Technology 3(5): 397-413.

Humphrey, P. E. and Zavala, D. 1989. A technique to evaluate the bonding reactivity of thermosetting adhesives. Journal of Testing and Evaluation. JTEVA 17(6): 323-328.

Kim, J., and Y. Mai. 1991. Effect of interfacial coating and temperature on the fracture behaviors of unidirectional kevlar and carbon fiber reinforced epoxy resin composites. Journal of Material Science, 1991(26): 4702 – 4720.

Kirlin, C.P. 1996. Experimental and finite-element analyses of stress distributions near the end of reinforcement in partially reinforced glulam. Masters thesis. Oregon State University, Corvallis, OR.

Kootenay Forest Products Ltd. 1964. KFP Silverlam products, Post and beam. Bulletin no. 1. CMHC Acceptance no. 4501. Nelson, British Columbia, Canada.

Lantos. G. 1970. The flexural behavior of steel reinforced laminated timber beams. Wood Science 2(3): 136-143.

Lin, R. Y., and S.G. Warrier. 1993. Silver coating on carbon and SiC fibers. Journal of Material Science, 1993(28): 4868 – 4877.

Leichti, R. J. and Groom, L. H. 1991. Influence of adhesive stiffness and adherend dissimilarity on stress distributions in structural finger joints. Adhesive and Bonded

Lounder, R. 1987. Electrical transport and optical properties of inhomogeneous media. American Institute of Physics Conference Proceedings, No. 40, P. 2. American Institute of Physics, New York, NY.

Mark, R. 1961. Wood-aluminum beams within and beyond the elastic range. Part I: Rectangular sections. Forest Products Journal 11(10): 477-484.

Mark, R. 1963. Wood-aluminum beams within and beyond the elastic range. Part II: Trapezoidal sections. Forest Products Journal 13(11): 508-516.

Moulin, G.P. and P. Jodin. 1990. FGRG: Fiberglass reinforced glulam, a new composite. Wood Science and Technology (24): 289-294.

Mufti, A. A. 1992. Pultrusion process in manufacturing of FRP-wood composite beams. Technical Bulletin University of Nova Scotia Halifax, Nova Scotia, Canada.

Orfeuil, M. 1987. Electric process heating. Technology/Equipment/Applications. Battelle Press, Columbus, OH.

Rowlands, R. E., R. P. Van Deweghe, T. L. Laufenberg, and G. P. Krueger. 1986. Fiber-reinforced wood composites. Wood and Fiber Science, 18(1): 39-57.

Saucier, J. R. and Holman, J. A. 1975. Structural particleboard reinforced with glass fiber-progress in its development. Forest Products Journal 25(9): 69-72.

Sliker, A. 1962. Reinforced wood laminated beams. Forest Products Journal 12(12): 91-96.

Smulski. S. and Ifju, G. 1987a. Creep behavior of glass fiber reinforced hardboard. Wood and Fiber Science 19(4): 430-438.

Smulski. S. and Ifju, G. 1987b. Flexural behavior of glass fiber reinforced hardboard. Wood and Fiber Science 19(3): 313-327.

Spaun, F. D. 1981. Reinforcement of wood with fiberglass. Forest Products Journal 31(4): 26-33.

Spicer, J., D. Wilson, and R. Osiander. 1999. Evaluating of high thermal conductivity graphite fibers for thermal management in electronics applications. Proceeding of SPIE-The International Society for Optical Engineering v 3700. Apr 6-Apr-8 1999. Society of Photo Instrumentation Engineers: 40-47.

Tingley, D. A. and R. J. Leichti. 1994. Glued Laminated beams having a high-strength fiber-reinforcement: The bi-material interface. In: Proceeding of the Pacific Timber Engineering Conference. Gold Coast, Australia. Vol. 2:665-675.

Volkersen O. 1938. Rivet strength distribution in tensile-stressed rivet joints with constant cross section. Luftfahrtforsch (15): 14-47.

Wangaard, F. F. 1964. Elastic deflection of wood-fiberglass composite beams. Forest Products Journal 14(6): 256-260.

CHAPTER 3

CARBON FIBER AS A RESISTIVE HEAT GENERATOR TO ACCELERATE ADHESIVE CURE IN REINFORCED WOOD LAMINATES. PART I: CHARACTERIZING THE HEATING EFFECT.

J. Liem*, R. J. Leichti[+], and P. E. Humphrey[+]

*Graduate Research Assistant and [+] Associate Professors,

Department of Forest Product, Oregon State University

119 Richardson Hall, Corvallis, OR, 97331

For Submission to Wood and Fiber Science

ABSTRACT

As a result of its atomic structure, carbon fiber produced from mesophase pitch has a high electrical conductivity and high tensile strength. Others have used carbon fiber as a resistive heating unit to accelerate matrix solidification in carbon fiber-polymer matrix composites.

In this study, a unidirectional carbon-fiber-reinforced-polymer (CFRP) strip was laminated with wood as reinforcement. It was hypothesized that the high conductivity of carbon fiber could be used in a low voltage circuit to generate heat to cure thermosetting adhesive at the interface layer.

The CFRP strip was a unidirectional composite of carbon fibers (9-μm diameter) in a 60 percent carbon fiber volume fraction. The polymer matrix was an epoxy. Due to the carbon fiber alignment and its molecular structure, the thermal-electrical properties of the CFRP strips were orthotropic.

To connect the electrical circuit to the CFRP strip, the ends of the strip first were electroplated with copper. It was found that a tapered end-geometry and low power density combined with a long period for electroplating resulted in a porous copper deposition which was advantageous for subsequent solder connection.

The heating characteristics of CFRP were investigated by using thermocouples mounted in the interface between CFRP and wood samples. It was found that the circuit could produce approximately 34 percent energy conservation efficiency. Measurements showed that the CFRP strip heated quite uniformly over its length. It was concluded that CFRP could be effectively connected to low-voltage electrical circuit and used as a

resistive heater. Adhesion kinetics associated with such heating are described in a companion paper (Liem *et al.* in preparation (b)).

Keywords: carbon fiber, CFRP, wood laminates, electroplating, resistive heating.

INTRODUCTION

The success of synthetic fiber reinforcement in glulam beams and other wood-based engineered composites has opened opportunities for enhanced utilization of wood fiber. Decreased access to wood fiber and changes in the quality of lumber have driven studies to improve utilization and provide alternative fiber sources that will meet the future demands of structural applications.

The production processes of synthetic fiber-reinforced wood, e.g., glulam, use phenol resorcinol formaldehyde (PRF) adhesives and cold clamping. This manufacturing process requires eight hours or more of clamped time for adhesive cure. To facilitate increased production of reinforced glulam products, a process is needed that will accelerate adhesive cure.

The common synthetic fibers used in fiber-reinforced plastic (FRP) materials are made from aramid, E-glass, and carbon. The aramid and E-glass fibers are sometimes used alone, but carbon fiber alone is not common. This is because the price for carbon fiber is greater than the alternatives. However, only the carbon fiber has good electrical and heat conductivity and the potential to be used as a resistive heat generator. Studies by others (Sancaktar *et al.* 1993, van den Nieuwen *et al.* 1994, and Ramakrishnan *et al.* 1998) have demonstrated the use of carbon fiber to accelerate reactions of polymer

matrix materials. It is here hypothesized that an FRP lamina of carbon fiber could be used as a resistive heater to accelerate the adhesive reactions in glulam production.

OBJECTIVES

The objective of this project was to modify a carbon-fiber reinforced polymer (CFRP) strip so that it may function as a resistive heating element and then assess both the heat uniformity and efficiency of the CFRP strip. In order to develop the CFRP resistive heating element, it was necessary to connect the CFRP strip to an electrical circuit. Thus, there were three objectives:

- To create electrical contact surfaces at the ends of CFRP strips;
- To connect CFRP strips to an electrical circuit;
- To characterize the heating uniformity and heating efficiency of the CFRP strips.

TECHNICAL BACKGROUND

Carbon Fiber Conductivity

The electrical and thermal conductivity of carbon fiber have not been explored and published as extensively as have their mechanical material properties. The resistivity of carbon fibers along their axis can reach 15×10^{-8} Ωm at room temperature; this is almost as low as metallic materials such as pure silver or copper that have values in the order of 1.6×10^{-8} Ωm (Halliday, 1988). However, when carbon fibers are embedded in

a polymer matrix with 60 percent fiber volume fraction, the resistivity can significantly increase and reach value of 1×10^{-2} Ωm (Ashby, 1994).

The thermal conductivity property of carbon fiber is orthotropic. In the longitudinal direction the thermal conductivity is 650 to 1,100 W/mK and in the transverse direction is 15 to 50 W/mK. The orthotropic behavior suggests that carbon fiber can function like a thermal pipe (Spicer *et al.* 1999).

The crystalline molecular form of carbon-graphite, with carbon attached in the x-y plane by covalent and metallic bonding, gives the material its good electrical and thermal conductivity properties. In the direction perpendicular to the layers, Van Der Waals bonding provides the bonding between layers and imparts thermal and electrical insulating properties to the material (Chung 1994). This makes carbon fiber a good electrical and thermal conductor along the fiber axis, and a good thermal insulator across the fiber axis.

Blaszkiewicz *et al.* (1992) studied the resistivity of carbon fiber embedded in a polymer matrix. Using general effective media computer modeling, they tried to simulate the resistivity and thermal conductivity of the carbon-polymer composite, based on media theories (Lounder 1987). The carbon-polymer composite resistivity was found to depend on the volume fraction of the carbon fiber. As one would expect, the resistivity values of graphite-epoxy and carbon-epoxy composites are highly dependent on the fiber volume fraction and temperature applied.

At elevated temperatures, the resistivity of carbon-polymer composite increases, and a low filler volume fraction also will increase the resistivity. A low value of fiber volume fraction in the composite leads to a segregation of the fiber network inside the

composite body. A high value of the fiber volume fraction can result in a random array of graphite flakes with many inter-fiber contacts. Studies near the critical fiber volume fraction suggest a reasonable linear relationship and correlation between resistivity and temperature.

Some researchers have tried to make a conductive polymer by mixing carbon fibers into polyethersulfone using extrusion and injection molding techniques at high temperature (Guoquan and Ping 1997). They found that a network of discontinuous carbon fiber (length = 2.00 mm) with a high fiber aspect ratio (length/diameter = 285) made an excellent conductive composite.

Carbon Fiber as a Heat Generator

Sancaktar *et al.* (1991) investigated electrical-resistive heating using a single graphite fiber to cure an epoxy matrix. The heating characteristics and results seemed to be similar to heating via convective thermal post curing.

Ramakrishnan *et al.* (1998) consolidated a thermosetting-matrix composite by embedding conductive carbon mats within the matrix. The carbon mats that were embedded inside the composite and were used to generate resistance heat. The carbon mats provided sufficient temperature to enhance curing uniformity throughout the composite cross-section.

Nakanishi and Hayashi (1992) have made a composite laminate from carbon fiber papers and epoxy resin. By stacking and hot pressing four laminae of carbon fiber paper (with 5 percent carbon fiber volume fraction) with an alternating or direct current, they

were able to easily heat the lamination and cure the laminates. This finding demonstrated that the carbon fiber paper could be a good plane heater.

Creating a Metal Contact on the CFRP

A major challenge in the present project concerned establishing an electrical connection with the CFRP. After careful consideration, electroplating was identified as a possible means of establishing such contact. Therefore, electroplating processes related to synthetic fiber were reviewed.

Many studies relating CFRP coating processes have been conducted since 1992. The purpose of these studies was to affect heating, enable current conduction, or to improve specific mechanical properties of the composites. Kim and Mai (1991) tried to coat aramid (Kevlar®) fiber and carbon fiber with polyvinyl-alcohol (PVA) to increase the transverse fracture toughness of the fibers by promoting interface bonds between fiber and matrix. They found that coating the aramid and carbon fibers with PVA led to enhanced fiber toughness. Embrittlement can lead to catastrophic failure when objects are subjected to impact loading.

Abraham and Satyanarayana (1992) tried to coat carbon fiber with copper and nickel by an electroless coating and cementation surface deposition technique. They used the electroless coating technique to deposit a copper layer onto the carbon fibers with a copper thickness of up to 0.2-μm. This was done so that the copper would act as a coupling agent for the carbon fiber when it was embedded in an aluminum matrix. The copper and nickel layers on the carbon fiber enhanced the wettability of carbon fiber with molten aluminum. A metal layer on the fiber surface also prevented surface deposits of

refractory materials on the carbon fiber and reduced the chemical reaction of the carbon fiber surface during wetting with molten aluminum. This research demonstrated that the use of an electroless-coating technique is feasible and that the coating does not reduce the ultimate tensile strength of the fiber. However, cementation coating resulted in lower ultimate tensile strength values of the product. It was thought that surface discontinuities in the coating lead to stress concentrations and consequent fracture initiation.

Lin and Warrier (1993) studied the electroless silver coating of carbon fiber using a silver-nitrate solution when working on a project for the aerospace and electrical industries. They found that the rate of coating deposition and the coating thickness depended on the carbon fibers degree of graphitization. Their findings suggested that the PAN-based carbon fiber could not be electroplated.

Kulkarni *et al.* (1979) used cementation technique to deposit metals (copper, nickel, and cobalt) on carbon fiber. The method used vacuum heating of the carbon fiber at 700 ^{0}C for about 15 minutes and then suspending them in an aqueous solution of metal (copper, nickel, and cobalt) salt. This contained glacial acetic acid and additional displacing agent (ferro, magnesium, aluminum, and zeng). The metal was displaced from the solution to the carbon fiber and the thickness of the coating depended on the metal-salt and surface activation (glacial acetic acid) solution concentration.

Shiota and Watanabe (1974) used an electroplating technique to nickel coat yarns and sheets of carbon fiber. A uniform and compact nickel deposit layer was formed by tensioning the yarn and controlling the current density in the electrolyte bath. Takato *et al.* (1976) found the adhesive force of an electroplated copper layer on a CFRP plate with 60 percent fiber volume fraction could be increased by increasing the roughness of the

substrate surface or by chemical pretreatment. Johnson and Browning (1990) used an electrochemical technique to copper and nickel coat the carbon fiber. The thick metal coating was used as a diffusion barrier to protect the carbon fiber from degradation at high temperatures. This electroforming was used mostly to fabricate inexpensive and strong electro-magnetic induction (EMI) shielding.

Bavarian *et al.* (1990) used a chemical vapor-deposition technique to deposit ternary hafnium-silicon-carbon compounds on a carbon-carbon composite which is usually used for rocket nozzles, re-entry shields for space vehicles, brake disks, and heating elements. Ordinary carbon-carbon composite only has oxidation resistance in the range of 500 to 600 ^{0}C. Coating the carbon-carbon composite with ternary hafnium-silicon-carbon compounds improved the composite's oxidation resistant up to 1900 ^{0}C under cyclic heating and cooling in air conditions.

Many of the cited studies have provided evidence that it may be possible to use the CFRP as reinforcement in the composite material as well as a heating element to expedite the manufacturing process.

MATERIALS AND METHODS

To use the CFRP for resistive heating, the CFRP must conduct electrical current. The carbon fiber is orthotropic, is of 9-μm diameter, and is embedded in a polymer-matrix when used as a CFRP. Therefore, an attachment between the CFRP and the electrical circuit was needed. Early bench tests with CFRP strips and mechanical clamps with metal paste greases to enhanced contact demonstrated that mechanical clamping

would not provide adequate electrical contact. It was decided that connection would be most efficient if the connection could be solder attached. Thus, a method was needed to electroplate the ends of the CFRP. With electroplated ends, a solder connection is possible. Then the efficiency and heating characteristics of the CFRP strip could be assessed.

Electroplating Process

Three conditions were assessed to determine the electroplating results. The geometry of the acceptor material was identified as a potentially important feature. In addition, the electrolyte acidity and current density are known to have an affect on metal deposition.

Shaping the deposit area. - CFRP strips, 270 × 20 × 1.03 mm, were shaped into either of two end geometries: square or tapered as shown in Figure 3.1.

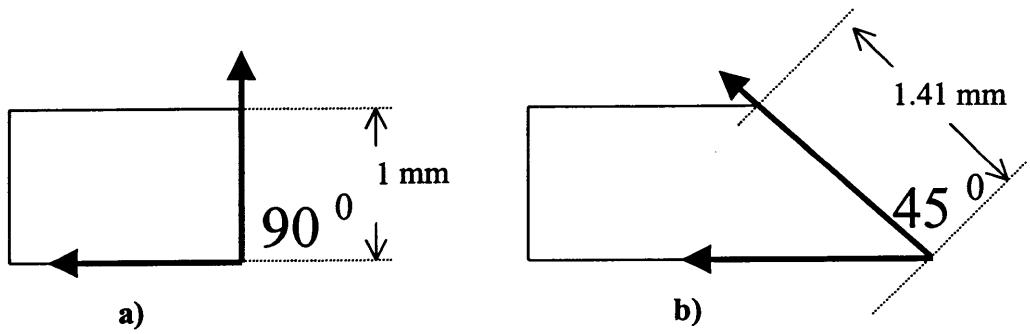

Figure 3. 1. CFRP end geometry; a) square-end sample, area = 20 mm^2, and b) tapered-end sample, area = 28.2 mm^2.

The prepared ends were cleaned by dipping them into a 50 percent ethanol solution and rinsing with clean water. The cleaned CFRP samples were dried using a blower to remove particulates and evaporate the residue. Masking tape was used to cover the lateral surfaces of the CFRP strip so that only the square-end or tapered-end surface would be exposed to the electroplating process.

The electroplating solution. – Electroplating processes for copper and nickel are fully described by Parthasaradhy (1989). The metal donors in electroplating processes are copper, chromium and silver. However, the copper electrolyte solution is the least expensive, and copper is a good conductor. Therefore, a strip of copper plate 200 × 6.33 × 0.69 mm was used as the metal donor.

The metal ions from the donor material are deposited on an acceptor material, which in this case was a strip of CFRP. It was made of carbon fiber (60 percent fiber volume fraction with epoxy matrix) produced from a pitch precursor with 66 percent graphitization. The resistivity value was 1×10^{-2} Ω.m (Ashby, 1994), and the thermal conductivities were 650 to 1,100 W/mK longitudinally and 15 to 50 W/mK transversely. The CFRP strips were 270 × 20 × 1 mm.

The electrolyte solution was produced by diluting 24 g of crystal cupric sulfate ($CuSO_4 \bullet 5H_2O$) into 100-ml water at room temperature in a large beaker. Then, 3 ml of 95 to 98 percent H_2SO_4 was added. The pH of the $CuSO_4$+H_2SO_4 solution was 0.7. This was stirred for 15 to 20 minutes using a remote stirrer/hot-plate. When the electrolyte was ready, it was stored in a sealed container to prevent moisture loss.

Electroplating process. - The electroplating apparatus is illustrated in Figure 3.2. After the electrolyte was ready, the metal donor and the CFRP strip were suspended in the electrolyte solution.

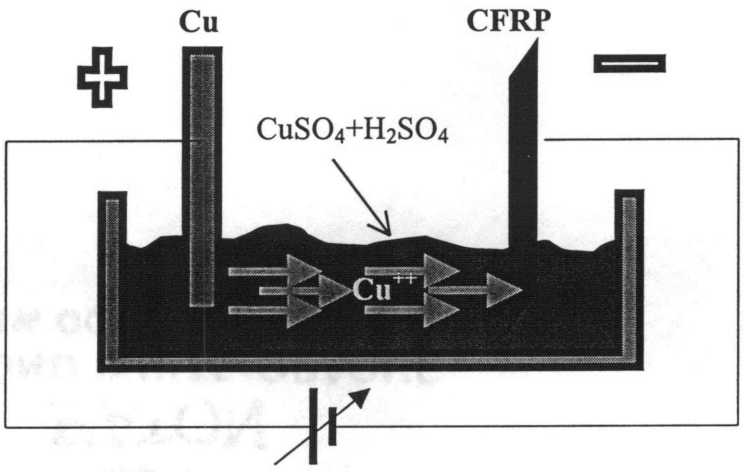

Figure 3. 2. Schematic of the electroplating apparatus.

The donor copper strip was connected to the positive pole of the power supply with a metal clamp, and the CFRP strip was clamped with aluminum bars as shown in Figure 3.3. The bars were connected to the negative pole of the power supply. When all of the connections were fixed, the electroplating process was started by applying the potential to the donor and acceptor.

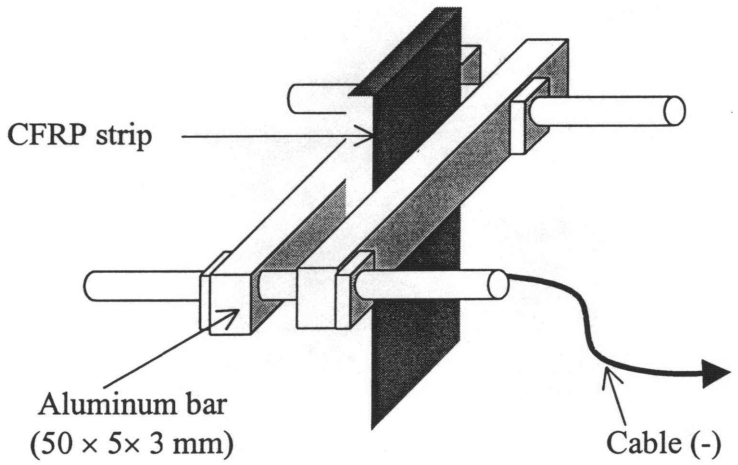

Figure 3. 3. Connection to the CFRP strip for the electroplating process.

Applied current density. - When applying the potential, the current density should not to exceed 0.16 mA/mm^2 (Parthasaradhy 1989). Based on the area of the sample and the current density, square-end CFRP samples with 20 mm^2 area were electroplated by applying a maximum current of either 32 mA or 6 mA (0.03 A/mm^2). Tapered-end CFRP samples had an area of 28.3 mm^2 and were electroplated receiving the maximum current supply of 45 mA or minimum current density 8.4 mA.

A copper deposit having a thickness of 25 μm to 50 μm was considered sufficient to carry the expected current in the heating application (Parthasaradhy 1989). Based on Faraday's Law of Electrolysis (Parthasaradhy 1989), the fastest recommended plating duration of the square-end CFRP sample, where area was 20 mm^2 and maximum current 32 mA, was determined by:

Volume of copper deposited $= Area \times thickness$

$= (1 \times 20 \text{ mm}) \times 25 \times 10^{-3} \text{ mm}$

$$= 0.5 \text{ mm}^3.$$

Weight of deposited material = *Volume* × *density*

$$= 0.5 \text{ mm}^3 \times 0.00892 \text{ g/mm}^3$$

$$= 4.46 \times 10^{-3} \text{ g}$$

Using Faraday's law of electrolysis:

$$W_g = 4.46 \times 10^{-3} g = \frac{It}{96{,}500} \times \frac{A_g}{z} = \frac{0.032 \times t}{96{,}500} \times \frac{63.54}{2}$$

$$t = \frac{4.46 \times 10^{-3} \times 96{,}500 \times 2}{0.032 \times 63.54} = 421.15 \text{sec} \cong 7 \text{min}.$$

Where:

I = current (A)

A_g = atomic weight of Copper (g/mole)

t = time (sec)

W_g = metal deposit weight (g)

Z = valence or charge (copper = +2)

It was calculated that the square-end CFRP strip would need approximately 7 minutes with maximum current density (32 mA) and 37 minutes at the minimum current density (6 mA). For the tapered-end samples, the electroplating process would need 10.5 minutes with maximum current density (45 mA) and 40 minutes with minimum current density (8.4 mA). The electroplating progress was assessed by macro- and-micro- scopic inspection at 5, 10, 15, 30, and 45 minutes to assess the distribution and the microstructure of deposited copper during the electroplating process.

Electrical Circuit Connection

The copper leads (18 gauge) to the electrical circuit were soldered to the electroplated ends of the CFRP strips. To facilitate a good solder result, the copper plated ends were prepared by rinsing them with clean water and drying. Then the copper plated surfaces were degreased, activated with flux, and the CFRP was soldered to the power supply wires. Figure 3.4 illustrates the electrical connection.

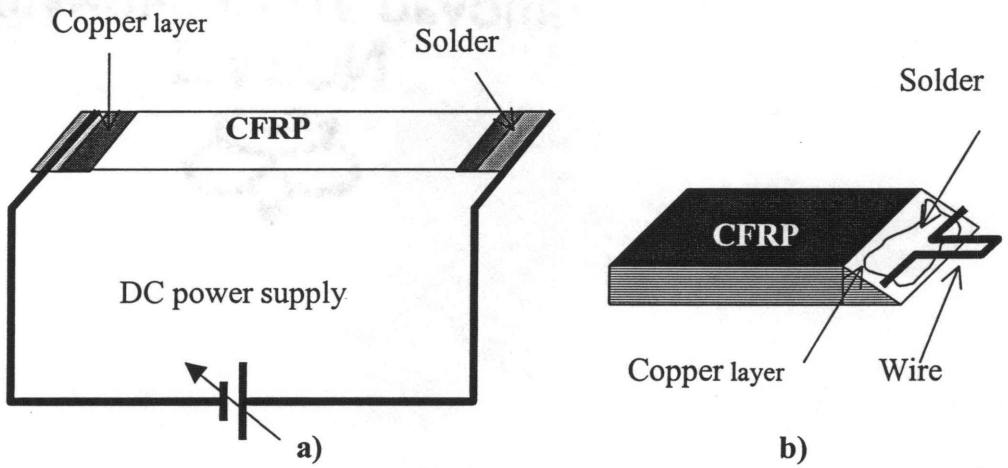

Figure 3. 4. A schematic showing the connection between the CFRP strip and the electrical circuit; a) circuit connection, and b) detail of the wire-to-CFRP connection showing the electroplated area.

Characterizing CFRP Heat Generation and Efficiency

Temperature distribution on the CFRP surface. - This study was conducted to explore the temperature profile of CFRP heating in a wood composite product. Thermocouples were used to explore the temperature distribution on an CFRP strip that was inserted between two alder (*Alnus rubra spp.*) wood laminae. The alder laminae were at ambient conditions and had an 8 percent moisture content.

Figure 3.5 illustrates the thermocouple alignment on the centerline of the CFRP strip between the two wood laminae. Ten T-type thermocouple was used on ten locations representing the entire length of CFRP surface. The results were records of interfacial temperature distribution during heating at 5 V. A data logger was used to record the temperature on the CFRP every 5 seconds until the CFRP surface temperature reached 100 ^{0}C.

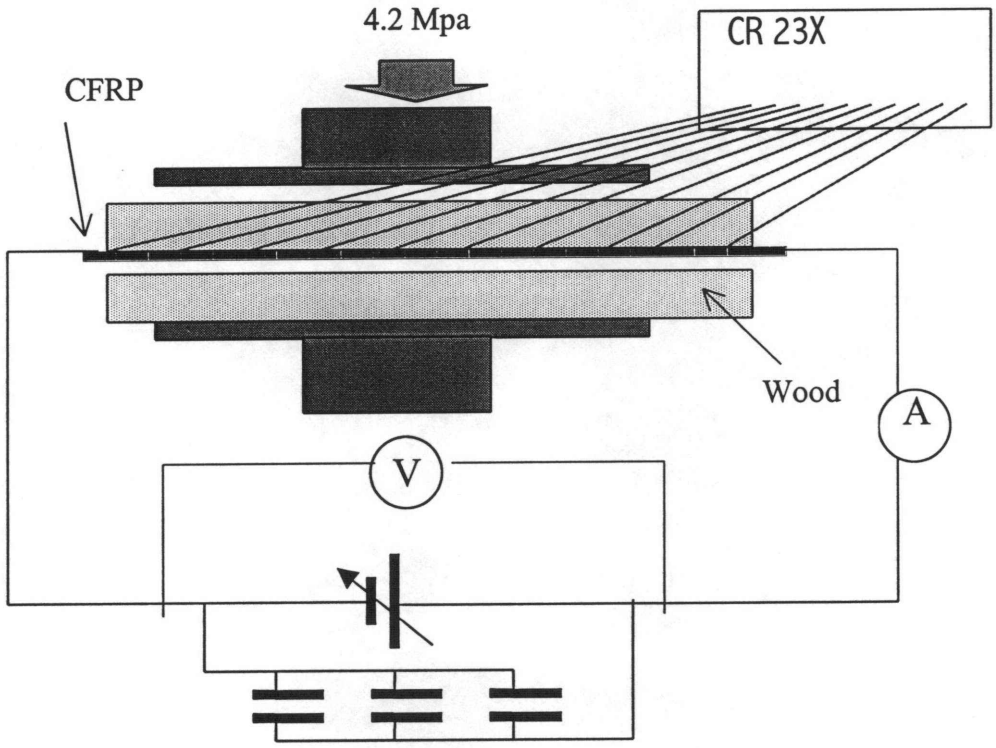

Figure 3. 5. Measuring temperature distribution at CFRP interface during the resistive heating process when the CFRP was between two wood laminae.

Rate of heating generation. – This study was conducted to determine the rate of heat generation given certain power inputs values. For the rate of heating measurements,

the heating was controlled by regulating current flow. The circuit used a variable DC power supply with capacity of 35 V and 12 A. The heating circuit shown in Figure 3.6 had two parallel loops; one loop included the CFRP strip and the other incorporated a set of non-polarized capacitors 12,000-pF, which were used to filter out 60-Hz noise.

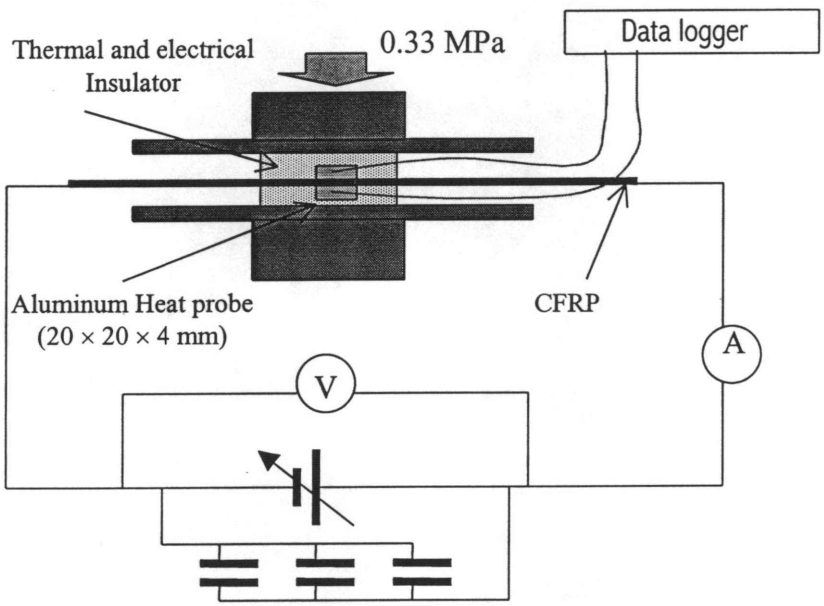

Figure 3. 6. Measuring energy generation on the CFRP surfaces.

Two specially designed heat probes, made from T-type thermocouples embedded in aluminum blocks inserted into the center of separate aluminum blocks, were used to measure heat generation from the CFRP surface. The aluminum blocks were 20 × 20 × 4 mm, and they were placed in direct contact with the CFRP surfaces at the center of the CFRP strips. The center of the CFRP strip was used as a measurement site because it was expected to have the slowest heating response. An insulation pad (70 × 70 × 50 mm) was placed over both aluminum heater probes and the surface of the CFRP. A hydraulic press

illustrated in Figure 3.6 was used to simulate the pressure that would exist during manufacturing of a laminated product, such as glulam. The manual hydraulic press was set up to press the CFRP sandwich at 0.33 MPa.

A data logger was used to record the heating data. The data logger was programmed to read room temperature, two thermocouples, voltage and current at 1-sec intervals. A separate voltmeter and ammeter were used to visually monitor the power supply during the heating test. Figure 3.6 illustrates the test apparatus including the heat probes, insulation pads, circuits, and clamping pressure.

Heating efficiency. - The purpose of this study was to measure the efficiency of the heat generation on the CFRP surface. The efficiency of CFRP to convert electrical power into heat used a fixed electrical power of 10 W to heat the CFRP.

The heating efficiency test was conducted by repeating the "rate of heating test" five times at different positions along the CFRP surface. Figure 3.7 shows the sequential measurement sites. The insulation around the heat probes and pressure were as described in the 'rate of heating test'.

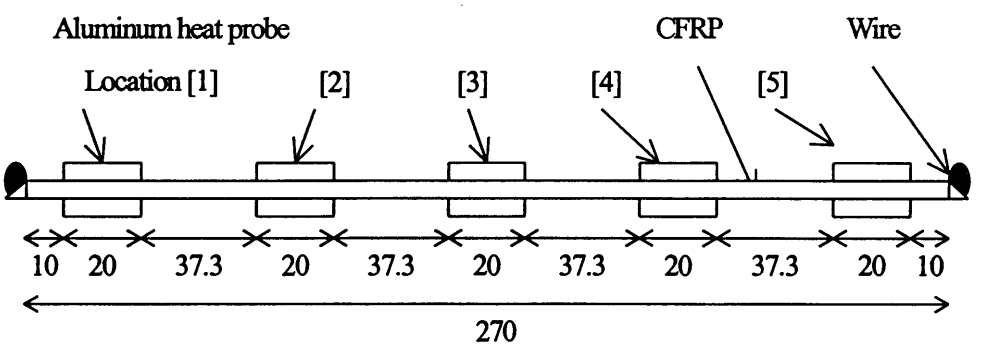

Figure 3. 7. Heat probes measurement positions.

RESULT AND DISCUSSIONS

Effect of Electroplating Parameters

End shape. - The result of electroplating specimens with each end shape was evaluated during and at the end of the process. Square-end CFRP strips required more time for electroplating than predicted. The square-end geometry minimized the carbon fiber exposure to the electrolyte solution. As a result, the copper deposit was poor. Macroscopic examination during the electroplating was sufficient to observe the inadequate results. Therefore the square-end geometry was dropped from the study.

Tapered-end CFRP samples were electroplated more successfully. The electroplating duration was close to the predicted time, which was approximately 30 minutes. These results showed that the tapered-end geometry offered enough exposed carbon fiber that the copper could be successfully deposited. Thus, only tapered-specimens were used in subsequent heat rate and heat uniformity tests.

Current density. - The copper deposit on the electroplated surface can be described as either porous or smooth. The copper plating results in $CuSO_4$+H_2SO_4 electrolyte with tapered-end CFRP sample shapes that were subjected to two different current densities applied were observed.

High current density (0.16 mA/mm^2) produced a thick and smooth copper layer. Under 1000 times magnification, it was possible to observe copper grains on the ends of an individual carbon fiber. Eventually, the grains bridged together forming a thick, smooth, and dense copper layer.

The low current density (0.03 mA/mm^2) produced a porous copper deposit on the CFRP strip. At the low current density, the copper deposit formed a spiral-branched network of copper on the tips of carbon fibers.

Electrical Circuit Connection

To maximize the performance of CFRP as a resistive-heating strip, low resistive lead wire (18 gauge, 0.00033 Ω.m) was used. A mechanically strong and low resistance intermetalic connection between the copper layer and the wire can be formed by soldering. However, for a liquid material to attach to a solid surface, the liquid must effectively wet the surface.

A high temperature solder (370 ^0C) was used to make solder connection. However, because the glass transition of the epoxy matrix in the CFRP was around 125 ^0C, the allowable wetting time for the soldering alloy was very short. Therefore, the copper surface was tinned with solder droplets. A contact time longer than a quick touch usually caused the copper plate to peel off of the CFRP strip. Flux and rosin agents helped to facilitate wetting and had to be used to achieve the solder connection. The character of the copper deposit also influenced the soldering process. The thick and smooth copper deposit layer had a surface wetting problem when the solder was applied, the copper-layer tended to peel off. High temperature of solder above 125 ^0C melted the matrix beneath the copper layer and caused the copper deposit to detached from the carbon fiber.

The porous copper layer was more tolerant to soldering. The high temperature solder did not disturb the porous copper deposit. In the porous copper structure, the

copper deposit was attached to the ends of carbon fibers and was not in direct contact with matrix surface. The carbon fibers conducted the heat away from the heat source and prevented the matrix from melting and peeling. The porous copper structure also allowed the solder to flow into the porous structure providing a mechanical connection to the CFRP. This finding suggested that the porous copper deposit structure was more tolerant to soldering and should be used for subsequent studies.

The resistance of the connected CFRP sample results was 0.06 Ω for the 270 mm strip with 28.2 mm^2 end area. It is desirable for resistivity to be low so that the CFRP heats with minimum energy requirements but still the resistivity of the CFRP must be greater than that of the circuit wires or else the wire will heat up rather than the CFRP. It was found that the resistivity of the circuit wires was 0.00033 Ω.m, and when the total length of wire was considered, then the resistance of the wire circuit was 0.00132 Ω. This resistance value was lower than the 0.06 Ω measured for the CFRP.

Ashby (1994) reported the resistivity of carbon fiber as 10 to 3.98×10^{-3} Ωm and the resistivity of the epoxy was 1×10^{19} to 1×10^{21} Ωm. The measured value of 0.06 Ω (in a sample size of 270 × 20 × 1 mm) or 900 Ωm for the CFRP is an expected intermediate value close to the 10 Ωm reported by Ashby (1994).

Others (Phelan et al. 1992 and Chen et al. 1994) have shown a resistance is created by interface of dissimilar materials, and this contributes to the apparent resistance of the CFRP and large difference relative to carbon fiber.

Characterizing CFRP Heat Generation and Efficiency

Temperature distribution in the CFRP plate. – The main purpose of resistive heating is to accelerate the curing of an adhesive in the interface layer of CFRP/wood surfaces. The data in Figure 3.8 shows that end heating was different than in the middle of the strip. It is thought that the contact resistance of dissimilar materials and some measurement errors might cause these observations. However, these demonstrate that CFRP resistive heating method may be able to produce a uniform heat across the CFRP surface inside the laminates.

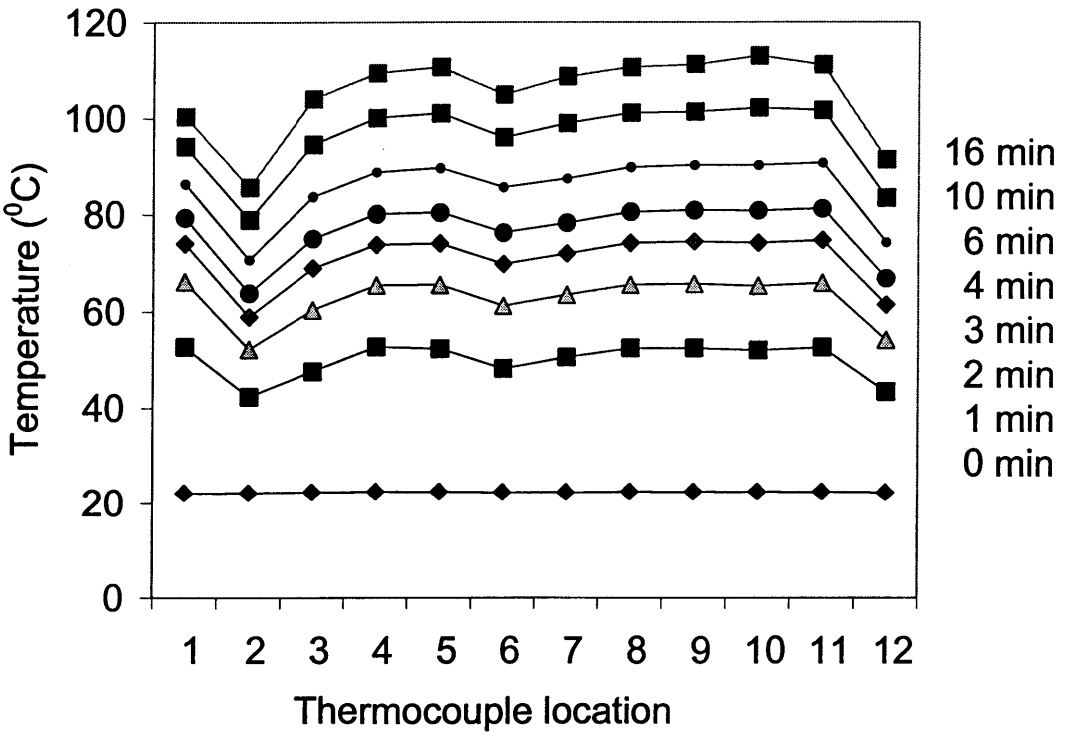

Figure 3. 8. CFRP resistive heating distribution inside the CFRP/woods laminate.

Rate of heating. - The CFRP resistive heating has a linear heat development in response to the power input. The illustration in Figure 3.9 shows the effect of power input into CFRP plate in four minutes. Temperature rise in the first 10 sec was slow but then increased with time. This shows that temperature in the CFRP strip is a function of both time and power.

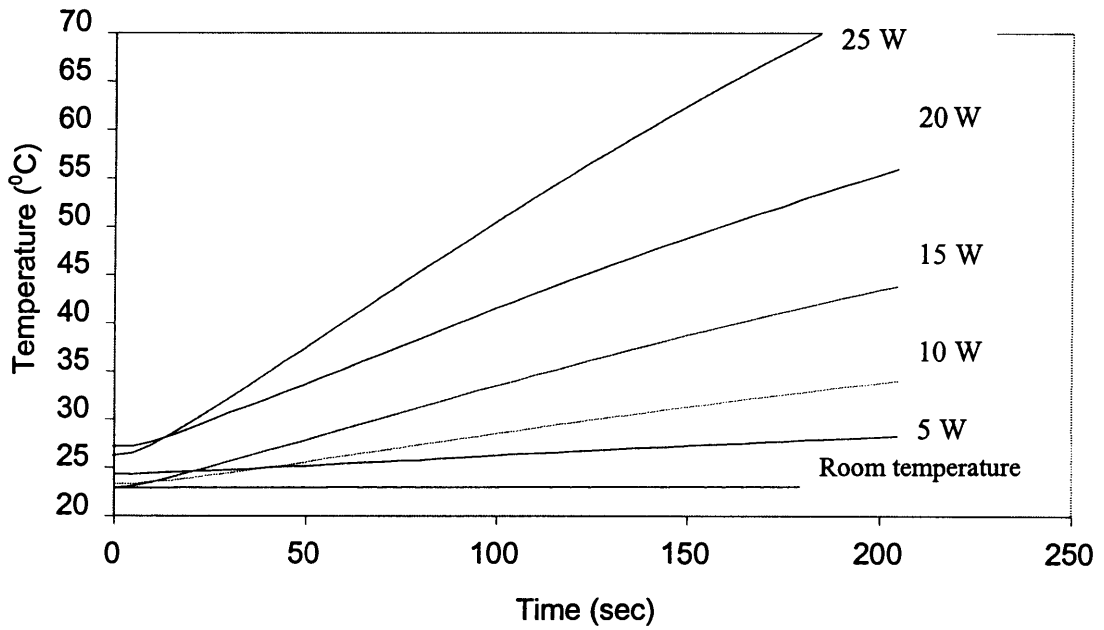

Figure 3. 9. CFRP surface temperature readings measured for up to 200 seconds at five power levels.

The information in Figure 3.9 was used to determine the heating rate, and the power density (W/m^2) for the CFRP strip was calculated for each of the power levels. Figure 3.10 shows the heating rate as a function of power density. It is seen that there is a linear relationship between power density and heating rate. This relationship would be used to calculate the time required achieving given temperature, given power and size

criteria. For example, if the CFRP was to provide resistive heating to 100 ^{0}C and the strip was 270 x 20 mm and 15 W of power was provided, then the time required would be 500 sec. This would be an important calculation with respect to adhesive kinetics.

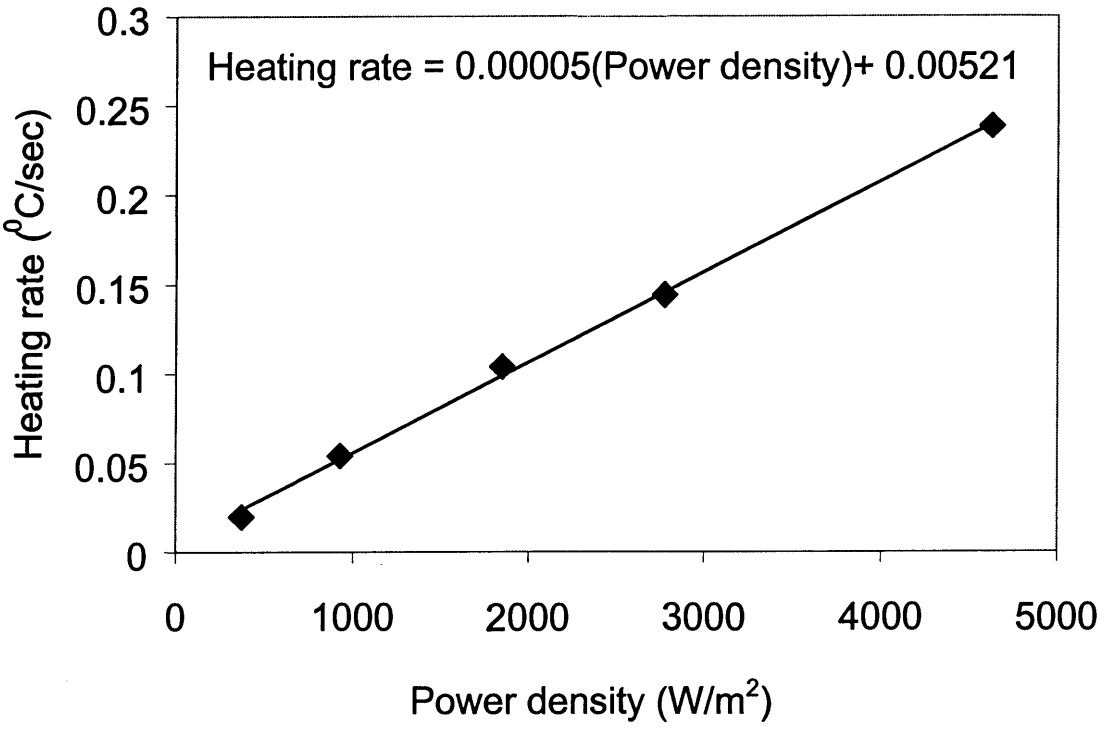

Figure 3. 10. Rate of heating CFRP resistive heating method.

Heating efficiency. - The temperature development illustrated in Figure 3.11 shows uneven distributions on the CFRP surface. The lines represent temperatures at the measurement sites over a 3-min heating period. The chart shows that the ends of CFRP strip tend to have higher temperature than the middle part of the strip. It is thought that some of the temperature differential from site-to-site was caused by the partial insulation; covering the whole sample would have improved this data.

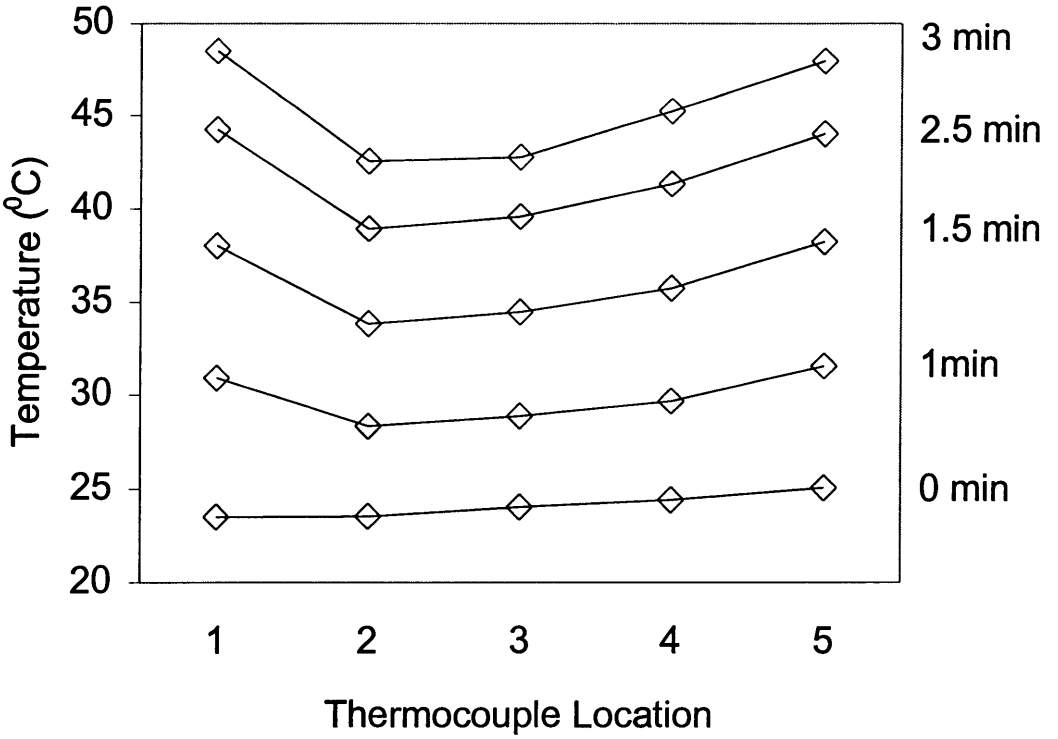

Figure 3. 11. Temperature development at several locations on 270 × 20 × 1 mm CFRP at 10 W power input and amperage of 0.7 amps.

A fixed power at 10 W and 0.7 amps was input to the CFRP strip and temperature readings at 30-sec intervals were recorded. As much as both surfaces of CFRP generate the same amount of energy, only the results from one CFRP surface was used for calculating the energy heating efficiency. Small amount of CFRP sample and the difficulty to achieve low resistance wired CFRP strip have prevented us to reproduce more sampling. The heat energy loss from the edge of the strip was ignored. Given the specific heat capacity of aluminum, the heat energy from the CFRP strip was calculated using the equation (2):

$$W = \frac{Q}{t} = c \cdot m \cdot (T_f - T_i) \qquad (2)$$

Where:

W = energy (W)

Q = heat (1 j = 0.239 cal)

t = time (180 sec)

c = specific heat capacity of aluminum (900 J/kg ^{0}K)

m = aluminum mass (0.00439 kg)

T_i = initial temperature (296 ^{0}K)

T_f = final temperature (T/C$_1$=320.5 ^{0}K, T/C$_2$=314.8 ^{0}K, T/C$_3$= 315.3 ^{0}K, T/C$_4$ =317.3 ^{0}K, T/C$_5$= 320.2 ^{0}K)

The results of equations were used with the surface area of the CFRP strip to calculate the energy density (W/m^2). The energy density results were plotted with position and a best fit third degree polynomial was fitted as shown in Figure 3.12. The total heat generation from CFRP was determined integrating the area under the curve line of equation (4).

$$W_o = \int_{0.27}^{0} (-132774\ x^3 + 72993\ x^2 - 11118\ x + 1529\ )dx \qquad (4)$$

Where:

W_o = CFRP energy generation (W)

x = length (m)

The integration result for heat generation from one CFRP surface was 310 W/m^2, and therefore, 620 W/m^2 of heat were generated from both CFRP surfaces. When the thin piece of CFRP with an area of 5400 mm^2, the heat generation from both side of CFRP sample was 3.4 W. Because these were 10 W input to the CFRP sample, the efficiency of CFRP heating was 34 percent.

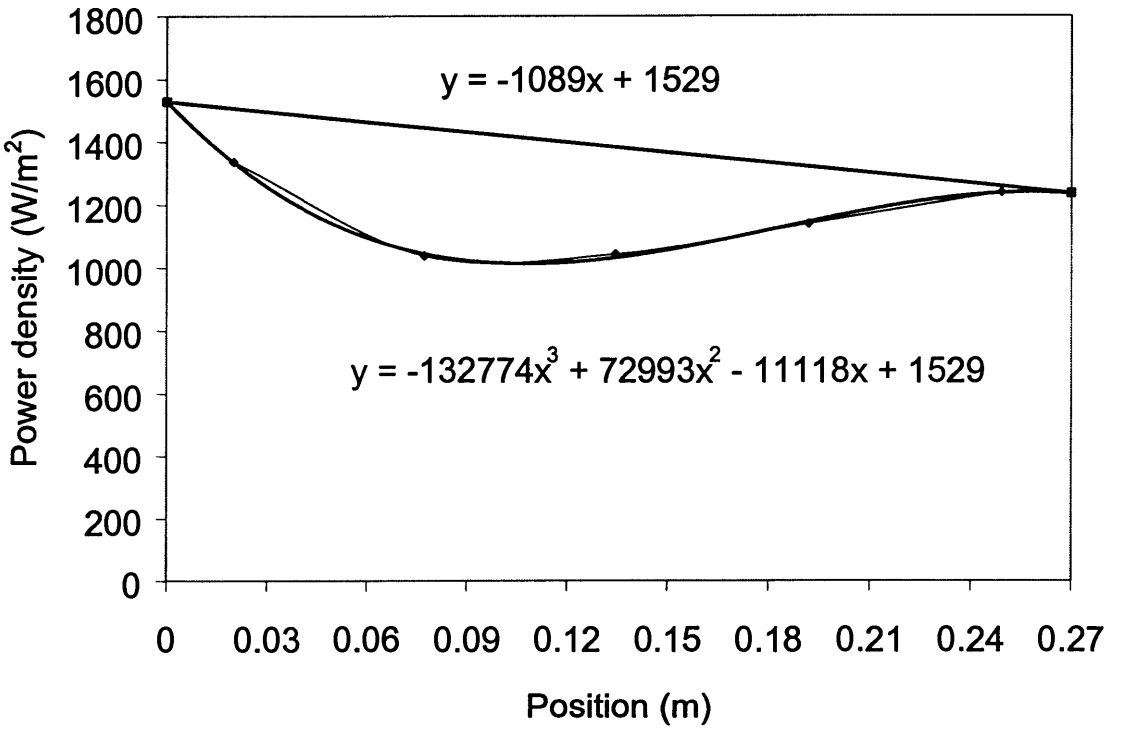

Figure 3. 12. Heating efficiency of CFRP (curve) and correction line (linear).

Under ideal conditions, the heat generation would be nearly a linear line with a higher heat generation at the positive pole then sloping down to the negative pole over the surface of the CFRP strip. The Kirchhoff loop rule requires that the potential into a junction must equal the potential leaving the junction (Halliday 1988). However, the

imperfect insulation and resulting heat loss lead to the nonlinear results of equation (3). To estimate the effect of heat loss on the heating efficiency, a corrected energy line was constructed by connecting the ends of the Position-Power density curve in Figure 3.12. The corrected heating efficiency was obtained by integrating equation (4):

$$W_i = \int_{0.27}^{0} [-1089x + 1528]dx \qquad (4)$$

Where:

W_i = corrected CFRP energy generation (W)

x = length (m)

The efficiency of the corrected heating, in a thin plate was 373 W/m^2 on each surface or 746 W/m^2 for both CFRP surfaces. With a 10 W power input the sample CFRP with 5400 mm^2 area the heating conversion was 4 W, thus the heating efficiency was 40 percent. This was compared to the result of equation (3), which was 34 percent, and therefore there was a 6 percent heat energy loss during the test.

CONCLUSIONS AND FUTURE STUDIES

CFRP can be used as reinforcement in glulam and wood composites. However it may serve a role in the production process if mechanism capable of providing heat to accelerate adhesive kinetics is developed. The CFRP can be used as a resistive heater. Success of CFRP as a heating element greatly depends on the connection to the electrical circuit. It was shown that the CFRP could be electroplated at the ends. A porous copper

circuit. It was shown that the CFRP could be electroplated at the ends. A porous copper deposit on CFRP ends provided good solder site and conductivity. In this case, a connected CFRP strip had a resistance of 0.06 Ω.

The heat generated from CFRP was quite uniform along the surfaces, although the temperatures were lower at the ends than in the middle of the CFRP strip. The energy needed to generate heat in the CFRP was relatively low and had an energy conversion efficiency of about 34 percent.

The result of this preliminary study led to additional research questions related to:

- The time period required for adhesive to development bonding strength using the CFRP resistive heating method;
- Predictions for guidance to achieving optimum heating results with CFRP resistive heating;
- The practicalities of using CFRP in trial laminates.

These issues will be addressed in a companion paper (Liem *et al.* in preparation (b)).

REFERENCES

Abraham, S., B.C. Pai, and K.G. Satyanarayana. 1992. Copper coating on Carbon fiber and their composites with aluminum matrix. Journal of the Material Science (27): 3479 – 3486.

Ashby, M. 1994. Cambridge material selector 2.0 (CMS). Granta Design Ltd., Trumpington, Cambridge CB2 2LS, UK.

Ashkinazi, L.A. 1993. New opportunities for application of carbon as a material for heaters. Pribory I Tekhnika Eksperimenta (3): 224-227.

Bavarian, B., V. Arrieta, and M. Zamanzadeh. 1990. Chemical vapor deposition of HF/SI compounds as a high temperature coating for carbon/carbon composites. National SAMPE Symposium and Exhibition (Proceeding) v 35 pt 2. April 1990. SAMPE: 1348-1362.

Blaszkiewicz, M., D. Mclachan, and R.Newnham. 1992. The volume fraction and temperature dependence of the resistivity in carbon black and graphite polymer composites: An effective media-percolation approach. Polymer Engineering and Science 32(6): 421-425.

Chen, Z.K., and S. Koichiro. 1995. Polarity effect of unisymmetrical material combination on the arc erosion and contact resistance behavior. Electrical Contacts, Proceeding of the Annual Holm Conference on Electrical Contact. Oct 17-19 1994. IEEE IEEE: 79-88.

Chung, D. D. L. 1994. Carbon fiber composites. Butterworth-Heinemann, Newton, MA.

Guoquan, W. and Z. Peng. 1997. Electrical conductivity of poly (vinyl chloride) plastisol-short carbon fiber composite. Polymer Engineering and Science 37(1): 96-100.

Halliday, D., and R. Resnick. 1988. Fundamentals of Physics.Third edition. John Willey & Sons Inc., New York, NY.

Johnson, C., and M. Browning. 1990. Status of electrocomposites Proceeding of the . American Electroplaters and Surface Finishers (AESF) Annual Technical Conference. July 9-12 1990. American Electroplaters and Surface Finishers Soc. Inc., 1203-1226.

Kim, J., and Y. Mai. 1991. Effect of interfacial coating and temperature on the fracture behaviors of unidirectional kevlar and carbon fiber reinforced epoxy resin composites. Journal of Material Science (26): 4702 – 4720.

Kulkarni, A., N. Balasubramanian, and B. Pai. 1979. Cementation technique for coating carbon fibers. Journal of Materials Science 14(3): 592-598.

Liem, J., R. J. Leichti, and P. E. Humphrey. in preparation (b). Carbon fiber as a resistive heat generator to accelerate adhesive cure in reinforced wood laminates. Part II: Characterizing wood-to-reinforcement bonding kinetics. Masters thesis. Oregon State University, Corvallis, OR.

Lin, R. Y., and S.G. Warrier. 1993. Silver coating on carbon and SiC fibers. Journal of Material Science (28): 4868 – 4877.

Lounder, R. 1987. Electrical transport and optical properties of inhomogeneous media. American Institute of Physics Conference Proceedings, No. 40, P. 2. American Institute of Physics, New York, NY.

Nakanishi, Y., and Y.Hayashi. 1992. Preparation of composite materials from carbon fiber paper and those several properties, Journal of the Textile Machinery Society of Japan 45(7): T101-T106.

Parathasaradhy, N.V. 1989. Practical Electroplating Handbook. Prentice Hall, Englewood Cliffs, NJ.

Phelan P.E., O. Nakabeppu, K. Ito, K. Hijikata, T. Ohmori, and K. Torikoshi. 1992. American Society of Mechanical Engineers, Heat Transfer Division, HDT v 200. Aug 9-12 1992. ASME Heat Transfer Div: 63-69.

Ramakrishnan, B., L. Zhu., and L. van der Shuur. 1998. Accelerated curing using supplemental internal resistive heating. International SAMPE Symposium and Exhibition (Proceeding) v 43 n 1. May 31-June 4 1998. SAMPE 243-253.

Sancaktar, E., W. Ma, and S. Yurgartis. 1991. Electric resistive heat curing of the fiber-matrix interphase in graphite/epoxy composites. American Society of Mechanical Engineers, Design Engineering Division (30): 127-137.

Shiota, I., and O. Watanabe. 1974. Continuous uniform nickel electroplating on carbon fibers. Nippon Kinzoku Gakkaishi/Journal of Japan Institute of Metals 38(9): 788-794.

Spicer, J., D. Wilson, and R. Osiander. 1999. Evaluating of high thermal conductivity graphite fibers for thermal management in electronics applications. Proceeding of SPIE-The International Society for Optical Engineering v 3700. Apr 6-Apr-8 1999. Society of Photo Instrumentation Engineers: 40-47.

Takato N., O. Maeda, and N. Yamada. 1976. Electroplating on plastic material reinforced with carbon-fibers and properties of the plated layer. Journal of Society of Material Science, Japan/Zairyo 25(279): 1153-1158.

Nieuwenhuizen, V.D., S.C. Robin, and A.K. Miller. 1994. Full insitu consolidation of thermoplastic matrix carbon fiber composite materials using direct electrical heating. American Society of Mechanical Engineers, Material Division (12): 29-41.

CHAPTER 4

CARBON FIBER AS A RESISTIVE HEAT GENERATOR TO ACCELERATE ADHESIVE CURE IN REINFORCED WOOD LAMINATES. PART II: CHARACTERIZING WOOD-TO-REINFORCEMENT BONDING KINETICS.

Liem J.*, P. E. Humphrey[+], and R. J. Leichti[+]

*Graduate Research Assistant and [+] Associate Professors,

Department of Forest Products, Oregon State University,

119 Richardson Hall, Corvallis, OR, 97330

For Submission to Wood and Fiber Science

ABSTRACT

The compatibility of carbon (CFRP) and E-glass (EFRP) fiber reinforced polymer-to-wood bonding with phenol resorcinol formaldehyde (PRF) and phenol formaldehyde (PF) adhesives has been explored. Of particular concern was the effect that temperature had on isothermal strength development rates. This is because the objective was to predict strength development with time of resistively heated bonds in CFRP reinforced glulam beams.

In order to evaluate the responsiveness of PRF bond-strength development rates to temperature, miniature adhesive bonds were formed and tested under a range of time and temperature conditions using the Automated Bonding Evaluation System (ABES). Isothermal strength development with time was linear in the early stages of bond formation, and the effect of temperature on regressed isothermal strength development rates followed an exponential relationship for both wood-CFRP and wood-EFRP adherend combinations. Maximum bond strengths at 100 ^{0}C reached approximately 3 MPa. Bond strengths up to 4.5 MPa were gained when PRF adhesive-to-wood test bonds were rapidly cooled to room temperature after pressing hot, but before pulling.

Tests with PRF adhesive failed to produce viable bonding results. This was probably because of temperature limitations.

An algorithm using numerical methods of integration and CFRP-PRF bonding kinetics data was established, which enables bond strength development to be predicted under changing temperature conditions. This may be used as a tool to select how much energy and pressing-time is needed to reach optimum bond strengths when making reinforced glulam beams using resistive heating.

Keywords: Wood laminates, reinforcement, carbon fiber, resistive heating, adhesion kinetics.

INTRODUCTION

Replacing one percent of the wood in structural glued laminated beams (glulam) with fiber reinforced polymer (FRP) has been found to greatly increase beam stiffness and strength. Such reinforcement may enable low wood grades to be utilized to make high performance beams (Davalos and Barbero 1991, Sonti 1995). However, bonding between the dissimilar materials in the glulam must be efficient if the potential of the products is to be realized. Therefore, the compatibility of wood-adhesive-FRP needs to be explored. Furthermore, production speed of beams is presently limited by the need for prolonged clamping in order that the room temperature curing adhesive develops sufficient strength to hold the glulam together upon release. Increasing bonding speed could therefore also increase production efficiency and thus add to the economic viability of fiber reinforcement.

A method of making reinforced glulam products which uses an electrical resistive heating method with carbon fibers and thermosetting adhesive has been reported in the companion paper (Liem *et al.* in preparation (a)). The present paper concerns the rate and magnitude of adhesion between wood and CFRP associated with the heating.

In order to evaluate the responsiveness of adhesive-adherend combinations to temperature, miniature adhesive bonds were formed and tested under a range of time and temperature conditions using the Automated Bonding Evaluation System (ABES). ABES is a laboratory desktop device in which lap-shear bonds are formed under highly

controlled conditions of temperature, pressure and time, and immediately thereafter tested in tensile mode. Provision is made for rapid heat transfer to gluelines. This instrument already has been successfully used to study the bonding kinetics of diverse adhesive (including urea formaldehyde, phenol formaldehyde and urathene) and adherend test sample types (Humphrey and Zavala 1989, and Humphrey 1999). The instrument enables strength development to be explored for a range of times under near-isothermal temperature conditions. This procedure may be repeated for a range of temperatures. The effect of temperature on isothermal bonding rate may therefore be investigated. Such information will, in this present study, enable links between electrical heating parameters and resultant strength development in trial beams to be established.

The compatibility and performance of bonding fiber-reinforced polymer (FRP) materials to wood were therefore observed in the present project by using ABES. The results of this study may help to optimize the production of reinforced glulam when using the resistive heating method.

TECHNICAL BACKGROUND

Synthetic Fiber-to-Wood Bonding

The concept of bonding synthetic fibers to wood was first reported in the 1960's when Wangaard (1964) and Biblis (1965) used glass-fiber reinforced plastic strips to reinforce the compression and tensile zones of solid wood samples loaded in bending mode. Spaun (1981) used E-Glass to reinforce finger jointed wood in the high stress region of beams. Rowland (1986) subsequently used unidirectional and cross-woven

carbon and Kevlar ® fibers and various adhesive types (epoxy, resorcinol formaldehyde, phenol resorcinol formaldehyde, and phenol formaldehyde) in studies of reinforcement.

The study of reinforcing wood has progressed over the last decades toward the use of high strength synthetic fibers. Those who have reported research studies on these types of reinforcement include Tingley 1996, Triantifillou and Deskovic (1992), Davalos *et al.* 1992, Barbero *et al.* 1993, Moulin *et al.* 1990, and Kirlin (1996). The present discussion will be largely limited to the use of carbon fiber since this combines high stiffness and strength with the ability to conduct electricity: a pre-requisite of the resistive heating method.

Adhesion mechanisms in CFRP bonding

To date, most studies have addressed bonding of carbon fibers within epoxy matrices and resultant epoxy matricised CFRP laminates onto metal substrates. Little work on bonding CFRP onto wood substrates has, however, been reported in literature. In the absence of such wood bonding studies, CFRP bonding onto non-wood substrates will therefore be summarized here.

Allen (1984) investigated the effect of volatile material in epoxy adhesive used in CFRP-CFRP bonding. This was done since volatile formed bubbles in the interface layer and reduced the CFRP-CFRP composite's shear strength. Parker *et al.* (1985) subsequently explored the effect of water, surface contamination, and thermal mismatch between two adherends on CFRP metal joints for composite patches in aircraft structures. Further, Lee *et al.* (1986) improved the compatibility of CFRP to epoxy adhesive by

applying copolymer and additional bisphenol into the matrix during CFRP manufacturing.

Menningen and Weiss (1995) stated that bonding between CFRP and metal primarily depends upon mechanical interlocking and Van der Walls forces, and that bond failure was influenced by the CFRP surface condition. Therefore, a mechanical roughening process that increased the potential for surface interlocking and chemical addition on the CFRP surface was found to promote a strong bond. Clearly, such surface modification is controversial since roughening suggests damage to the carbon fibers and thence reduction of their ability to transfer stress. However, where the Young's modulus of the partner adherend is significantly lower than that of carbon, such damage may be advantageous. Stress intensity values between adherends of greatly differing elastic modulae can be high and lead to interfacial fracture. A damage zone may act to decrease the stress intensity factor and thence enhance efficiency of the system. This may be the case with wood and CFRP in our present situation of glulam reinforcement. Such roughening will not, however, be investigated in the present study but may be the subject of a future investigation. The influence of adherend property on stress distribution in bonds has received considerable attention. Such work will be relevant to analysis of damage-induced gradients in adherent properties through cross-sections of bonds.

Shear Testing of Adhesive to Wood Bonds

In the present work, the strength development of wood-to-CFRP bonds will be studied as they cure. This is with a view to designing and optimizing the resistive heating approach reported in the companion paper (Liem *et al.* in preparation(a)). Shear mode has

been employed both because the ABES technique is based upon the formation and testing of such bonds, but also because the principal stress at CFRP-to-wood interfaces in reinforced beams loaded in flexure is shear (Kirlin 1996). For these reasons, some uses of lap-shear testing methods for bond assessment are briefly reviewed here.

A large number of analyses of stresses in single-lap joints have been conducted over the past 60-plus years. Volkerson (1938) published the first known analysis of stresses arising from differential shearing. The analysis was then extended to calculate stresses due to both bending and shearing. Eventually, Goland and Reissner (1944) described the shear and transverse tensile stresses in the adhesive.

Further improvements in stress analysis were made by using finite element methods (FEM). An investigation using the then quite new method was conducted by Cooper and Sawyer (1979). These workers compared solutions, including non-linear behavior, with the results of Goland and Reisner who developed closed-form solutions. At the same time, the influence of thickness on stresses in the adhesive layer was explored by Ojalvo and Eidinoff (1978), who produced a more complete shear-strain equation.

Many researchers have investigated stress distributions in other test joint configurations. The intention of these investigations was often to determine the effect on bond strength of altering joint geometry and also to develop test methods which provided results which were independent of sample size. Improvement of test sample geometry by tapering edges and stepping joints was, for example, analyzed by Erdogan and Ratwani (1971).

Testing of lap shear bonds, - Using the Automated Bonding Evaluation System (ABES), the bonding reactivity of thermosetting adhesives can be evaluated in a small

lap-shear testing method developed by Humphrey (1999). This instrument imposes a hot-pressing action on a miniature scale by the use of small test bonds and controlled pressure and temperature blocks. The testing method enables bond strength development kinetics and the effect of modification of specific bond conditions to be investigated. Small lap-shear test bonds are pressed at a range of target temperatures, and tensile load is applied after certain designated time periods. Adherends are made thin or heat diffusive so that block temperature is reached at the glueline quickly; near isothermal conditions therefore prevail for most of each pressing period. Derived bond test data can be used to construct plots of isothermal shear strength development with time. Providing that such isothermal strength development plots display linearity in their early stages, then a value of bond formation speed can be derived by regressing bond strength against time. The effect of temperature on bonding rate may then be explored by collecting data for a range of pressing temperatures and then plotting the regressed isothermal bonding rates against temperature.

Several factors effect the results of ABES testing for a given adhesive; these include (but are not limited to) adherend properties, adhesive distribution over the glueline, and overlap area. When using ABES, adherend thickness must be sufficient to enable the maximum shear load to be transferred to the bond area without tensile failure in the wood away from the bond. The thickness must also be sufficient to prevent adhesive penetration right through the wood sample during the bond pressing; this would interfere with bond formation. On the other hand, if near-isothermal conditions are to be reached quickly at the bond line (necessary for the above mentioned kinetics analysis), the adherend material must not be too thick. The adherend's thermal conductivity (or

diffusivity) should therefore also be considered before selecting adherend sample thickness.

The overlap area used in ABES testing must be selected so that the loading capacity of the instrument is not exceeded when bonds are allowed to reach high levels of cure. When strong adhesive or well cured bonds are to be tested, a small overlap area is therefore preferred. In single lap joint tests, the effect of adherend geometry on the shear stress as considered by Goland and Reissner (1944), may expressed in the following way:

$$S_s = \sqrt{2\frac{G \cdot c^2}{E \cdot n \cdot t}} \qquad (1)$$

$$S_n = \sqrt[4]{\frac{3E_c \cdot c^4}{8 \cdot E \cdot n \cdot t^3}} \qquad (2)$$

Where:

S_s = shear stress concentration (Pa)

S_n = normal stress concentration (Pa)

G = adhesive shear modulus (Pa)

E = adherend tensile elastic modulus (Pa)

E_c = adhesive tensile elastic modulus (Pa)

c = overlap length (mm)

n = adhesive layer thickness (mm)

t = adherend thickness (mm)

The predicted variation of shear stress along the interface layer in the axial direction is parabolic (Figure 4.1). This is caused by material interactions imposed by the tensile load. Furthermore, a bending effect occurs within the joint due to its transverse

asymmetry. The interaction of such forces can promote propagation of fracture from the ends of the overlap towards its center and thus cause premature catastrophic failure. These effects can mask the measurement of true shear strength values. All of the above factors were considered in the design of the test method used in the present study.

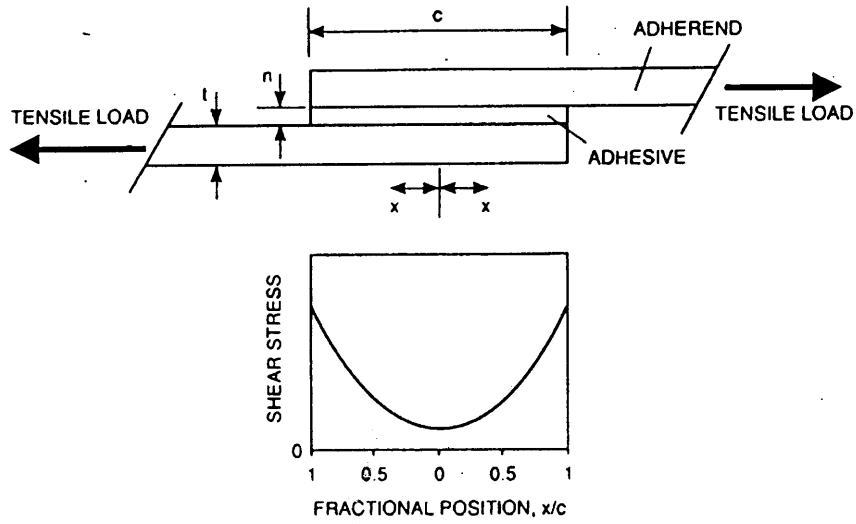

Figure 4. 1. Variation of shear stress at the adhesive-adherend interface in a lap-shear bonding test during pulling (Humphrey and Zavala 1989).

Opportunities do, however, still exist to further optimize test bond design, and the use of FEM methods is presently under way in a complimentary project. Such optimization is, however, complicated by the fact that the adhesive's properties change with time as cure progresses.

OBJECTIVES

The objective of this project was to study the bonding characteristics of FRP-to-wood and how the rate of bond strength development is effected by temperature. In order to effectively apply the CFRP resistive heating method to cure bonds in glulam beams, it was necessary to understand the bonding kinetics of thermosetting adhesive (PF and PRF). Thus, there were three objectives:

- To study bonding kinetics of PRF and PF resin when used with FRP and wood.
- To obtain numerical estimates of bond cure (strength development) in relation to the resistive heating method.
- To identify failure modes for bonds between FRP and wood.

MATERIALS AND METHODS

Materials

Wood specimens. - Sliced birch (*Betula spp.*) veneer (0.8 mm thick) with radial faces were cut into 20 × 120-mm strips with a metal shear cutting tool. This wood species has high uniformity and the ABES machine has been standardized with this and similar species. Birch was also chosen in preference to the Douglas-fir material used to fabricate trial beams because variability in the latter's structure leads to scatter in test bond data. Comparative trials with Douglas-fir and birch (Humphrey 1999) have, however, indicated that underlying trends are similar for the two species. Still, ongoing work concerns evaluation of the species-dependent variability in bonding and how this may influence industrial wood processing.

Five hundred wood strips were prepared for the test. The veneers came in 2.4 × 1.2-m sheets (8 × 4-ft), and were conditioned at room temperature (23 ^{0}C and 65 percent RH) to 8 to 9 percent moisture content prior to use. No attempt was made in the present research to investigate the effect of moisture content on bonding. This is, however, of concern in ongoing research. The thickness of the wood adherends was selected with consideration of the heat transfer, tensile strength and glue penetration.

Synthetic fibers. – Carbon FRP (CFRP) and E-glass FRP (EFRP) were used in the tests. The FRP came in 895 × 130 × 1-mm sheets and was precision cut into 20- × 10- × 1-mm strips with a specially designed precision cutting table incorporating a 50 mm diameter circular metal cutting blade rotating at 1,000 RPM (peripheral speed of 2.6 m/sec). The CFRP was made of carbon fiber (60 percent fiber volume fraction) from a pitch precursor with 66 percent graphitization. This material has a thermal conductivity in the longitudinal direction of 650 to 1,100 W/mK and 15 to 50 W/mK in the transverse direction. All the FRP samples were cleaned with ethanol (Davalos, 1994), soaked in clean water, and dried and stored in plastic bags prior to use.

Adhesives. - PRF adhesive (type GP 4554) and hardener (type GP 4242) produced by the Georgia Pacific Company and commonly used in glulam beam manufacturing was used in the study. This adhesive has also been used in the manufacture of reinforced beams. Since very small quantities were necessary for bonding studies, PRF batches were mixed and prepared in a 50-ml syringe tube. The mixing weight proportions were 70 percent PRF glue, 12 percent hardener, and 18 percent water. After mixing, the adhesive was kept in a sealed container at 10 ^{0}C to minimize pre-cure and the maximum storage time was 48 hours (increases in viscosity were detectable beyond this time).

Base-catalyzed PF adhesive with pH 12 and 50 percent solids content produced by Borden Chemical Inc. was used for a comparative adhesive study.

Methods

The ABES approach. - The ABES applied heat and pressure at the overlapping area of bonds with two heated aluminum blocks (faced with stainless steel anvils). The ABES device is shown in Figure 4.2, a conceptual schematic is shown in Figure 4.3, and the materials alignment used in the present studies are shown in Figure 4.4. In this arrangement, the heat was rapidly transferred from the blocks, through the wood to the adhesive at the interface layers between the wood strips and CFRP sample. Such heating was rapid since the wood strips were thin (0.8-mm). Target temperature was typically approached within 2 ^{0}C in 8 seconds. A family of typical glueline heating curves for a range of target pressing temperatures are shown in Figure 4.5.

There are two options for breaking the sample: while it is still hot or after it has been cooled down to room temperature by the automatic application of pressurized air. Cooling may be affected by activation of a cooling head which rises up on either side of the hot bond once the pressing blocks are retracted as shown in Figure 4.6. Figure 4.7 shows the glueline time-temperature sequence after the selected pressing time has been reached. In either case, once pressing and optional cooling was complete, the free ends of the wood samples were gripped and the pulling head activated to break the bond in the lap-shear mode while it was still hot or after being cooled. The stress to fail the bond was applied at a controlled rate of approximately 2.2 MPa/sec (both of pressing and pulling). The result was a shear strength value specific to the selected pressing time and

temperature. This procedure was repeated for a range of times and temperatures in order to construct sets of isothermal strength development plots as described below.

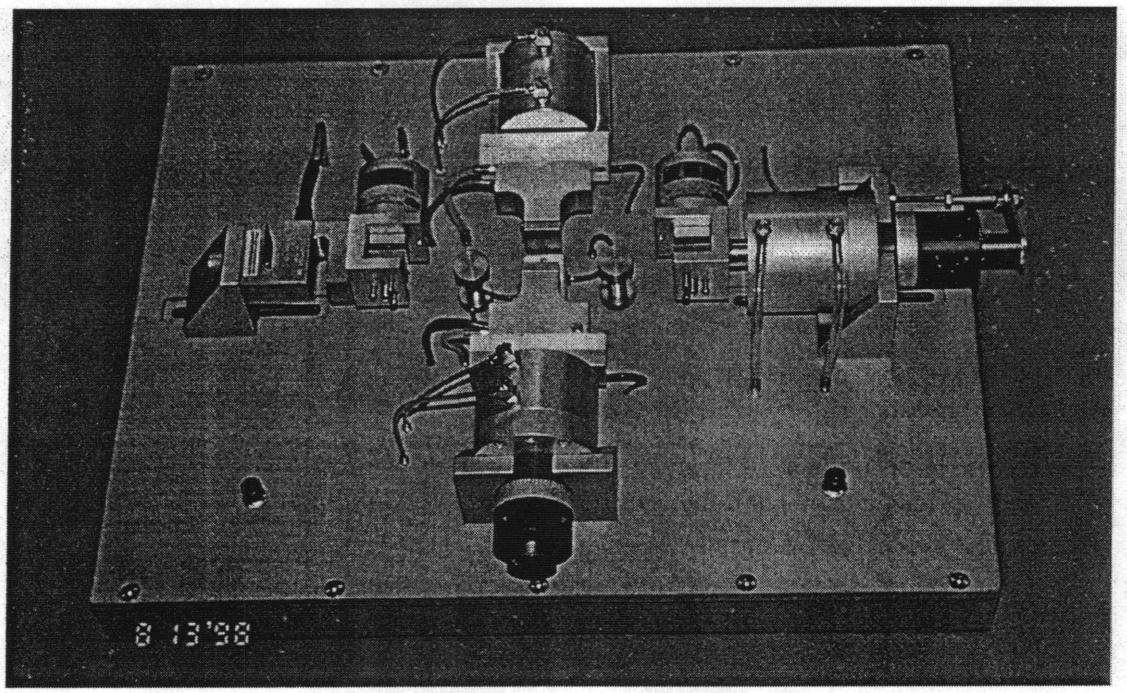

Figure 4. 2. An overview of the main module of the ABES system (Humphrey 1999).

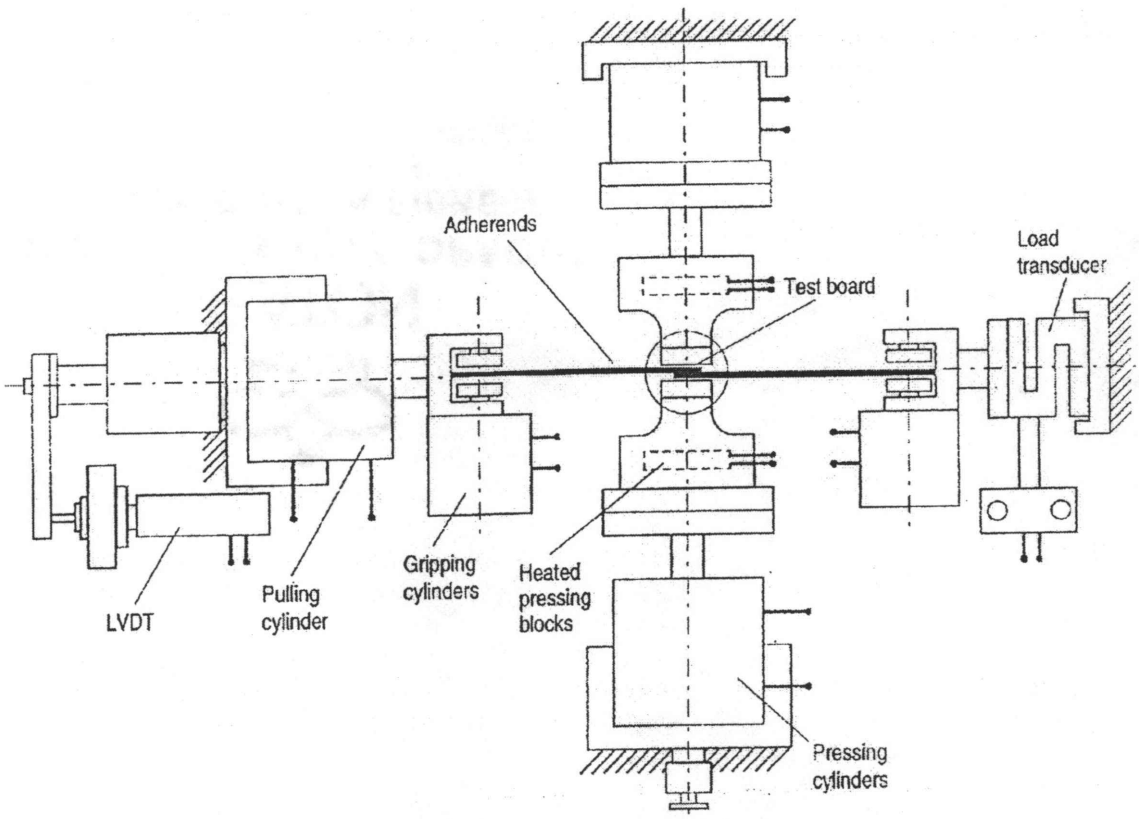

Figure 4. 3. A schematic of the ABES testing system (Humphrey 1999).

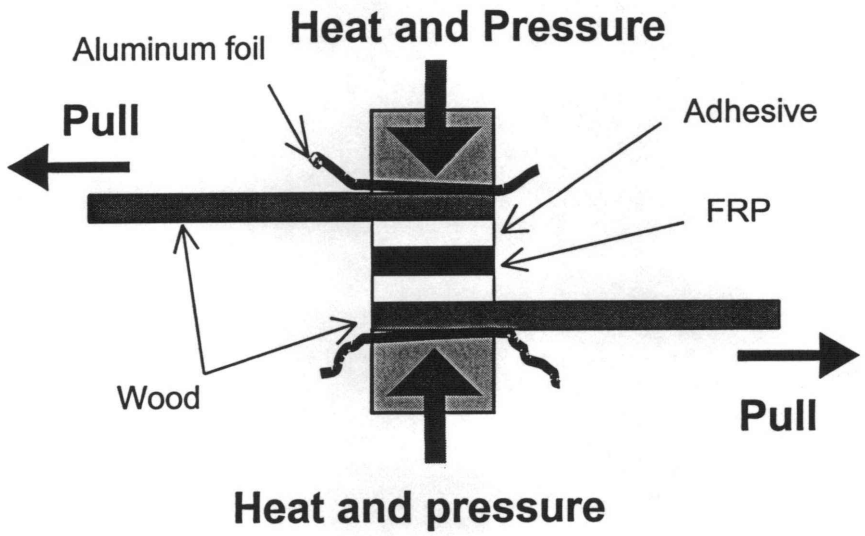

Figure 4. 4. Schematic concept of the lap-shear test in ABES for the present investigation (not to scale).

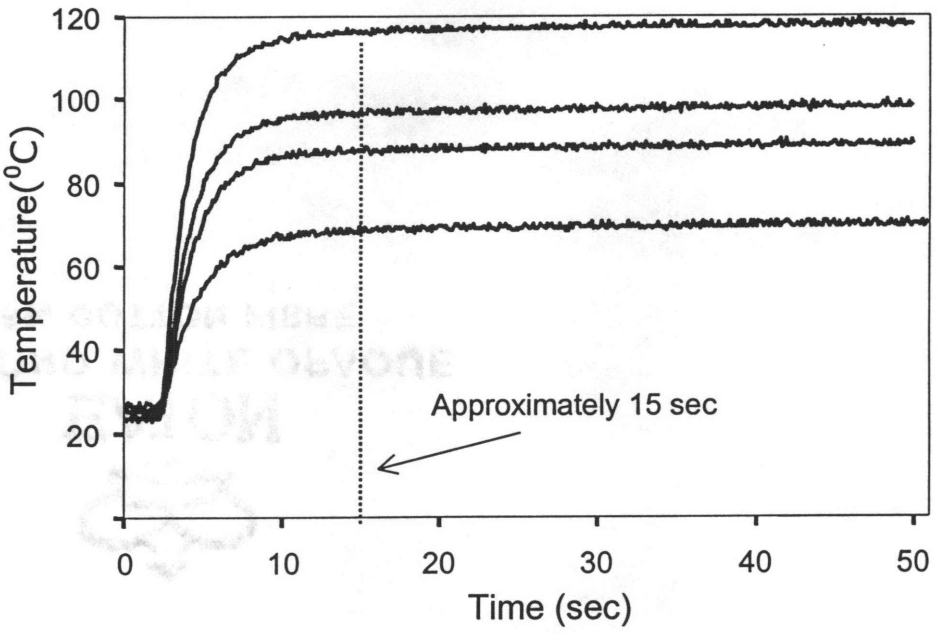

Figure 4. 5. Glueline heating curves for a range of target temperatures. Measured by inserting miniature thermocouple probes into bonds which were pressed but not pulled (Humphrey 1999).

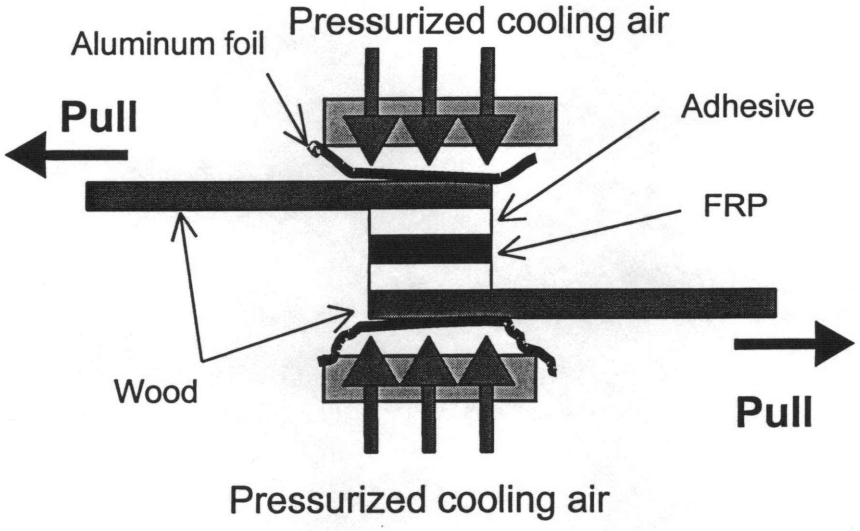

Figure 4. 6. Schematic of the bond cooling arrangement mounted on the ABES system (not to scale). The cooling head blocks pop up and cool the glueline area after the heat and pressure sequence, then the bond sample was pulled.

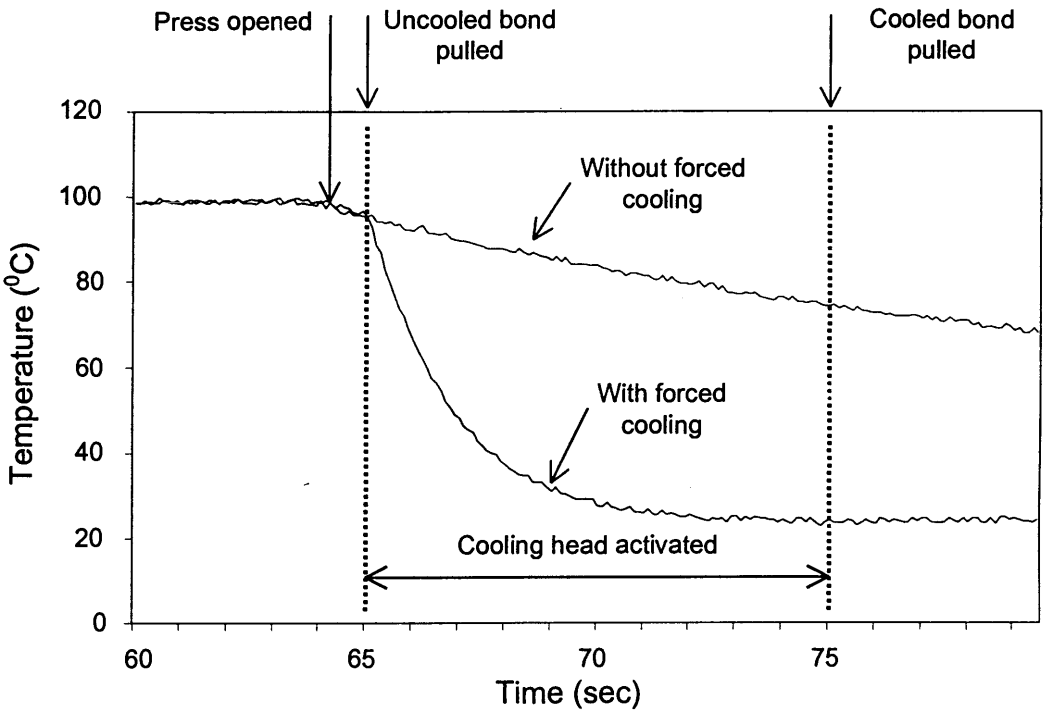

Figure 4. 7. Typical glueline cooling curves after normal pressing: a) without and b) with forced cooling (Kim and Humphrey 1999).

Adhesive application. - In preparation for bond formation, individual droplets of adhesive (weighing 0.0552 grams each) were applied near the end of each FRP surface and then carefully and rapidly spread with a clean flat metal spatula over the bonding area (20 × 10-mm). This resulted in a spread rate of approximately 130 g/m^2. Care was taken to apply adhesive in a similar fashion for each bond and to minimize variability in spread rate and open assembly time.

To further minimize variability in adhesive spread rate among gluelines, the two heating blocks pressed the glueline with controlled and consistent pressure; a small excess of adhesive was squeezed out of the sandwich formation and only a thin and

uniform layer of adhesive was left. Consequently, adhesive remaining in the pressed glueline had a spread rate somewhat less than 130 g/m ^{2}. A pressing pressure of 2 MPa was used for all tests. This pressure is typical of that used in wood laminating processes. The effect of pressure on adhesion will be a concern in future investigations.

A thin aluminum sheet (0.01-mm thick) was placed at the interface between the heating blocks and the adherend samples before pressing began (Figure 4.6). The aluminum sheet prevented interference of small quantities of squeezed out PRF adhesive by isolating adhesive spread from the heat-blocks. The high thermal conductivity of aluminum (235 W/m ^{0}K) meant that heat transfer into test bonds was not impeded.

Experimental Plan for FRP-to-Wood Bonding Kinetics Studies. - The bonding kinetics study covered three pressing-testing modes (the pressing and pulling modes are shown in Table 4.1) using two adhesive types (PRF and PF). Each pressing mode had three adherend formations (CFRP-, EFRP-, and wood-to-wood) and each adherend formation was subjected to four target-temperature pressing conditions. Ten sample bonds were formed for each target pressing temperature and each sample was pressed for a different time and treated as an individual data point. Plots of bond strengths versus time were than analyzed with a regression method to find an isothermal bond strength development rate for each temperature employed. Regressed bonding rates were than plotted against pressing temperature for each adherend type. In this way, the compatibility and bonding characteristics of FRP was also investigated and compared to wood-to-wood bonding.

Table 4. 1. Experimental plan for bond strength kinetics evaluation.

<table>
<tr><th>Adhesive Type</th><th>Pressing and pulling modes</th><th>Adherend</th><th colspan="4">Glueline temperature test</th></tr>
<tr><td rowspan="7">Phenol Resorcinol Formaldehyde (PRF)</td><td rowspan="3">Press: -hot
Pull: -hot</td><td>CFRP and wood</td><td rowspan="3">Press: 40°C
Pull: 40°C
Pressing time:
120, 240, 360, 420, 480, 540, 600 sec.</td><td rowspan="3">Press: 70°C
Pull: 70°C
Pressing time:
60, 90, 120, 150, 180, 210, 300 sec.</td><td rowspan="3">Press: 100°C
Pull: 100°C
Pressing time:
30, 45, 60, 75, 90, 115, 120 sec</td><td rowspan="3">Press: 130°C
Pull: 130°C
Pressing time:
15, 17, 20, 22, 25, 30, 40 sec.</td></tr>
<tr><td>EFRP and wood</td></tr>
<tr><td>Wood and wood</td></tr>
<tr><td rowspan="3">Press: -hot
Pull: -cool</td><td>CFRP and wood</td><td rowspan="3">Press: 40°C
Pull: 22°C
Pressing time:
120, 240, 360, 420, 480, 540, 600 sec.</td><td rowspan="3">Press: 70°C
Pull: 22°C
Pressing time:
60, 90, 120, 150, 180, 210, 300 sec.</td><td rowspan="3">Press: 100°C
Pull: 22°C
Pressing time:
30, 45, 60, 75, 90, 115, 120 sec</td><td rowspan="3">Press: 130°C
Pull: 22°C
Pressing time:
15, 17, 20, 22, 25, 30, 40 sec.</td></tr>
<tr><td>EFRP and wood</td></tr>
<tr><td>Wood and wood</td></tr>
<tr><td rowspan="3">Extended
Press: -hot
Pull: -hot</td><td>CFRP and wood</td><td colspan="4" rowspan="3">Pressing temperature = 100°C
Pulling temperature = 100°C
Pressing time = 180, 240, 300, 360, 420, 480, 540, 600, 1200 seconds</td></tr>
<tr><td>EFRP and wood</td></tr>
<tr><td>Wood and wood</td></tr>
<tr><td rowspan="3">Phenol Formaldehyde (PF)</td><td rowspan="3">Press: -hot
Pull: -hot</td><td>CFRP and wood</td><td rowspan="3">Press: 70°C
Pull: 70°C
Pressing time:
60, 120, 180, 240, 300, 360, 420, sec.</td><td rowspan="3">Press: 80°C
Pull: 80°C
Pressing time:
60, 90, 120, 150, 180, 240, 300 sec.</td><td rowspan="3">Press: 90°C
Pull: 90°C
Pressing time:
60, 90, 120, 150, 180, 210, 240, 270, 300, 360 sec</td><td rowspan="3">Press: 100°C
Pull: 100°C
Pressing time:
60, 75, 90, 120, 150, 180, 210, 240, 270 sec.</td></tr>
<tr><td>EFRP and wood</td></tr>
<tr><td>Wood and wood</td></tr>
</table>

Details of each treatment combination were:

- *FRP-to-wood bond strength development in press-hot-pull-hot test with PRF adhesive.*

  The samples were subjected to one of four target pressing temperatures (40 ^{0}C, 70 ^{0}C, 100 ^{0}C, and 130 ^{0}C) for times ranging from 15 to 600 sec. Pressing times less than 15 sec were not employed since the glueline needed at least 15 seconds to reach target temperature from room temperature condition (Figure 4.5). After the

target pressing time had been reached, the samples were pulled apart in hot condition. EFRP-to-wood and wood-to-wood bonding characteristics were also studied by repeating the above test regimen. Isothermal strength development plots were then constructed.

- *FRP-to-wood maximum bond strength in press-hot-pull-cool test with PRF adhesive.*

  The purpose of this treatment was to measure the final bond strength of CFRP-to-wood when the bonds were fully cured and quickly cooled to room temperature. For this purpose, bonds were formed on the ABES at 100 ^{0}C and subsequently cooled using pressurized room temperature air for 20 seconds prior to being pulled in the normal fashion. Using the cooling system (Figure 4.6), glueline temperatures can be reduced to room temperature within 15 seconds (Figure 4.7). An extra 5 seconds of cooling time was added to the cycle in order to minimize variability of the temperature at which bonds were tested. This extra time is unlikely to have had a significant effect due to further adhesive curing; curing was almost halted once the temperature approached that of the cooling air.

- *FRP-to-wood maximum bond strength in extended-press-hot-pull-hot test with PRF adhesive.*

  The purpose of this treatment to explore the maximum bond strength of CFRP-to-wood when the bonds were cured at a fixed temperature (100 ^{0}C) for a prolonged pressing period ranging from 120 to 1200 seconds. After the target pressing time had been reached, the samples were subsequently tested in the hot condition.

- *CFRP-to-wood bonding development with PF adhesive.*

  PF adhesive has been widely used in the forest products industry. The performance of PF adhesive was tested here since it is inexpensive compared to PRF. These include its low cost relative to PRF and the fact that it is widely used and accepted in wood products industries as an exterior adhesive. These bonds were pressed hot and pulled hot. There was some concern that the temperature limitations may prevent resin polymerization.

Numerical Prediction of Bond Strength Development in resistively heated laminates. - The numerical prediction of bond strength development was conducted since it may be used to provide information of time, temperature, and resistive heating power necessary to form strong bonds or to achieve bond strengths sufficient for the clamps to be safely removed during beam manufacture.

Failure Modes. - The adhesion failure modes of the broken samples from the lap-shear test were surveyed. A digital image-enhancing system with 280× magnification was used to study the adhesive spread onto the adherends. The results were used to consider the chronology of bonding development and issues that may effect the minimum time needed to form acceptable bonds.

RESULTS AND DISCUSSION

FRP-to-Wood Bonding Characteristics Studies

FRP-to-wood bond strength in hot-pull tests using PRF adhesive. - A plot of CFRP-to-wood bond-strength versus pressing time using PRF glue at several pressing

temperature conditions is shown in Figure 4.8. These data show that the strength developed in a nearly-linear fashion once the target temperature was reached. Clearly, such strength development could not continue indefinitely; polymerization rate must eventually decrease as full cross-linking is approached. In addition, limitations were imposed by the cohesive and tensile strengths of the adherends and the loading limits of the ABES system. However, over the range of temperatures and times explored in the present study, linear strength development is suggested and isothermal strength developed rates may be derived by linear regression. Regressed lines and associated correlation coefficient (r^2) are therefore included in Figure 4.8.

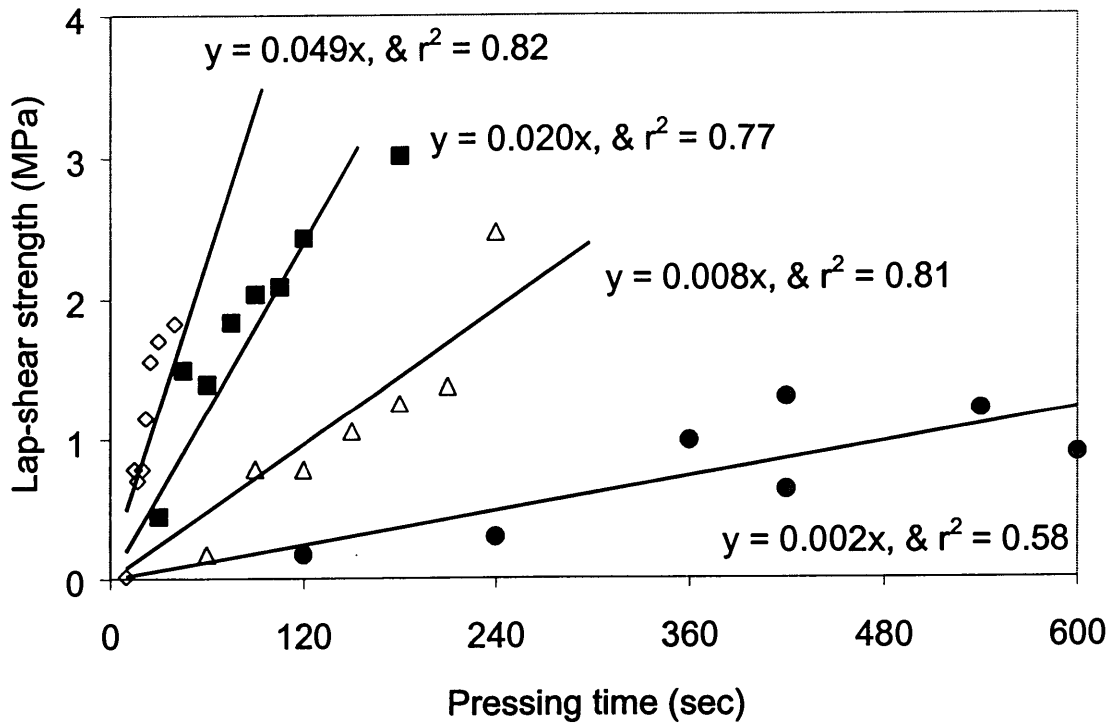

Figure 4. 8. CFRP-to-wood bond strength development data using PRF adhesive in press-hot-pull-hot test. Each point group represents: ◇) 130 ^{0}C, ■) 100 ^{0}C, Δ) 70 ^{0}C, and ●) 40 ^{0}C pressing temperature

For a comparison with carbon fiber bonding, a chart of EFRP-to-wood bonds with PRF adhesive is also illustrated in Figure 4.9.

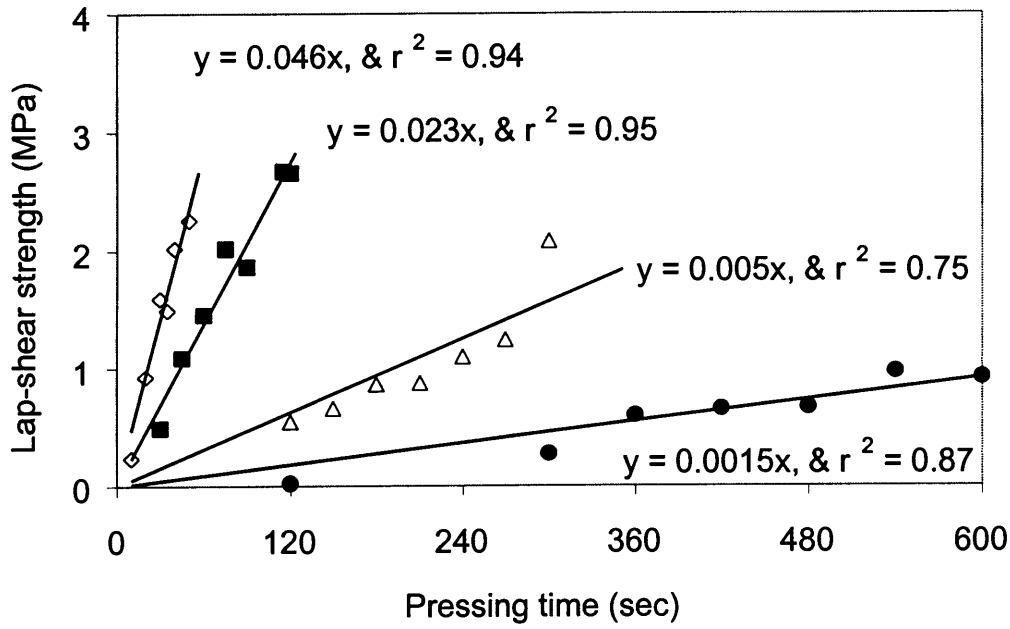

Figure 4. 9. EFRP-to-wood bond strength development data using PRF adhesive in press-hot-pull-hot test. Each point group represents: ◇) 130 ^{0}C, ■) 100 ^{0}C, Δ) 70 ^{0}C, and ●) 40 ^{0}C pressing temperature.

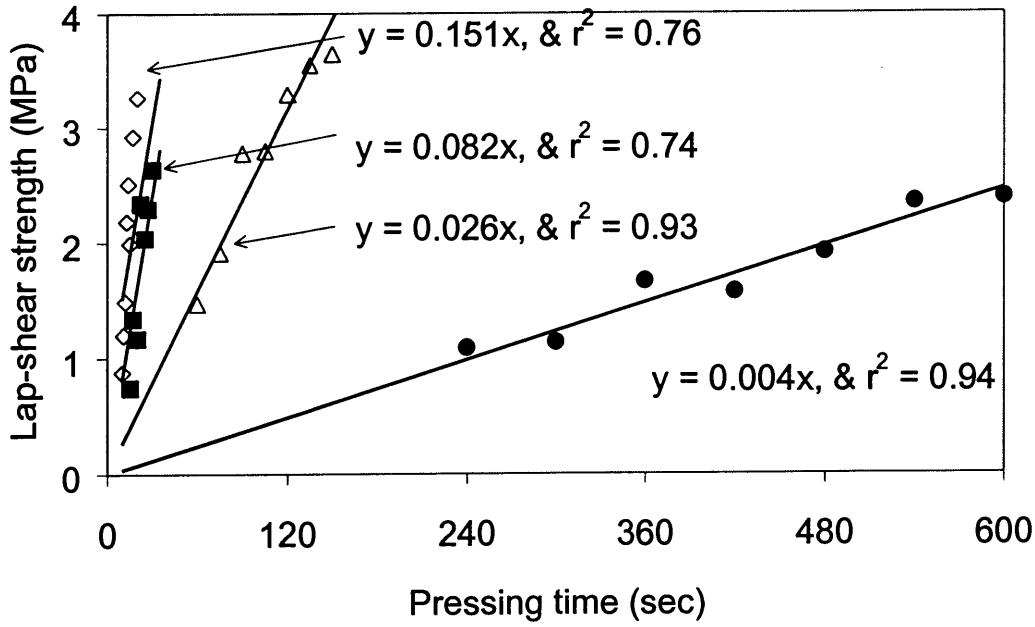

Figure 4. 10. Wood-to-wood bond strength development data using PRF adhesive in press-hot-pull-hot test. Each point group represents: ◇) 130 ^{0}C, ■) 100 ^{0}C, Δ) 60 ^{0}C, and ●) 40 ^{0}C pressing temperature.

FRP-to-wood bonding kinetics studies. - By obtaining the slopes of the regressed isothermal bonding strength development plots (Figures 4.8, 4.9, and 4.10), the bonding rate at each temperature for CFRP-to-wood, EFRP-to-wood, and wood-to-wood were derived (Table 4.2).

Table 4. 2. Regressed isothermal bond strength development rates of: a) CFRP-to-wood bonds, b) E-glass FRP-to-wood, and c) Wood-to-wood.

Pressing temperature (^{0}C)	Regressed Isothermal bonding strength development rate (kPa/sec)	r^2
CFRP-to-wood		
40	2	0.58
70	8	0.81
100	20	0.77
130	49	0.82
E-glass FRP-to-wood		
40	1.5	0.87
70	5	0.75
100	23	0.95
130	46	0.94
c) Wood-to-wood		
40	4	0.94
70	26	0.93
100	82	0.74
130	151	0.76

Plots of isothermal bond strength development rate versus temperature are shown for all three adherend types in Figure 4.11. The results suggest an exponential relationship between the pressing temperature and isothermal bonding development rate. Such a relationship suggests that the measured bond strength is due to a first-order activated process - - most likely the polymerization reactions associated with the adhesive cure. The curves for CFRP- and EFRP- wood adherends are very similar. This may be

due to the fact that the reinforcing fibers in both materials are completely encased in epoxy matrix; the bonding surface for each may therefore be similar (epoxy rather than fiber).

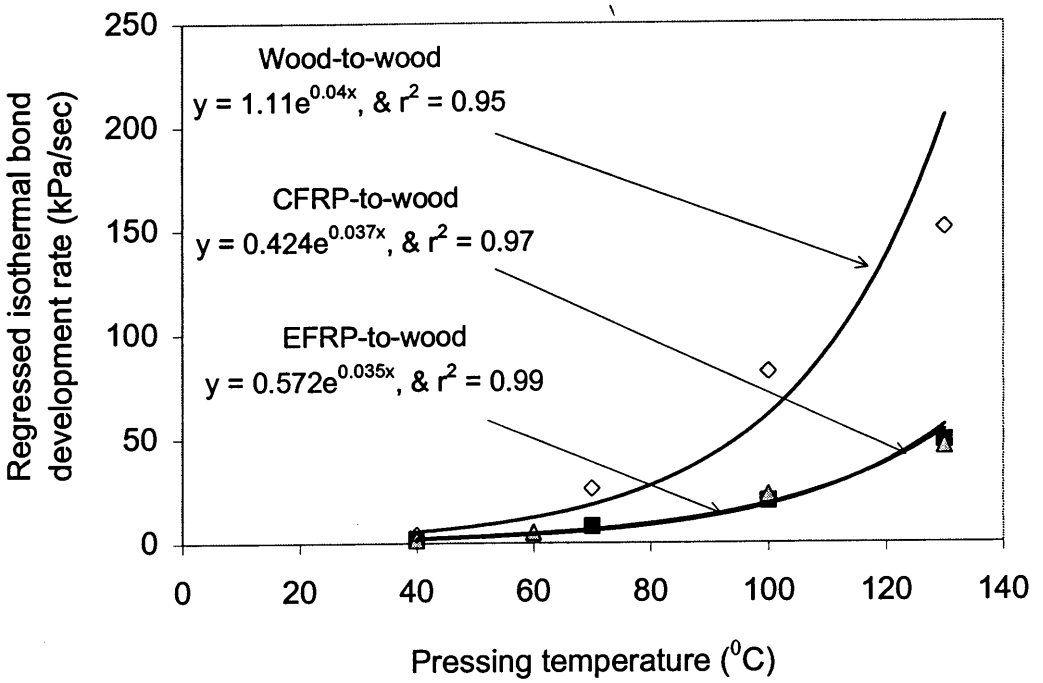

Figure 4. 11. Regressed rate of isothermal bond strength development versus temperature for all material combinations with PRF adhesive.

One may, however, expect differences in measured strengths for strong bonds since the stiffness of carbon and E-glass differ. Stress distributions along the length of the bond overlaps are influenced by the relative stiffnesses of the adherends (Nono 1993, and Wu 1947). This effect is not examined here because the strengths of partially cured bonds are low compared to the stiffness of the FRP; thus the distribution of shear stress is likely almost uniform except at the ends of bond.

Bonds between wood adherends show substantially higher strengths at all stages of cure; rates are greater than those for CFRP- and EFRP-wood adherends at all temperatures. This difference may be due to the porosity of wood and the attendant penetration of adhesive into the surface structure prior to increase in viscosity associated with cross-linking. It is reasonable, however, to expect that epoxy surfaces may be superior when adhesives with a greater propensity for chemical bonding are used.

The results suggest that the inert nature and lack of porosity of FRP surfaces limits mechanical interlocking of the adhesive to them and reduces the shear strength of bonds. To increase FRP-to-wood bonding, modification of the FRP's surface to enhance interactions such as by surface roughening may be needed (Gardner 1994, Tingley *et al.* 1996). Coupling agent such as amino-salane (Spaun 1981) and copolymer bisphenol (Lee *et al.* 1985) may also be helpfull. Still, the rate for CFRP strength development is fast compared to that which occurs at room temperature and this is encouraging for the resistive heating approach.

In addition, mechanical interlocking that is largely absent with the epoxy-filled FRP adherends of vitrified adhesive in wood adherends may lead to high bond strengths. Wood-to-wood bonds may also display superior strengths because of greater mechanical compatibility when like adherends are used; stress uniformity is greater within bonds with adherends consisting of material of similar stiffness.

The effect of cooling bonds. – Resistively heated bonds in FRP glulam will cool once the electrical supply is terminated. It was hypothesized that such cooling may lead to increases in bond strength since Kim and Humphrey (1999) have detected a significant

influence of testing temperature on the strength of partially cured wood–to-wood bonds with PF and UF adhesives. For this reason, a small number of CFRP-to-wood bonds were pressed in the present study for a range of times at 100 ^{0}C and were subsequently cooled prior to the tensile test. Because the test bonds in the present study were thicker than those in Kim and Humphrey (1999), a cooling period of 20 seconds was employed. This ensured that bonds had reached a stable temperature prior to being tested.

Bond strength data for cooled bonds are shown in Figure 4.12. Data for bonds tested hot are also shown. Increased bond strength at every press-time is clear; strengths based on regressed rates are approximately 45 percent higher due to cooling where the regressed rates were 1.85 and 3.14 kPa/sec respectively.

These results may be due to the cooling of the PRF adhesive reducing the glueline temperature below the glass transition. However, bond strengths without cooling are likely to reach values which are sufficient to hold laminates together after clamping is released.

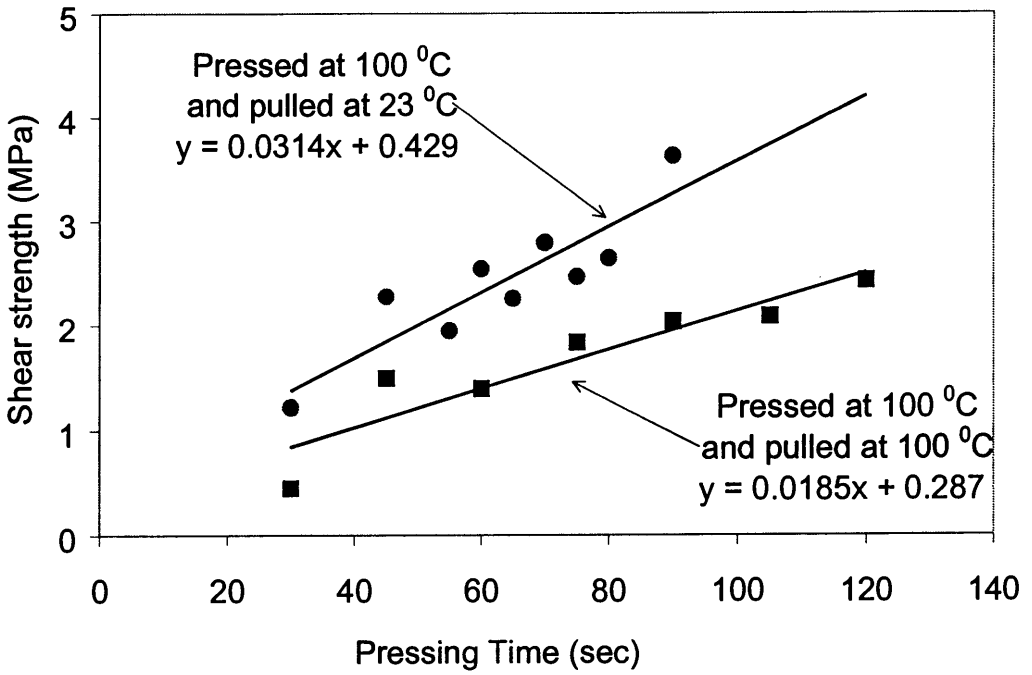

Figure 4. 12. Isothermal bond strength development for CFRP-to-wood bonds and PRF adhesive pressed at 100°C and pulled: a) at 100 °C, and b) at 23 °C (± 3 °C).

Strength of bonds cured for extended periods. – Most test bonds were pressed for relatively short periods prior to being pulled in the hot condition. This facilitated the study of early bond strength development. A set of bonds were, however, also pressed for extended periods (150 to 1200 seconds) at 100 °C. This was done in order to observe the maximum strength attainable under an elevated temperature condition. These data are shown as Figure 4.13. A maximum strength of approximately 3 MPa was reached within approximately 200 seconds. While not very high, this value would likely be great enough for clamping to be removed in an industrial lamination process. Further strength development may be possible due to subsequent cooling of the product.

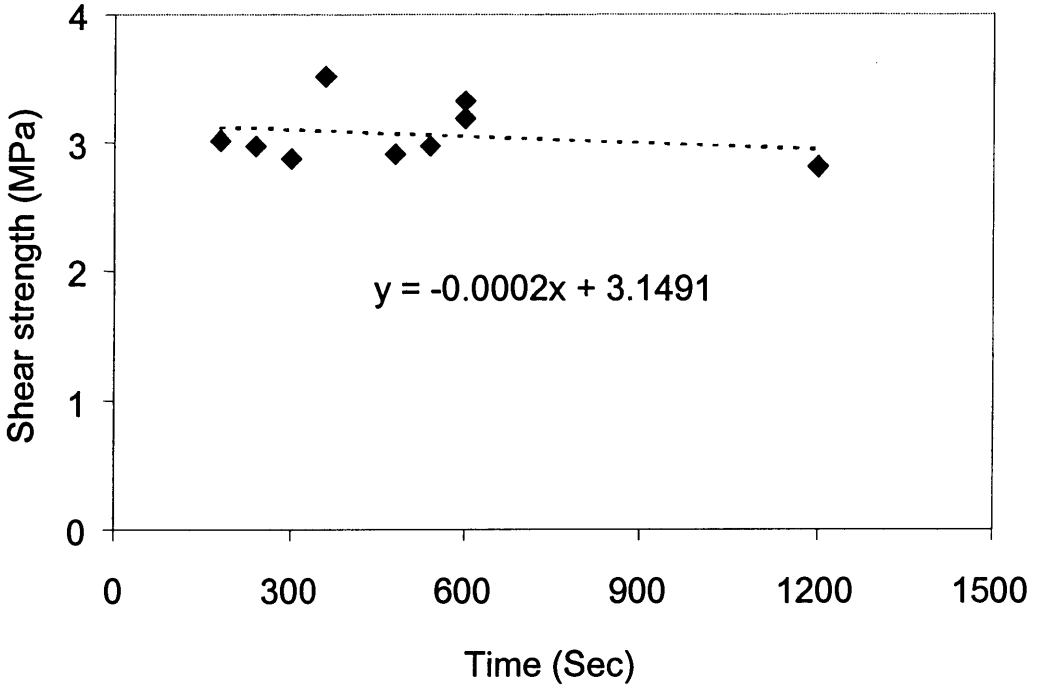

Figure 4. 13. Strength of CFRP-to-wood bonds cured at 100 ^{0}C for a range of extended-press-hot-pull-hot test mode prior to being tested at 100 ^{0}C.

CFRP-to-wood bonding development using PF glue, - The bonding characteristic of an alternative thermoset adhesive, phenol formaldehyde (PF), was studied over a temperature range of 70 to 100 ^{0}C, which is below CFRP matrix melting point (130 ^{0}C). However, this may not have been sufficiently hot to affect the resin polymerization. Results in Figure 4.14 shows maximum strength values of only approximately 1 MPa when the temperature was applied for 4 to 5 minutes and the bonds were tested in the hot condition. Further, the effect of temperature on bonding rate was very small. After maximum bond strength (1 MPa) was reached, strength tended to decrease somewhat. Deficiency in PF-to-CFRP bonding was probably caused by the inert surface structure of the CFRP material and should be investigated further.

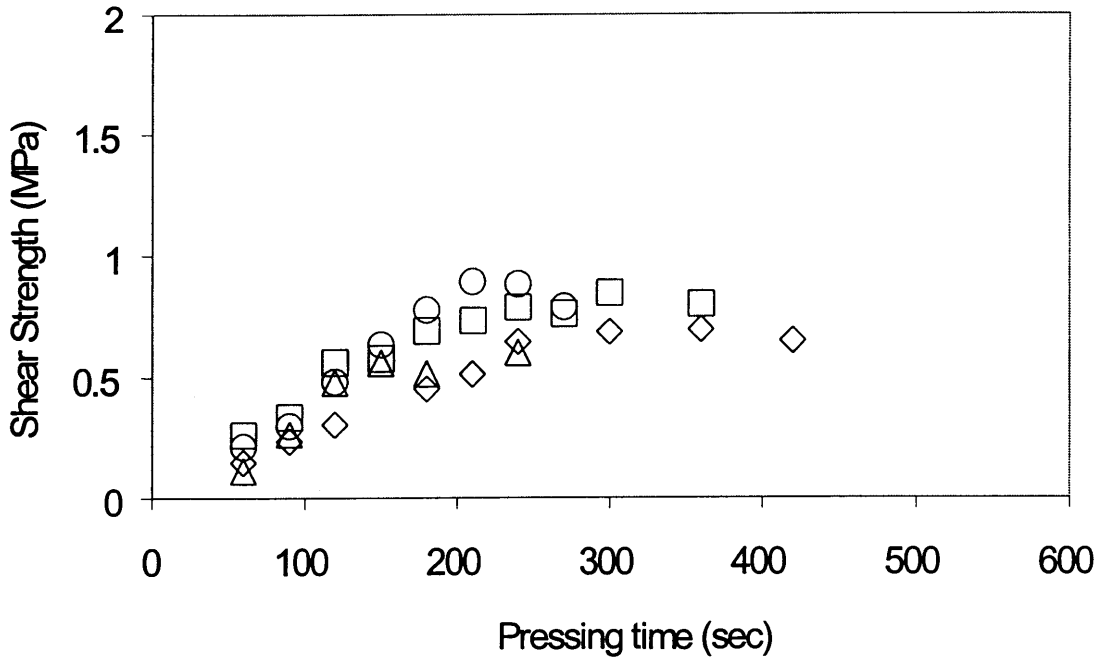

Figure 4. 14. Isothermal CFRP-to-wood bond strength development data using PF adhesive in hot tension test condition. Each point group represents: ○) 100 ^{0}C,) 90 ^{0}C, Δ) 80 ^{0}C, and ◇) 70 ^{0}C pressing temperature.

Numerical estimation of bond strength development of resistively heated bonds

One of the principal reasons that ABES has been used to study bonding kinetics is that derived data may be used to estimate the development of bond strength during resistive heating of reinforcement laminations in glulam. Selection of appropriate voltage and time will depend upon the relationship between bonding rate to temperature. In the companion paper (Liem *et al.* in preparation (a)), the relationship between applied voltage and the spatial distribution of heating at CFRP-wood interfaces has been explored. Optimization of the heating process may be defined in terms of minimization of time needed to achieve a glulam with sufficient integrity to enable clamps removal and

safe handling. It is reasonable to expect that full bond strength may be reached in subsequent cure as temperatures decline to room temperature, adhesive cross linking is completed, and localized stresses relax as moisture gradients in the vicinity of bonds normalize.

The bonding kinetics studies for CFRP and PRF adhesive resulted in an equation relating temperature at the glueline (T_A) to isothermal bond strength development rate (R). This relationship is of the form:

$$R = a \cdot e^{b \cdot T_A} \qquad (1)$$

Where:

R = Isothermal bond strength development rate (Pa/sec).

T_A = Glueline temperature (^{0}C)

a, b = Constants specific to the adhesive-adherend combination

For the CFRP-to-wood combination used in heating trials in the companion paper, the relationship between applied voltage and heating rate was investigated. A number of factors clearly influenced this relationship. These include the resistivity of CFRP in the conducting direction and the heat capacity and thermal diffusivity of the CFRP and wood adherends. The relationship is further complicated by the anisotropy of the CFRP electrical properties. In spite of these complexities, temperature development rate ($\overset{0}{T}$) for a given power input (P_I) to the CFRP may be approximated here by the following expression:

$$\overset{0}{T} = t \cdot P_i + d \qquad (2)$$

Power input in relation to the resistance across the CFRP contacts (R_{CFRP}) and applied voltage (V) is described as:

$$P_i = \frac{V^2}{R_{CFRP}} \qquad (3)$$

Where:

$\overset{0}{T}$ = Temperature development rate (^{0}C/sec)

t = pressing time (sec)

d = room temperature (^{0}C)

P_I = Power input (Watts)

V = Voltage (V)

R_{CFRP} = CFRP strip's resistance (Ω)

Numerical computation. – Heating rate in the present situation has been simplified to a linear function (temperature rise at a constant rate from a fixed starting value). Bond strength development with time could therefore be predicted by developing a closed-form solution for the exponential expression of bonding rate with temperature together with the heating expression (by integration). However, when the resistive heating method will be used with real glulam, more complex non-linear variations of glueline temperature with time have been found and closed-form solutions for bond strength prediction are not feasible. For this reason, a simple numerical method of integration is used here.

In this approach, the heating period was divided into small time steps. Constant temperature may be approximated for each time step if they are sufficiently small. An isothermal bond strength development rate may therefore be calculated using equation (1)

for each time step. The principle of superposition may then be used to construct a predicted bond strength development plot for any given heating curve. The superposition equation with temperature and bond strength relation is described as:

$$BS_1 = (\Delta t_{1-0} \cdot R) + BS_0 \qquad (4)$$

Where:

Δt_{1-0} = time step duration (sec),

R = Isothermal bond strength development rate (Pa/sec),

BS_1 = Current bond strength value (MPa),

BS_0 = Previous bond strength value (MPa).

A spreadsheet was used to implement these solutions. Time steps of 10 seconds were used and an initial bond strength of zero was assumed. A resultant predicted bond strength development plot (for V= 5 V, R_{CFRP} = 0.6 Ω) is shown as Figure 4.15.

Predicted bond strength development plots for a range of input voltages are shown in Figure 4.16. These are included to demonstrate the sensitivity of the resistive heating and consequent bonding to input voltage. The usefulness of the numerical construction lies in gaining approximate times to reach certain minimum strengths, but this procedure provides no limit on bond strength values. Strength predictions have here been truncated at 4 MPa because bond strength between CFRP and wood at elevated temperature were found rarely to exceed 3 MPa in tests.

The predicted bond strength development data may be used to ascertain the time needed to reach a target strength. Figure 4.17 shows such data for a 3 MPa target bond strength.

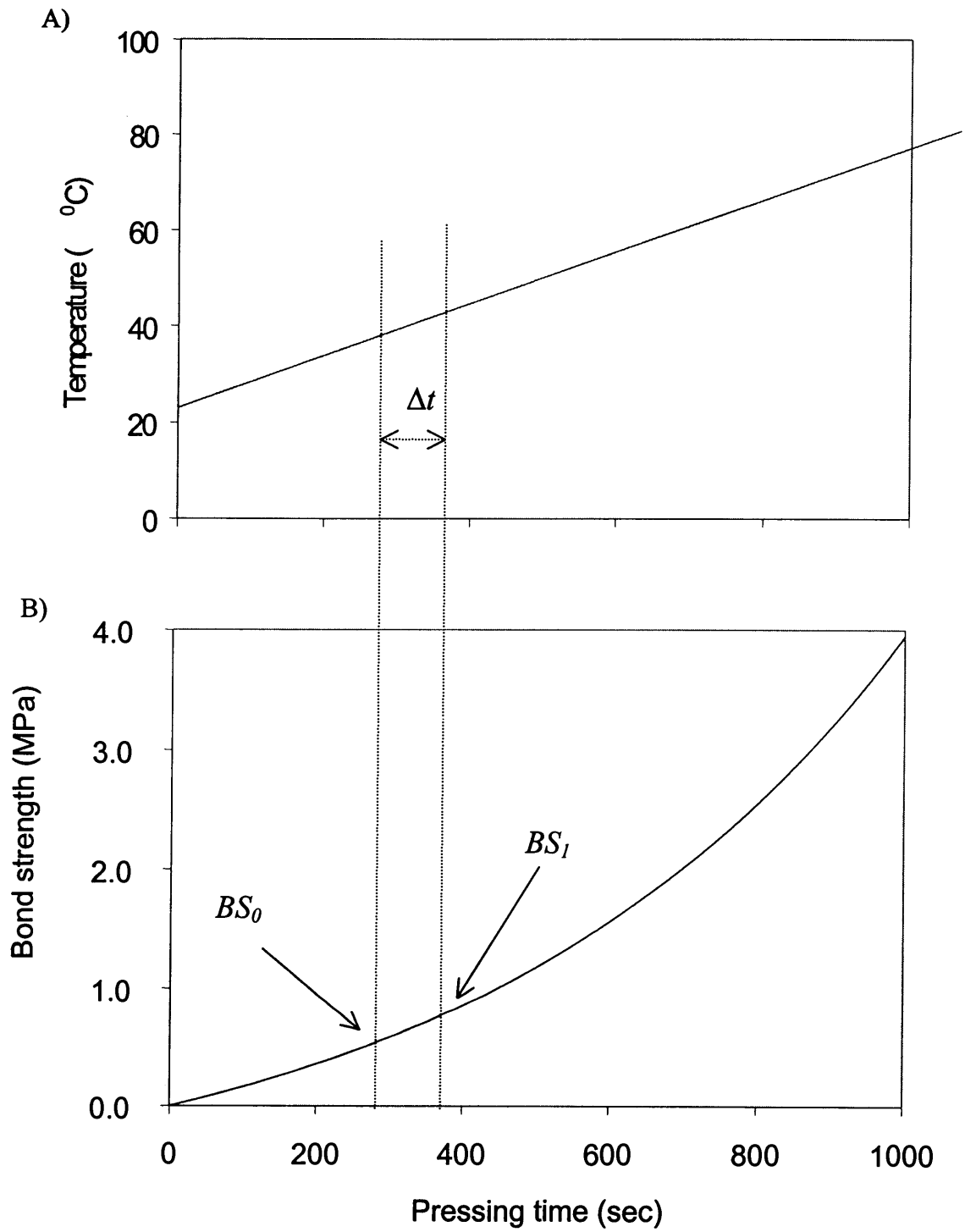

Figure 4. 15. A) Glueline temperature development at 5V applied to a 270 × 20 × 1 mm CFRP strip, and B) Prediction of bond strength development versus pressing time.

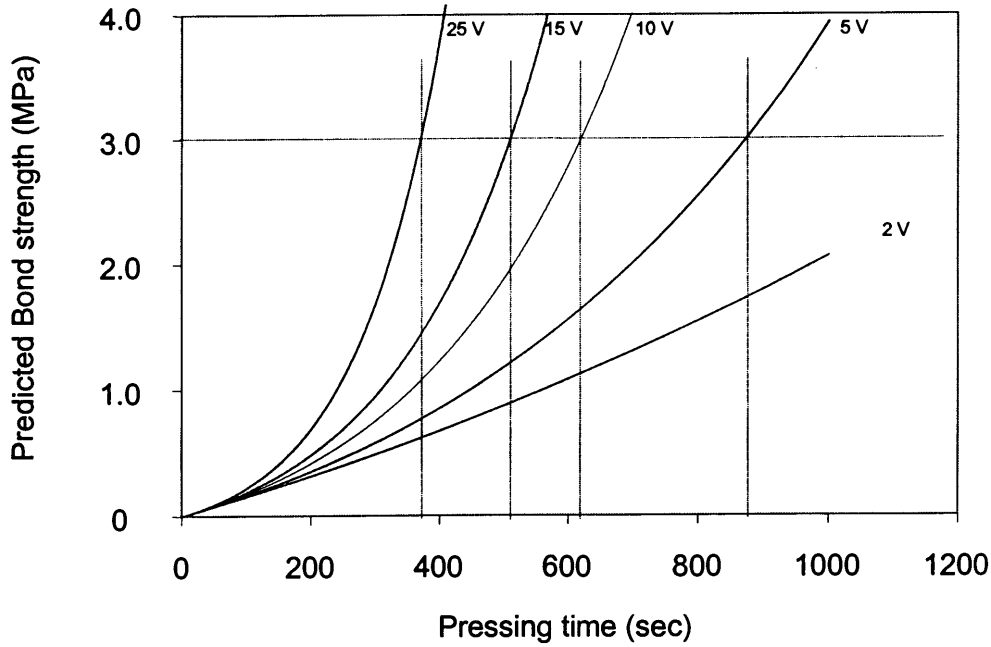

Figure 4. 16. A family of predicted bond strength development curves for a range of input voltages applied to an experimental CFRP-to-wood combination.

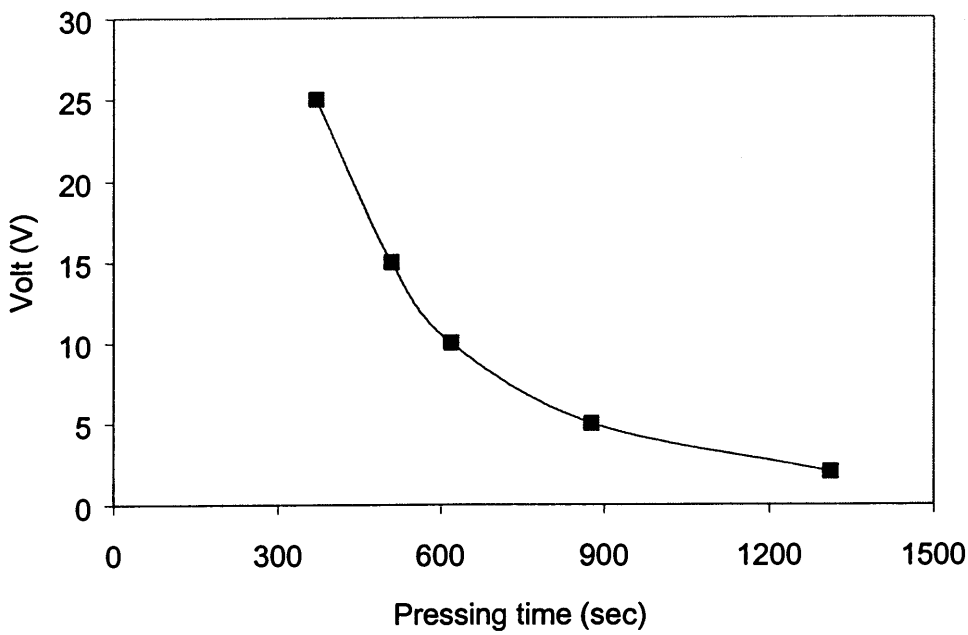

Figure 4. 17. Relationship between time and voltage needed for a 0.6 Ω CFRP strip to reach a predicted bond strength of 3 MPa.

A further limitation was imposed by the temperature tolerance of the epoxy CFRP matrix material; temperatures above 120 ^{0}C were known to cause unacceptable epoxy degradation. For this reason, maximum temperature attained during the modeled bonding system are presented as Figure 4.18.

The previous computation suggests that approximately 22.5 V is an optimal voltage to affect the most rapid bonding of the trial sample to 3 MPa without incurring thermal damage of the epoxy matrix (assuming a conservative maximum temperature of 110 ^{0}C).

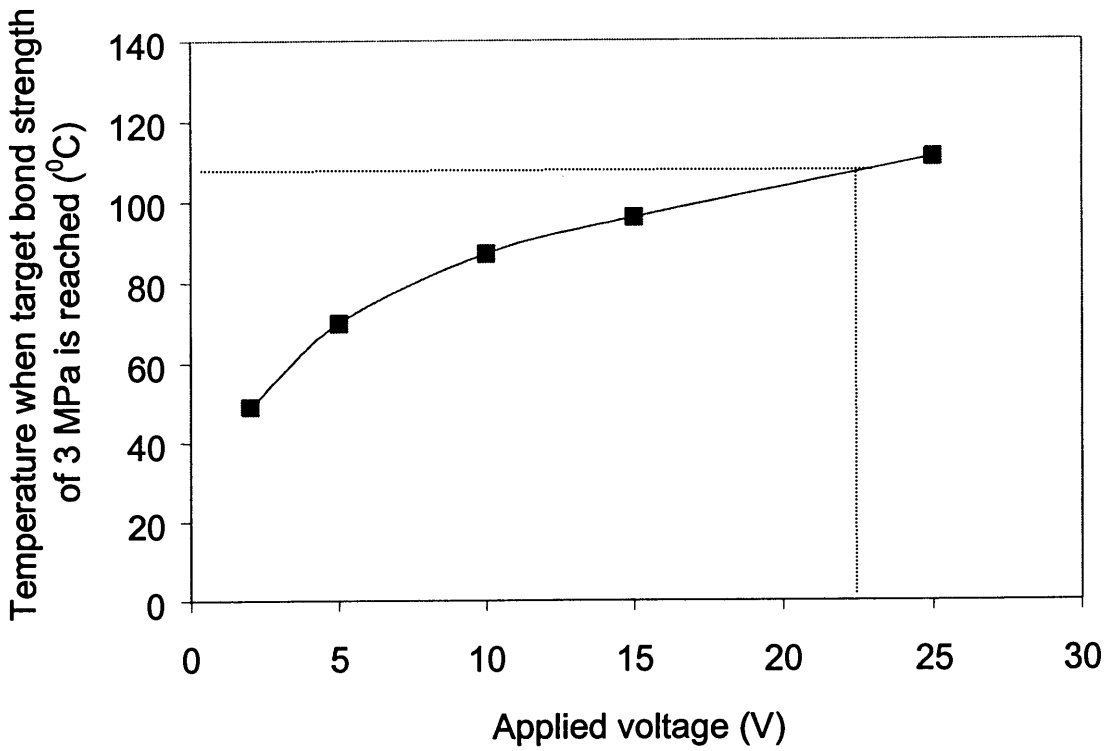

Figure 4. 18. Relationship between temperature and voltage needed to reach a predicted bond strength of 3 MPa using the bonding system model from Figure 4.17.

Failure modes

Failure surfaces of CFRP-to-wood samples that were pressed and tension tested at 100^0C were observed in a preliminary investigation. By comparing the broken sample surfaces to the clean sample surfaces, the failure modes were categorized into three types. Figure 4.19 illustrates the failure types of the CFRP-to-wood using PRF adhesive.

Adhesive failure. - At the early stages of bond cure, image-enhanced analysis showed an adhesion failure with no adhesive absorption and penetration into the CFRP surfaces (Figure 4.20-b). Figure 4.20-c shows that the PRF adhesive had spread and wet both adherend (CFRP and wood) surfaces and some adhesion processes occurred but there was not enough time for the adhesive to polymerize.

Adherend failure. - The image-enhanced result that is illustrated in Figure 4.22-d shows a fiber failure zone where the fibers began to pull out from the substrate. In some samples, fibers were both pulled out and attached on the opposite adherends. This suggested that the PRF adhesive had solidified and formed a strong bond. Some parts of the carbon fiber were therefore pulled away. The bond strength of PRF at this stage had greatly improved and exceeded the adhesive interface capacity between the fiber and the polymer matrix in CFRP.

For long pressing times, wood fiber adherend failures occurred. These failures occurred when the bond strength of PRF glue had reached its maximum adhesive and cohesive strengths. Some of the lap-shear samples could not be broken in the geometry used in the present study.

The ratio of modulus elasticity between CFRP (200 GPa) and wood (13 GPa) was approximately 15. This adherend stiffness dissimilarity caused the stress concentration at

the ends of bond-layer that exceeded the bond strength. Then, an adhesive fracture occurred and propagated across the interface layer leading to catastrophic bond failure.

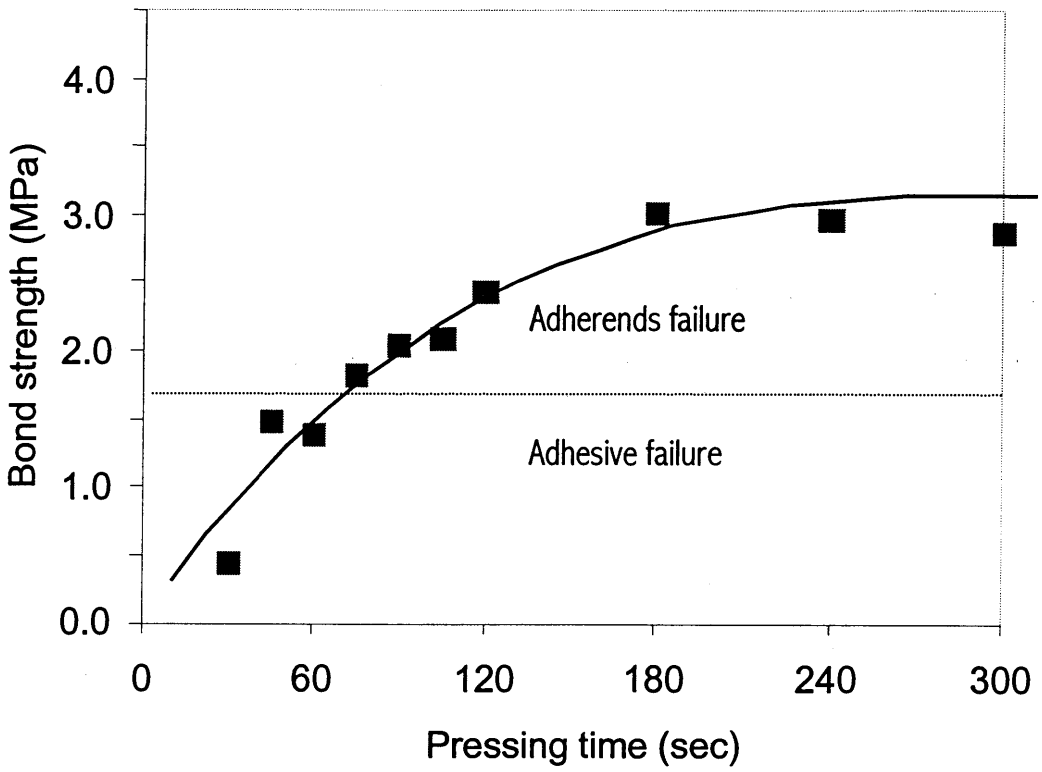

Figure 4. 19. Bond failure zones for CFRP-to-wood samples formed at 100 ^{0}C and tension tested at 100 ^{0}C using PRF adhesive.

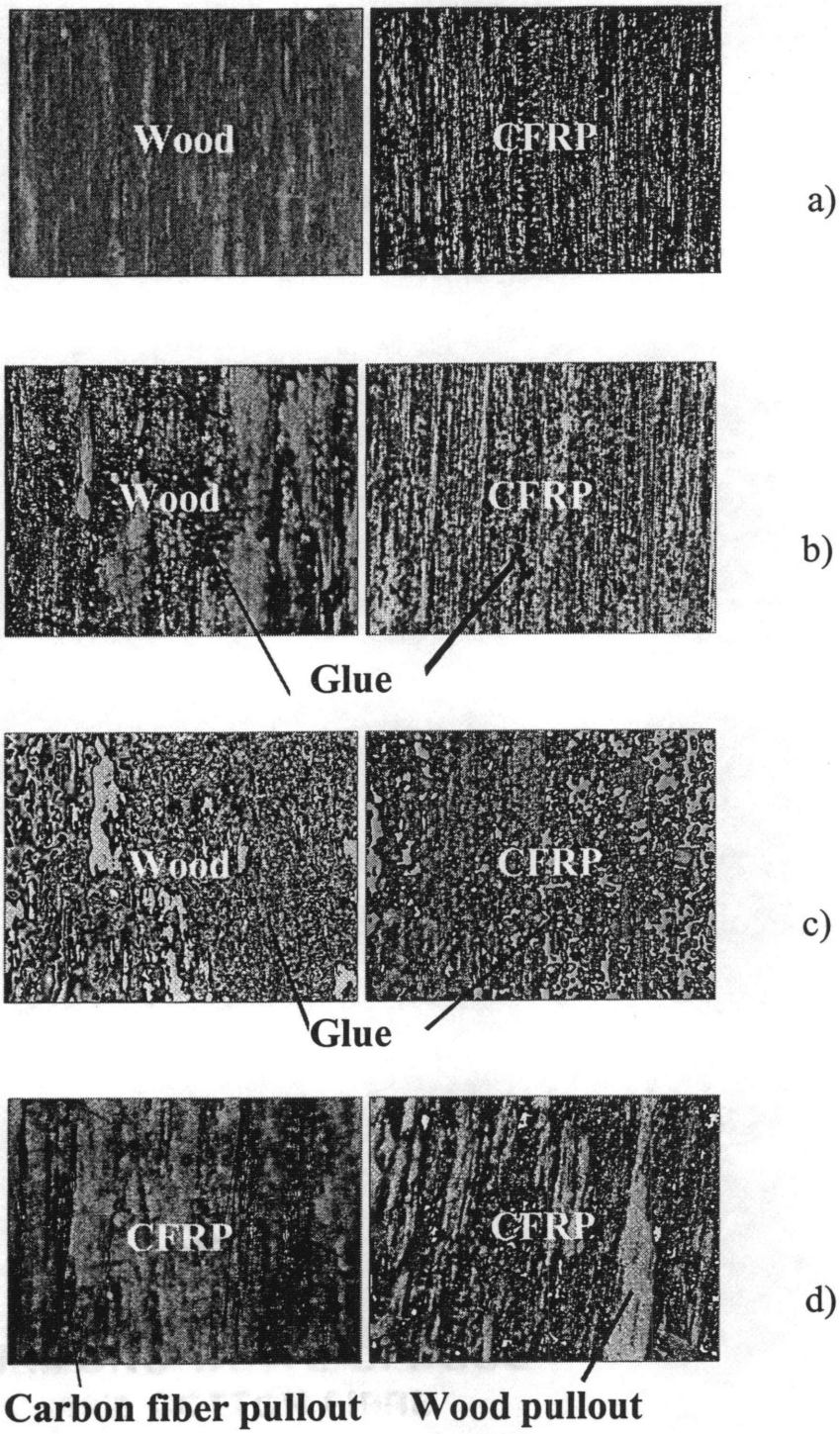

Figure 4. 20. Surfaces of broken samples from enhanced image analysis: a) clean CFRP and wood surfaces, b) adhesive failure caused by insufficient wetting and spreading, c) adhesive failure caused by insufficient adhesive cross-linking, and d) fiber pullout caused by a strong bond formation.

CONCLUSIONS

CFRP-to-wood bond strength development rate with PRF adhesive displayed an exponential dependence on temperature. This relationship suggests that increasing glueline temperature from ambient to 110 ^{0}C could lead to a substantial reduction in required pressing time. Maximum bond strengths do, however, appear to be limited by the surface properties of the FRP, which is rich in epoxy matrix. Values at 100 ^{0}C did not exceed 3 MPa. Similar limitations are evident for carbon and glass FRP. Cooling of bonds does lead to substantial (in the order of 43%) increases in bond strength at all stages of cure. Phenol formaldehyde adhesive does not appear compatible with CFRP with the pressing temperature maximum of 100 ^{0}C; bond strengths reached a maximum of about 1 MPa.

Kinetics data from ABES testing was used to estimate the effect of various process and material variables on the electrical resistive heating approach to bond cure. Design and optimization of glulam manufacturing processes with resistively heated CFRP reinforcement may therefore be possible. This approach may also be used to explore the effect of CFRP surface modification (to enhance bonding) and to aid in identifying adhesive types and formulations which are better suited to bonding CFRP-to-wood.

REFERENCES

Allen K. W. 1984. Bubbles in adhesive joints with CFRP adherends. Journal of Adhesion 17(1): 45-49.

Barbero, E.J., J.F. Davalos, and U. Munipalle. 1993. Bond strength of FRP-Wood interface. Journal of Reinforced Plastics and Composites 13(9): 835-854.

Biblis, E. J. 1965. Analysis of wood fiberglass composite beams: Within and beyond the elastic region. Forest Products Journal 25(24): 81-88.

Cooper P.A., and J.W. Sawyer. 1979. A critical examination of stresses in an elastic single lap joint. NASA, Langley Res Cent, Hampton, Va, Source: NASA Technical Paper n 1507. p: 58.

Davalos, J. F. and E. J. Barbero. 1991. Modelling of glass-fiber reinforced glulam beams. 1991 International Timber Engineering Conference, Vol 3. September 2-5, 1991. London, England. TRADA, High Wycombe, England p:3.234-3.241.

Davalos, J.F.; H. V. S. Ganga Rao S. S. Sonti, R. C. Moody, and R. Hernandez. 1994. Bulb-T and glulam-FRP beams for timber bridges. Proceedings of the Structures Congrees '94, Apr 24-28 1994. Sponsored by: ASME, Published by ASCE. p: 1316-1321.

Erdogan, F., and M. Ratwani. 1971. Stress Distribution in Bonded joints. Journal of Composite Materials (5): 378-393.

Gardner, D. J., J. F. Davalos, and U. M. Munipalle. 1994. Adhesive bonding of pultruded fiber-reinforced plastic to wood. Forest Product Journal 44(5): 62-66.

Goland, M. and Reissner, E. 1944. The stresses in cemented joints. Journal of Applied Mechanics (1): A17-A127.

Humphrey, P. E. and Zavala, D. 1989. A technique to evaluate the bonding reactivity of thermosetting adhesives. Journal of Testing and Evaluation 17(6): 323-328.

Humphrey, P. E. 1999. Personal references. Proceedings of the Washington State University International Particleboard/Composite Materials Series Symposium Apr 10-11 1991. Published by Washington State Univ. p: 99-108.

Kim, J. W. and P. E. Humphrey, 1999. The effect of temperature on the strength of partially cured phenol-formaldehyde adhesive bonds. Final seminar for Forest Products Department at Oregon State University, Corvallis, OR.

Kirlin, C.P. 1996. Experimental and finite-element analyses of stress distributions near the end of reinforcement in partially reinforced glulam. Masters thesis. Oregon State University, Corvallis, OR.

Lee, Y. D., S. K. Wang, and W. K. Chin. 1986. Liquid-rubber-modified-epoxy adhesive cured with dicyandiamide. II. Morphology and adhesion strength. Journal of applied Polymer Science 32(8): 6329-6338.

Liem, J., R. J. Leichti, and P. E. Humphrey. in preparation (a). Carbon fiber as a resistive heat generator to acceleraate adhesive cure in reinforced wood laminates. Part I: Characterizing the heating effect. Masters thesis. Oregon State University, Corvallis, OR.

Menningen, M. and H. Weiss. 1995. Application of fracture mechanics to the adhesion of metal coatings on CFRP. Surface and Coating Technology 76-77(12): 835-840.

Moulin, G.P. and P. Jodin. 1990. FGRG: Fiberglass reinforced glulam, a new composite. Wood Science and Technology (24): 289-294.

Nono, K., T. Sugibayashi, K. Mori, and H. Isono. 1993. Stress analysis of symmetric single lap-joints. Nippon Kikkai Gakkai Ronbunshu 59(559): 646-653.

Ojalvo, I.U. and H.L. Eidinoff. 1978. Bond thickness effects upon stressed in single-lap adhesive joints. Journal of American Institute of Aeronautics and Astronomic (16): 204-211.

Parker, B. M., P. Poole, M. H. Stone, G. R. Sutton, and R. N. Wilson. 1985. Problems in bonding of CFRP for aerospace use. ASE 85: Adhesives, Sealants and Encapsulants Conference - Conference Proceedings. v 2. Stress Analysis. Test Methods. Applications: Building Industry. Applications: Bonding of Fibre. Composites. Published by Network Events Ltd. Buckingham, England. p: 230-247.

Rowlands, R. E., R. P. Van Deweghe, T. L. Laufenberg, and G. P. Krueger. 1986. Fiber-reinforced wood composites. Wood and Fiber Science 18(1): 39-57.

Sonti, S. S. 1995. Laminated wood beams reinforced with pultruded fiber-reinforced plastic. 50th Annual Conference, Composite Institute, The society of the Plastics Industry, Cincinnati, OH.

Spaun, F. D. 1981. Reinforcement of wood with fiberglass. Forest Products Journal 31(4): 26-33.

Tingley, D. A. 1996. High-strength fiber-reinforced plastic reinforcement of wood and wood composite. International SAMPE Symposium and Exhibition (Proceedings) 41(1), Mar 24-28, 1996. Published by SAMPE . p: 667-678.

Tingley, D. A., J. Poland, and Kent, S. M. 1996. Shear stress distribution in American Society for Testing and Materials (ASTM) D143 shear blocks. Forest Products Society 1996 Annual Meeting, Minneapolis, MN.

Triantafillou, T. C. and N. Descovic. 1992. Prestressed FRP sheets as external reinforcement of wood members, Journal of Structural Engineering 118(5): 1270-1284.

Volkersen, O. 1938. Rivet strength distribution in tensile-stressed rivet joints with constant cross section. Luftfahrtforsch (15): 14-47.

Wangaard, F. F. 1964. Elastic deflection of wood-fiberglass composite beams. Forest Products Journal 14(6): 256-260.

Wu, Z. J., A. Romeijn, and J. Wardenier. 1997. Stress expressions of single-lap adhesive joints of dissimilar adherends. Composite Structure 38(1-4): 273-280.

CHAPTER 5

CONCLUSIONS

The results of tests reported in this thesis suggest that carbon fiber reinforced polymer (CFRP) resistive heating methods may be used to shorten conventional manufacturing processes of reinforced glulam beams by generating heat and curing the phenol resorcinol formaldehyde (PRF) adhesive inside the wood laminates. This localized heating method can effectively generate the heat through the CFRP surface and is highly controllable due to the low resistivity of CFRP.

Success of CFRP as a heating element greatly depends on the connection to the electrical circuit. It was shown that the CFRP may be electroplated at the ends. A porous copper deposit on the CFRP ends provided a good foundation for solder and conductivity. In this case, a connection to the CFRP strip had a resistance of 0.06 Ω for a measured strip of 270 × 20 × 1.03 mm.

The heat generated from CFRP was quite uniform along the surfaces of heated samples, although the temperatures were somewhat lower at the ends than in the middle of the CFRP strip. The energy needed to generate heat in the CFRP was relatively low and had an energy conversion efficiency of about 34 percent. This compares very favorably with bulk heating by hot pressing, where the whole body of wood has to be heated.

The CFRP heating pattern showed power dissipation when passing through the CFRP strip which was equivalent to resistors in series (wire, contact area of wire-to-

CFRP, CFRP strip, contact area of CFRP-to-wire, and wire). The peaks of heat concentration were on both ends at the contact area where two different materials (copper deposit and carbon fiber) met. Additional uneven heat distribution was contributed by the complexities of the carbon fiber network in the CFRP and the carbon fiber's orthotropicity.

Strength development tests for bonds between CFRP and wood in lap-shear tests using the Automated Bonding Evaluation System (ABES) with thermoset glue (PRF) were conducted. These have shown that the adhesive curing time is dependent on pressing temperature and time and an exponential dependency on temperature was found. In the lap shear testing using ABES, CFRP-to-wood bonds using PRF had an average maximum strength of 3 MPa at an elevated temperature of 100 ^{0}C. When the interface layer was cooled, bond strengths increased by up to 40%. This was detected in ABES tests with automatic cooling.

The phenol formaldehyde (PF) adhesive results showed slow bond formation processes and inferior strength. This finding suggests that the PF adhesive is not suitable for use in CFRP resistive heating methods. However, alternative PF adhesive types should be studied in the future since PF adhesive has been used as a major adhesive in wood industries and is widely accepted and less expensive than PRF.

From observation of broken samples of CFRP and wood, a bonding development chart was constructed. This result suggests that a 3 MPa bonding strength of cured PRF adhesive between the CFRP and wood may be considered as a strong bond where the bond could pull the carbon fiber out of the CFRP strip.

Prediction graphs of CFRP-to-wood bonding strength development using CFRP resistive heating was formed by combining ABES data with trial beam heating data. Numerical methods were used for the construction. This prediction can be used to provide guidance for the manufacturer to estimate sufficient energy input to accomplish optimum bond strength development efficiently.

Most of this thesis has been devoted to find ways of affecting resistive heating and evaluating adhesion kinetics of CFRP-to-wood bond tests. Preliminary trials were also conducted in which an actual laminate (measuring one meter in length) was formed. Due to time limitations, only one trial beam was formed. Effective heating was detected (from embedded thermocouples) and a strong laminate was formed within about 30 minutes. This test is not included in this thesis because it is felt that levels of replication are not sufficient. Further trials will, however, be conducted and reported in a future publication.

The CFRP resistive heating method offers a cheaper, faster and better method to enhance existing laminated wood composite manufacturing processes with high control. Since the CFRP has good mechanical reinforcement in composite products, this additional heating function makes CFRP even more favorable to be applied.

BIBLIOGRAPHY

Abel-Majid, B., H. J. Dagher, and T. Kimball. 1994. The effect of composite reinforcement on structural wood. Infrastructure: New materials and methods of repair. American Society of Civil Engineers, p.: 417-424.

Abraham, S., B.C. Pai, and K.G. Satyanarayana. 1992. Copper coating on Carbon fiber and their composites with aluminum matrix. Journal of the Material Science (27): 3479 – 3486.

Allen K. W. 1984. Bubbles in adhesive joints with CFRP adherends. Journal of Adhesion. 17(1): 45-49.

Ashby, M. 1994. Cambridge material selector 2.0 (CMS). Granta Design Ltd., Trumpington, Cambridge CB2 2LS, UK.

Asbury Carbons, Inc. 1966. P O. Box 144. Asbury, NY, 08802.

Ashkinazi, L.A. 1993. New opportunities for application of carbon as a material for heaters. Pribory I Tekhnika Eksperimenta (3): 224-227.

Ballinger, C. A. 1994. Specification needs for FRP composite products. Infrastructure: New material and methods of repair. Proceeding of the Third Material Engineers Conference in San Diego, CA, Nov 13-16, 1994, Published by American Society of Civil Engineers, (ASCE) 1852 p: 56-63.

Barbero, E.J., J.F. Davalos, and U. Munipalle. 1993. Bond strength of FRP-wood interface. Journal of Reinforced Plastics and Composites, 13(9): 835-854.

Bavarian, B., V. Arrieta, and M. Zamanzadeh. 1990. Chemical vapor deposition of HF/SI compounds as a high temperature coating for carbon/carbon composites. National SAMPE Symposium and Exhibition (Proceeding) v 35 pt 2. April 1990. SAMPE 5(35): 1348-1362.

Biblis, E. J. 1965. Analysis of wood fiberglass composite beams: Within and beyond the elastic region. Forest Products Journal 25(24): 81-88.

Blaszkiewicz, M., D. Mclachan, and R.Newnham. 1992. The volume fraction and temperature dependence of the resistivity in carbon black and graphite polymer composites: An effective media-percolation approach. Polymer Engineering and Science 32(6): 421-425.

Bohannan, B. 1962. Prestressing wood members. Forest Products Journal 12(12): 596-602.

Bulleit, M. W., B. L. Sandberg, and G. J. Woods. 1989. Steel reinforced glued laminated timber. Journal of Structural Engineering 115(2): 433-444.

Chen, Z.K., and S. Koichiro. 1995. Polarity effect of unisymmetrical material combination on the arc erosion and contact resistance behavior. Electrical Contacts, Proceeding of the Annual Holm Conference on Electrical Contact. Oct 17-19 1994. IEEE IEEE 79-88.

Chung, D. D. L. 1994. Carbon fiber composites. Butterworth-Heinemann, Newton, MA.

Coleman, G. E. and H. T. Hurst. 1974. Timber structures reinforced with light gage steel. Forest Products Journal 24(7): 45-53.

Cooper P.A., and J.W. Sawyer. 1979. A critical examination of stresses in an elastic single lap joint. NASA, Langley Res Cent, Hampton, Va, Source: NASA Technical Paper n 1507. p:58.

Davalos, J. F. and E. J. Barbero. 1991. Modelling of glass-fiber reinforced glulam beams. 1991 International Timber Engineering Conference, Vol 3. September 2-5, 1991. London, England. TRADA, High Wycombe, England p:3.234-3.241.

Davalos, J.F.; H. V. S. Ganga Rao S. S. Sonti, R. C. Moody, and R. Hernandez. 1994. Bulb-T and glulam-FRP beams for timber bridges. Proceedings of the Structures Congrees '94, Apr 24-28 1994. Sponsored by: ASME, Published by ASCE. p: 1316-1321.

Dailey, T. H. Jr. 1995. Hybrid composites: Efficiency utilization of resources by enhancement of traditional engineered composites with pultruded sheets. In proceeding of the Composites Institute's 50th Annual Conference and EXPO'95, Cincinnati, OH.

Dorf, R. C. 1993. The electrical engineering handbook. CRC Press, Inc. Boca Raton, Florida, FL, 33431.

Guoquan, W. and Z. Peng. 1997. Electrical conductivity of poly (vinyl chloride) plastisol-short carbon fiber composite. Polymer Engineering and Science 37(1): 96-100.

Erdogan, F., and M. Ratwani. 1971. Stress Distribution in Bonded joints. Journal of Composite Materials, 1971:(5): 378-393.

Fink, B. K., R. L. Mccullough, and J. W. Gillespie Jr. 1992. Local theory of Heating in Cross-Ply Carbon Fiber thermoplastic Composites by Magnetic Induction", University of Delaware, Newark, Delaware. Polymer Engineering and Science 32(5): 357 – 369.

Galligan, P.E. 1999. Personal references. 5223 Verda Line NE., Salem, Oregon, 97303.

Gardner, G. P. 1991. A reinforced glued laminated timber system. International Timber engineering Conference London p.: 3.295-3.300.

Gardner, D. J., J. F. Davalos, and U. M. Munipalle. 1994. Adhesive bonding of pultruded fiber-reinforced plastic to wood. Forest Product Journal 44(5): 62-66.

Goland, M. and E. Reissner. 1944. The stresses in cemented joints. Journal of Applied Mechanic , 1944 (1): A17-127.

Guoquan, W. and Z. Peng. 1997. Electrical conductivity of poly (vinyl chloride) plastisol-short carbon fiber composite. Polymer Engineering and Science 37(1): 96-100.

Halliday, D., and R. Resnick. 1988. Fundamentals of Physics.Third edition. John Willey & Sons Inc., New York, NY.

Humphrey, P. E. and R. J. Leichti. 1997. Affecting enhanced adhesion in fiber-reinforced laminates wood systems. New project description, Oregon State University Center for Wood Utilization Research, Corvallis, 97331.

Humphrey, P. E. and S. Ren. 1989. Bonding kinetics of thermosetting adhesive system used in wood-based composites: the combined effect of temperature and moisture content. Journal Adhesion Science Technology 3(5): 397-413.

Humphrey, P. E. and Zavala, D. 1989. A technique to evaluate the bonding reactivity of thermosetting adhesives. Journal of Testing and Evaluation. JTEVA 17(6): 323-328.

Humphrey, P. E. 1999. Personal references. Proceedings of the Washington State University International Particleboard/Composite Materials Series Symposium Apr 10-11 1991. Published by Washington State Univ. p: 99-108.

Johnson, C., and M. Browning. 1990. Status of electrocomposites Proceeding of the . American Electroplaters and Surface Finishers (AESF) Annual Technical Conference. July 9-12 1990. American Electroplaters and Surface Finishers Soc. Inc., 1203-1226.

Kim, J., and Y. Mai. 1991. Effect of interfacial coating and temperature on the fracture behaviors of unidirectional kevlar and carbon fiber reinforced epoxy resin composites. Journal of Material Science, 1991(26): 4702 – 4720.

Kim, J. W. and P. E. Humphrey, 1999. The effect of temperature on the strength of partially cured phenol-formaldehyde adhesive bonds. Final seminar for Forest Products Department at Oregon State University, Corvallis, OR, 97331.

Kirlin, C.P., T. C. Kennedy, and R. J. Leichti. 1996. Experimental and finite-element analyses of stress distributions near the end of reinforcement in partially reinforced glulam. Masters thesis. Oregon State University, Corvallis, OR.

Kootenay Forest Products Ltd. 1964. KFP Silverlam products, Post and beam. Bulletin no. 1. CMHC Acceptance no. 4501. Nelson, British Columbia, Canada.

Kulkarni, A., N. Balasubramanian, and B. Pai. 1979. Cementation technique for coating carbon fibers. Journal of Materials Science 14(3): 592-598.

Lantos. G. 1970. The flexural behavior of steel reinforced laminated timber beams. Wood Science 2(3): 136-143.

Lee, Y. D., S. K. Wang, and W. K. Chin. 1986. Liquid-rubber-modified-epoxy adhesive cured with dicyandiamide. II. Morphology and adhesion strength. Journal of applied Polymer Science. 32(8): 6329-6338.

Leichti, R. J. and Groom, L. H. 1991. Influence of adhesive stiffness and adherend dissimilarity on stress distributions in structural finger joints. Adhesive and Bonded

Liem, J., R. J. Leichti, and P. E. Humphrey. in preparation (a). Carbon fiber as a resistive heat generator to accelerate adhesive cure in reinforced wood laminates. Part I: Characterizing the heating effect. Masters thesis. Oregon State University, Corvallis, OR.

Liem, J., R. J. Leichti, and P. E. Humphrey. in preparation (b). Carbon fiber as a resistive heat generator to accelerate adhesive cure in reinforced wood laminates. Part II: Characterizing wood-to-reinforcement bonding kinetics. Masters thesis. Oregon State University, Corvallis, OR.

Lin, R. Y., and S.G. Warrier. 1993. Silver coating on carbon and SiC fibers. Journal of Material Science, 1993(28): 4868 – 4877.

Lounder, R. 1987. Electrical transport and optical properties of inhomogeneous media. American Institute of Physics Conference Proceedings, No. 40, P. 2. American Institute of Physics, New York, NY.

Mark, R. 1961. Wood-aluminum beams within and beyond the elastic range. Part I: Rectangular sections. Forest Products Journal 11(10): 477-484.

Mark, R. 1963. Wood-aluminum beams within and beyond the elastic range. Part II: Trapezoidal sections. Forest Products Journal 13(11): 508-516.

Menningen, M. and H. Weiss. 1995. Application of fracture mechanics to the adhesion of metal coatings on CFRP. Surface and Coating Technology. 76-77(12): 835-840.

Moulin, G.P. and P. Jodin. 1990. FGRG: Fiberglass reinforced glulam, a new composite. Wood Science and Technology (24): 289-294.

Mufti, A. A. 1992. Pultrusion process in manufacturing of FRP-wood composite beams. Technical Bulletin University of Nova Scotia Halifax, Nova Scotia, Canada.

Nakanishi, Y., and Y.Hayashi. 1992. Preparation of composite materials from carbon fiber paper and those several properties, Journal of the Textile Machinery Society of Japan 45(7): T101-T106.

Nieuwenhuizen, V.D., S.C. Robin, and A.K. Miller. 1994. Full insitu consolidation of thermoplastic matrix carbon fiber composite materials using direct electrical heating. American Society of Mechanical Engineers, Material Division (12): 29-41.

Nono, K., T. Sugibayashi, K. Mori, and H. Isono. 1993. Stress analysis of symmetric single lap-joints. Nippon Kikkai Gakkai Ronbunshu 59(559): 646-653.

Ojalvo, I.U. and H.L. Eidinoff. 1978. Bond thickness effects upon stressed in single-lap adhesive joints. Journal of American Institute of Aeronautics and Astronomic (AIAA), (16): 204-211.

Orfeuil, M. 1987. Electric process heating. Technology/Equipment/Applications. Battelle Press, Columbus, OH.

Parathasaradhy, N.V. 1989. Practical Electroplating Handbook. Prentice Hall, Englewood Cliffs, NJ.

Parker, B. M., P. Poole, M. H. Stone, G. R. Sutton, and R. N. Wilson. 1985. Problems in bonding of CFRP for aerospace use. ASE 85: Adhesives, Sealants and Encapsulants Conference - Conference Proceedings. v 2. Stress Analysis. Test Methods. Applications: Building Industry. Applications: Bonding of Fibre. Composites. Published by Network Events Ltd. Buckingham, England. p: 230-247.

Phelan P.E., O. Nakabeppu, K. Ito, K. Hijikata, T. Ohmori, and K. Torikoshi. 1992. American Society of Mechanical Engineers, Heat Transfer Division, HDT v 200. Aug 9-12 1992. ASME Heat Transfer Div 63-69.

Ramakrishnan, B., L. Zhu., and L. van der Shuur. 1998. Accelerated curing using supplemental internal resistive heating. International SAMPE Symposium and Exhibition (Proceeding) v 43 n 1. May 31-June 4 1998. SAMPE , 5(43): 243-253.

Rowlands, R. E., R. P. Van Deweghe, T. L. Laufenberg, and G. P. Krueger. 1986. Fiber-reinforced wood composites. Wood and Fiber Science, 18(1): 39-57.

Sancaktar, E., W. Ma, and S. Yurgartis. 1991. Electric resistive heat curing of the fiber-matrix interphase in graphite/epoxy composites. American Society of Mechanical Engineers, Design Engineering Division (30): 127-137.

Saucier, J. R. and Holman, J. A. 1975. Structural particleboard reinforced with glass fiber-progress in its development. Forest Products Journal 25(9): 69-72.

Shiota, I., and O. Watanabe. 1974. Continuous uniform nickel electroplating on carbon fibers. Nippon Kinzoku Gakkaishi/Journal of Japan Institute of Metals 38(9): 788-794.

Sliker, A. 1962. Reinforced wood laminated beams. Forest Products Journal 12(12): 91-96.

Smulski. S. and Ifju, G. 1987a. Creep behavior of glass fiber reinforced hardboard. Wood and Fiber Science 19(4): 430-438.

Smulski. S. and Ifju, G. 1987b. Flexural behavior of glass fiber reinforced hardboard. Wood and Fiber Science 19(3): 313-327.

Sonti, S. S. 1995. Laminated wood beams reinforced with pultruded fiber-reinforced plastic. 50th Annual Conference, Composite Institute, The society of the Plastics Industry January 1995, Cincinnati, OH, Session 10-B: 1-5.

Spaun, F. D. 1981. Reinforcement of wood with fiberglass. Forest Products Journal 31(4): 26-33.

Spicer, J., D. Wilson, and R. Osiander. 1999. Evaluating of high thermal conductivity graphite fibers for thermal management in electronics applications. Proceeding of SPIE-The International Society for Optical Engineering v 3700. Apr 6-Apr-8 1999. Society of Photo Instrumentation Engineers 5(3700): 40-47.

Takato N., O. Maeda, and N. Yamada. 1976. Electroplating on plastic material reinforced with carbon-fibers and properties of the plated layer. Journal of Society of Material Science, Japan/Zairyo 25(279): 1153-1158.

Tingley, D. A. and R. J. Leichti. 1994. Glued Laminated beams having a high-strength fiber-reinforcement: The bi-material interface. In: Proceeding of the Pacific Timber Engineering Conference. Gold Coast, Australia. Vol. 2:665-675.

Tingley, D. A., J. Poland, and Kent, S. M. 1996. Shear stress distribution in ASTM D143 shear blocks. Forest Products society 1996 Annual Meeting, Minneapolis, MN.

Tingley, D. A. 1996. High-strength fiber-reinforced plastic reinforcement of wood and wood composite. International SAMPE Symposium and Exhibition (Proceedings) 41(1), Mar 24-28, 1996. Published by SAMPE . p: 667-678.

Triantafillou, T. C. and N. Descovic. 1992. Prestressed FRP sheets as external reinforcement of wood members, Journal of Structural Engineering 118(5): 1270-1284.

Volkersen O. 1938. Rivet strength distribution in tensile-stressed rivet joints with constant cross section. Luftfahrtforsch (15): 14-47.

Wangaard, F. F. 1964. Elastic deflection of wood-fiberglass composite beams. Forest Products Journal 14(6): 256-260.

Wu, Z. J., A. Romeijn, and J. Wardenier. 1997. Stress expressions of single-lap adhesive joints of dissimilar adherends. Composite Structure. 38(1-4): 273-280.